



11 GENERAL CIRCULATION

Contents

- 11.1. Key Terms 330
- 11.2. A Simple Description of the Global Circulation 330
 - 11.2.1. Near the Surface 330
 - 11.2.2. Upper-troposphere 331
 - 11.2.3. Vertical Circulations 332
 - 11.2.4. Monsoonal Circulations 333
- 11.3. Radiative Differential Heating 334
 - 11.3.1. North-South Temperature Gradient 335
 - 11.3.2. Global Radiation Budgets 336
 - 11.3.3. Radiative Forcing by Latitude Belt 338
 - 11.3.4. General Circulation Heat Transport 338
- 11.4. Pressure Profiles 340
 - 11.4.1. Non-hydrostatic Pressure Couplets 340
 - 11.4.2. Hydrostatic Thermal Circulations 341
- 11.5. Geostrophic Wind & Geostrophic Adjustment 343
 - 11.5.1. Ageostrophic Winds at the Equator 343
 - 11.5.2. Definitions 343
 - 11.5.3. Geostrophic Adjustment - Part 1 344
- 11.6. Thermal Wind Effect 345
 - 11.6.1. Definition of Thickness 346
 - 11.6.2. Thermal-wind Components 346
 - 11.6.3. Case Study 348
 - 11.6.4. Thermal Wind & Geostrophic Adj.-Part 2. 349
- 11.7. Explaining the General Circulation 350
 - 11.7.1. Low Latitudes 350
 - 11.7.2. High Latitudes 352
 - 11.7.3. Mid-latitudes 352
 - 11.7.4. Monsoon 356
- 11.8. Jet Streams 357
 - 11.8.1. Baroclinicity & the Polar Jet 359
 - 11.8.2. Angular Momentum & Subtropical Jet 360
- 11.9. Types of Vorticity 362
 - 11.9.1. Relative-vorticity Definition 362
 - 11.9.2. Absolute-vorticity Definition 363
 - 11.9.3. Potential-vorticity Definition 363
 - 11.9.4. Isentropic Potential Vorticity Definition 364
- 11.10. Horizontal Circulation 365
- 11.11. Extratropical Ridges & Troughs (Rossby Waves) 367
 - 11.11.1. Barotropic Instability 367
 - 11.11.2. Baroclinic Instability 371
 - 11.11.3. Meridional Transport by Rossby Waves 374
- 11.12. Three-band Global Circulation 376
 - 11.12.1. A Metric for Vertical Circulation 377
 - 11.12.2. Effective Vertical Circulation 377
- 11.13. Ekman Spiral of Ocean Currents 378
- 11.14. Review 379
- 11.15. Homework Exercises 380

A spatial imbalance between radiative inputs and outputs exists for the earth-ocean-atmosphere system. The earth loses energy at all latitudes due to outgoing infrared (IR) radiation. Near the tropics, more solar radiation enters than IR leaves, hence there is a net input of radiative energy. Near Earth's poles, incoming solar radiation is too weak to totally offset the IR cooling, allowing a net loss of energy. The result is **differential heating**, creating warm equatorial air and cold polar air (Fig. 11.1a).

This imbalance drives the global-scale **general circulation** of winds. Such a circulation is a fluid-dynamical analogy to **Le Chatelier's Principle** of chemistry. Namely, an imbalanced system reacts in a way to partially counteract the imbalance. The continued destabilization by radiation causes a general circulation of winds that is unceasing.

Because buoyancy causes warmer air to rise and colder air to sink, you might guess that equator-to-pole overturning would exist (Fig. 11.1b). Instead, the real general circulation has three bands of circulations in the Northern Hemisphere (Fig. 11.1c), and three in the Southern. In this chapter, we will identify characteristics of the general circulation, explain why they exist, and learn how they work.

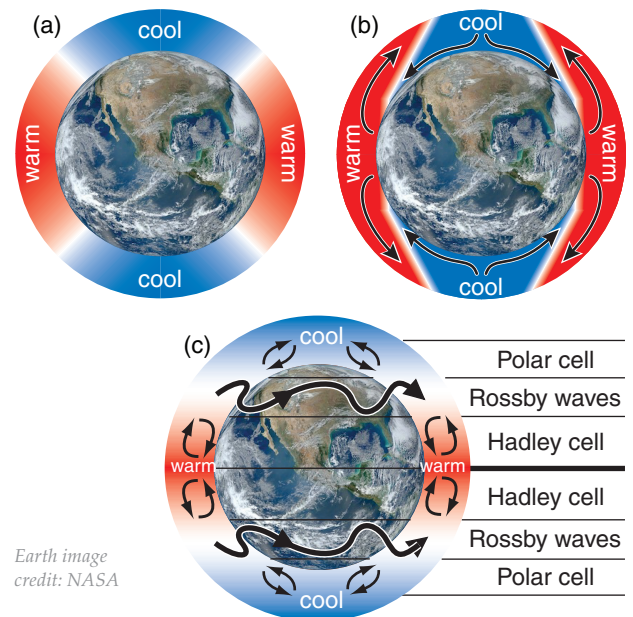


Figure 11.1 Radiative imbalances create (a) warm tropics and cold poles, inducing (b) buoyant circulations. Add Earth's rotation, and (c) three circulation bands form in each hemisphere.

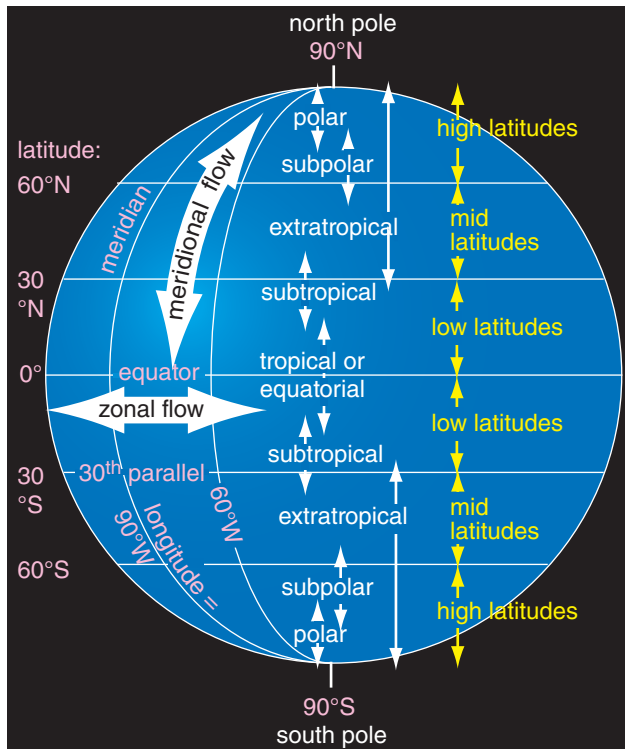


Figure 11.2
Global key terms.

A SCIENTIFIC PERSPECTIVE • Idealizations of Nature

Natural atmospheric phenomena often involve the superposition of many different physical processes and scales of motion. Large-scale average conditions are said to be caused by **zeroth-order** processes. Dominant variations about the mean are controlled by **first-order** processes. Finer details are caused by **higher-order** processes.

Sometimes insight is possible by stripping away the higher-order processes and focusing on one or two lower orders. Equations that describe such simplified physics are known as **toy models**. With the right simplifications, some toy models admit analytical solutions. Compare this to the unsimplified physics, which might be too complicated to solve analytically (although numerical solutions are possible).

A rotating spherical “aqua planet” with no continents and with uniform temperature is one example of a zeroth-order toy model. A first-order toy model might add the north-south temperature variation, while neglecting east-west and continent-ocean variations. With even more sophistication, seasonal or monthly variations might be explained. We will take the approach in this chapter to start with zeroth-order models to focus on basic climate concepts, and then gradually add more realism.

John Harte (1988) wrote a book demonstrating the utility of such toy models. It is “*Consider a Spherical Cow*”, by University Science Books. 283 pages.

11.1. KEY TERMS

Lines of constant latitude are called **parallels**, and winds parallel to the parallels are identified as **zonal flows** (Fig. 11.2). Lines of constant longitude are called **meridians**, and winds parallel to the meridians are known as **meridional flows**.

Between latitudes of 30° and 60° are the **mid-latitudes**. **High latitudes** are 60° to 90°, and **low latitudes** are 0° to 30°. Each 1° of latitude = 111 km.

Tropics, subtropics, subpolar, and polar regions are as shown in Fig. 11.2. Regions not in the tropics are called **extratropical**; namely, poleward of about 30°N and about 30°S.

For example, **tropical cyclones** such as **hurricanes** are in the tropics. Low-pressure centers (**lows**, as indicated by L on weather maps) outside of the tropics are called **extratropical cyclones**.

In many climate studies, data from the months of June, July, and August (**JJA**) are used to represent conditions in N. Hemisphere summer (and S. Hemisphere winter). Similarly, December, January, February (**DJF**) data are used to represent N. Hemisphere winter (and S. Hemisphere summer).

11.2. A SIMPLIFIED DESCRIPTION OF THE GLOBAL CIRCULATION

This section summarizes “what” happens. The subsequent sections explain “why” and “how”.

Consider a hypothetical rotating planet with no contrast between continents and oceans. The **climatological average** (average over 30 years; see the Climate chapter) winds in such a simplified planet would have characteristics as sketched in Figs. 11.3. Actual winds on any day could differ from this climatological average due to transient weather systems that perturb the average flow. Also, monthly-average conditions tend to shift toward the summer hemisphere (e.g., the circulation bands shift northward during April through September).

11.2.1. Near the Surface

Near-surface average winds are sketched in Fig. 11.3a. At low latitudes are broad bands of persistent easterly winds ($U \approx -7 \text{ m s}^{-1}$) called **trade winds**, named because the **easterlies** allowed sailing ships to conduct transoceanic **trade** in the old days.

These trade winds also blow toward the equator from both hemispheres, and the equatorial belt of convergence is called the **intertropical convergence zone (ITCZ)**. On average, the air at the ITCZ

is hot and humid, with low pressure, strong upward air motion, heavy convective (thunderstorm) precipitation, and light to calm winds except in thunderstorms. This **equatorial trough** (low-pressure belt) was called the **doldrums** by sailors whose sailing ships were becalmed there for many days.

At 30° latitude are belts of high surface pressure called **subtropical highs** (Fig. 11.3a). In these belts are hot, dry, cloud-free air descending from higher in the troposphere. Surface winds in these belts are also calm on average. In the old days, becalmed sailing ships would often run short of drinking water, causing horses on board to die and be thrown overboard. Hence, sailors called these miserable places the **horse latitudes**. On land, many of the world's deserts are near these latitudes.

In mid-latitudes are transient centers of low pressure (**mid-latitude cyclones, L**) and high pressure (**anticyclones, H**). Winds around lows **converge** (come together) and circulate **cyclonically** — counterclockwise in the N. Hemisphere, and clockwise in the S. Hemisphere. Winds around highs **diverge** (spread out) and rotate **anticyclonically** — clockwise in the N. Hemisphere, and counterclockwise in the S. Hemisphere. The cyclones are regions of bad weather (clouds, rain, high humidity, strong winds) and fronts. The anticyclones are regions of good weather (clear skies or fair-weather clouds, no precipitation, dry air, and light winds).

The high- and low-pressure centers move on average from west to east, driven by large-scale winds from the west. Although these **westerlies** dominate the general circulation at mid-latitudes, the surface winds are quite variable in time and space due to the sum of the westerlies plus the transient circulations around the highs and lows.

Near 60° latitude are belts of low surface pressure called **subpolar lows**. Along these belts are light to calm winds, upward air motion, clouds, cool temperatures, and precipitation (as snow in winter).

Near each pole is a climatological region of high pressure called a **polar high**. In these regions are often clear skies, cold dry descending air, light winds, and little snowfall. Between each polar high (at 90°) and the subpolar low (at 60°) is a belt of weak easterly winds, called the **polar easterlies**.

11.2.2. Upper-troposphere

The stratosphere is strongly statically stable, and acts like a lid to the troposphere. Thus, vertical circulations associated with our weather are mostly trapped within the troposphere. These vertical circulations couple the average near-surface winds with the average upper-tropospheric (near the tropopause) winds described here (Fig. 11.3b).

In the tropics is a belt of very strong equatorial

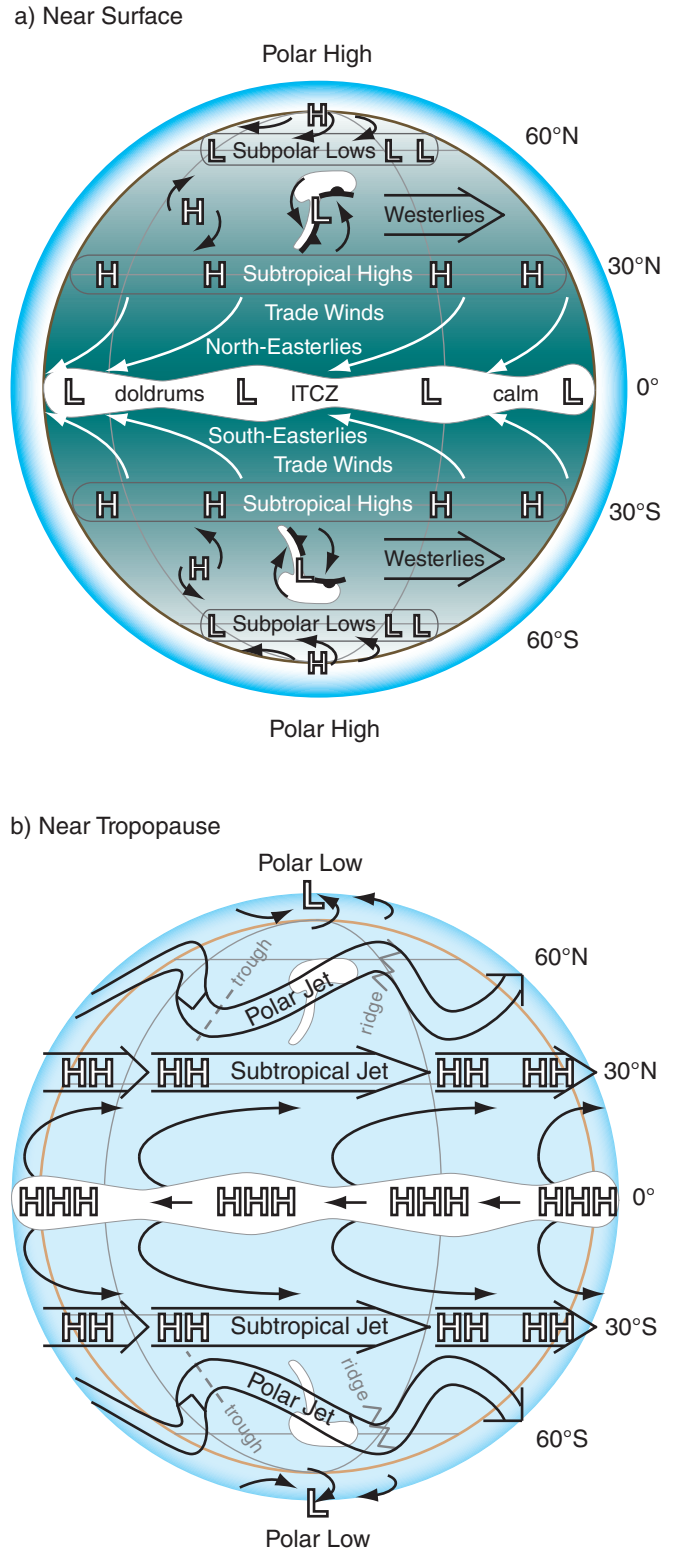
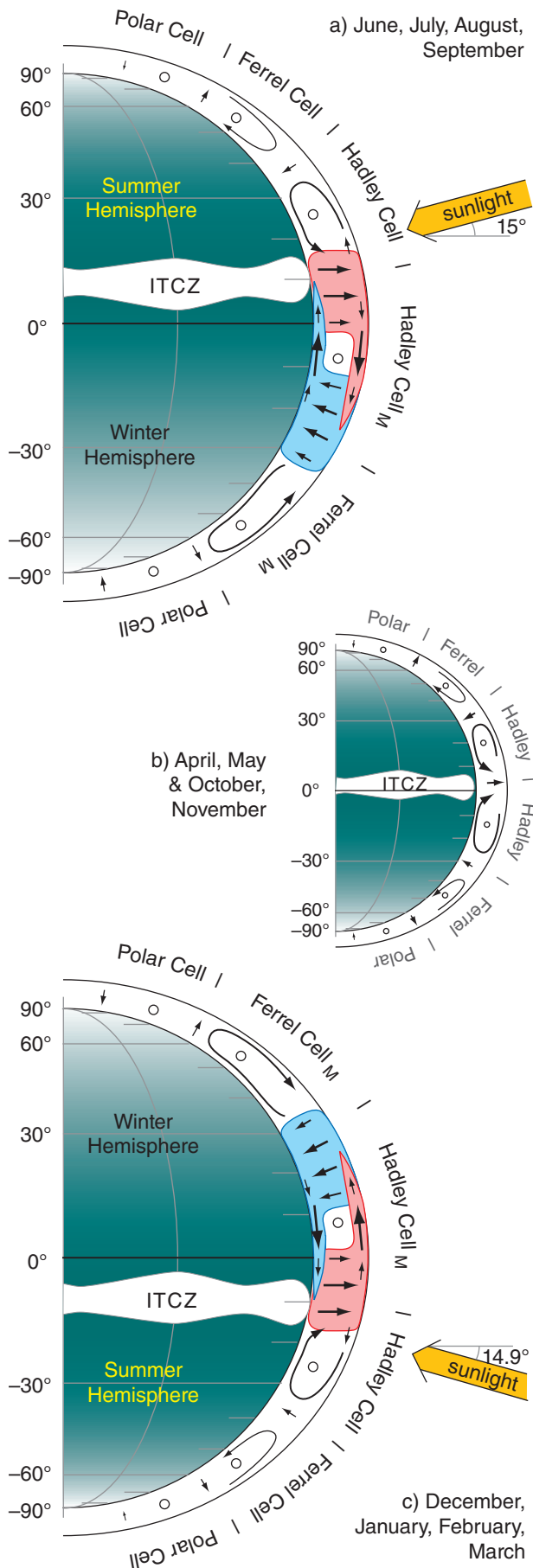


Figure 11.3
Simplified global circulation in the troposphere: (a) near the surface, and (b) near the tropopause. H and L indicate high and low pressures, and HHH means very strong high pressure. White indicates precipitating clouds. CAUTION: high and low pressures are RELATIVE to the average pressure AT THE SAME ALTITUDE. All absolute pressures near the tropopause are actually lower than the near-surface pressures.



high pressure along the tops of the ITCZ thunderstorms. Air in this belt blows from the east, due to easterly inertia from the trade winds being carried upward in the thunderstorm convection. Diverging from this belt are winds that blow toward the north in the N. Hemisphere, and toward the south in the S. Hemisphere. As these winds move away from the equator, they turn to have an increasingly westerly component as they approach 30° latitude.

Near 30° latitude in each hemisphere is a persistent belt of strong westerly winds at the tropopause called the **subtropical jet**. This jet meanders north and south a bit. Pressure here is very high, but not as high as over the equator.

In mid-latitudes at the tropopause is another belt of strong westerly winds called the **polar jet**. The centerline of the polar jet meanders north and south, resulting in a wave-like shape called a **Rossby wave** (or **planetary wave**), as sketched in Fig. 11.1c. The equatorward portions of the wave are known as low-pressure **troughs**, and poleward portions are known as high-pressure **ridges**. These ridges and troughs are very transient, and generally shift from west to east relative to the ground.

Near 60° at the tropopause is a belt of low to medium pressure. At each pole is a low-pressure center near the tropopause, with winds at high latitudes generally blowing from the west causing a cyclonic circulation around the **polar low**. Thus, contrary to near-surface conditions, the near-tropopause average winds blow from the west at all latitudes (except near the equator).

11.2.3. Vertical Circulations

Vertical circulations of warm rising air in the tropics and descending air in the subtropics are called **Hadley cells** or **Hadley circulations** (Fig. 11.4). At the bottom of the Hadley cell are the trade winds. At the top, near the tropopause, are divergent winds. The updraft portion of the Hadley circulation often contains thunderstorms and heavy precipitation at the ITCZ. This vigorous convection in the troposphere causes a high tropopause (15 - 18 km altitude) and a belt of heavy rain in the tropics.

The summer- and winter-hemisphere Hadley cells are strongly asymmetric (Fig. 11.4). The major Hadley circulation (denoted with subscript "M") crosses the equator, with rising air in the summer hemisphere and descending air in the winter hemisphere. The updraft is often between 0° and

Figure 11.4 (at left)

Vertical cross section of Earth's global circulation in the troposphere. (a) N. Hemisphere summer. (b) Transition months. (c) S. Hemisphere summer. The major (subscript M) Hadley cell is colored in red and blue. Minor circulations have no subscript.

15° latitudes in the summer hemisphere, and has average core vertical velocities of 6 mm s^{-1} . The broader downdraft is often found between 10° and 30° latitudes in the winter hemisphere, with average velocity of about -4 mm s^{-1} in downdraft centers. Connecting the up- and downdrafts are meridional wind components of 3 m s^{-1} at the cell top & bottom.

The major Hadley cell changes direction and shifts position between summer and winter. During June-July-August-September, the average solar declination angle is 15°N, and the updraft is in the Northern Hemisphere (Fig. 11.4a). Out of these four months, the most well-defined circulation occurs in August and September. At this time, the ITCZ is centered at about 9°N, but varies with longitude.

During December-January-February-March, the average solar declination angle is 14.9°S, and the major updraft is in the Southern Hemisphere (Fig. 11.4c). Out of these four months, the strongest circulation is during February and March, and the ITCZ is centered at roughly 6°S, but varies with longitude. The major Hadley cell transports significant heat away from the tropics, and also from the summer to the winter hemisphere.

During the transition months (April-May and October-November) between summer and winter, the Hadley circulation has nearly symmetric Hadley cells in both hemispheres (Fig. 11.4b). During this transition, the intensities of the Hadley circulations are weak.

When averaged over the whole year, the strong but reversing major Hadley circulation partially cancels itself, resulting in an annual average circulation that is somewhat weak and looks like Fig. 11.4b. This weak annual average is deceiving, and does not reflect the true movement of heat, moisture, and momentum by the winds. Hence, climate experts prefer to look at months JJA and DJF separately to give **seasonal averages**.

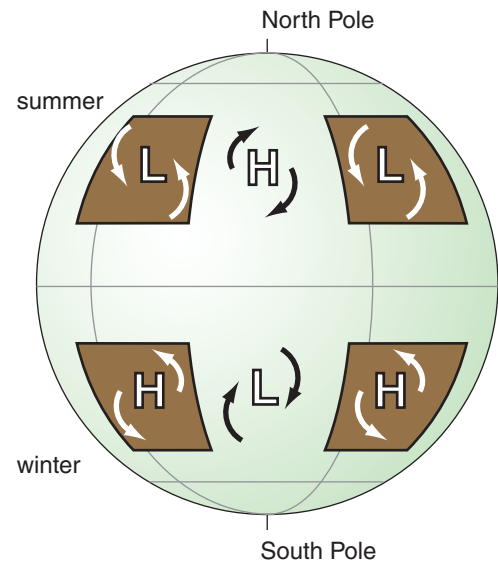
In the winter hemisphere, one or more jet streams circle the earth at mid-latitudes while meandering north and south as Rossby waves (Fig. 11.1c). When averaged around latitude bands, the net effect is a weak vertical circulation called a **Ferrel cell**. At high latitudes is a modest **polar cell**.

In the summer hemisphere, all the circulations are weaker. There are minor Hadley and Ferrel cells (Fig. 11.4). Summer-hemisphere circulations are weaker because the temperature contrast between the tropics and poles are weaker.

11.2.4. Monsoonal Circulations

Monsoon circulations are continental-scale circulations driven by continent-ocean temperature contrasts, as sketched in Figs. 11.5. In summer, high-pressure centers (anticyclones) are over the

a) June, July, August



b) December, January, February

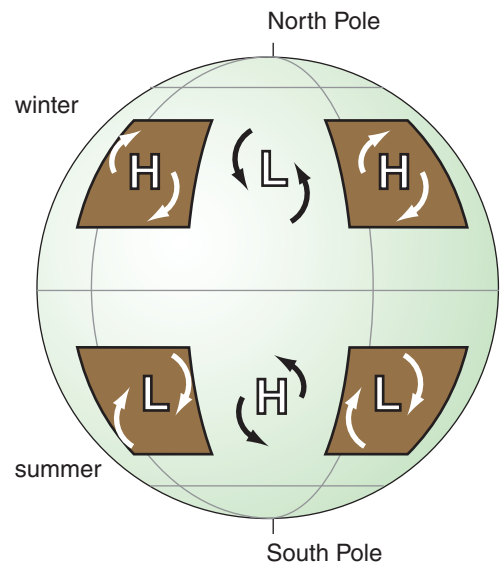


Figure 11.5

Idealized seasonal-average monsoon circulations near the surface. Continents are shaded dark brown; oceans are light green. H and L are surface high- and low-pressure centers.

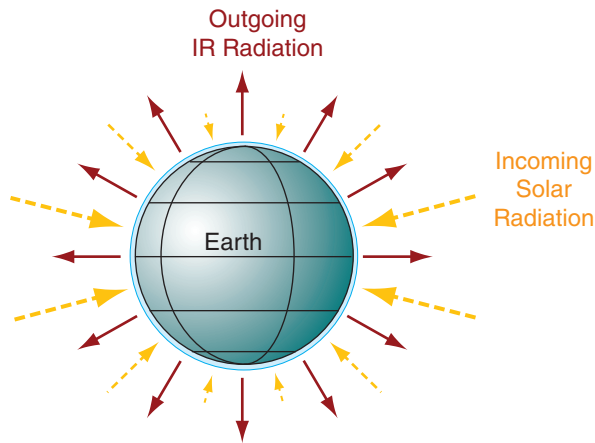


Figure 11.6
 Annual average incoming solar radiation (yellow dashed arrows) and outgoing infrared (IR) radiation (solid dark red arrows), where arrow length indicates relative magnitude. [Because the Earth rotates and exposes all locations to the sun at one time or another during the year, the incoming solar radiation is sketched as approaching all locations on the Earth’s surface.]

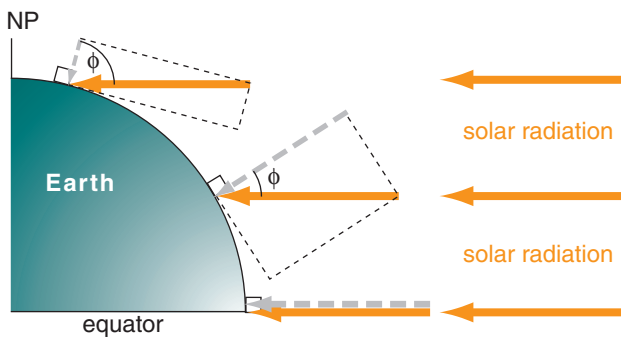


Figure 11.7
 Of the solar radiation approaching the Earth (thick solid yellow arrows), the component (dashed grey arrow) that is perpendicular to the top of the atmosphere is proportional to the cosine of the latitude ϕ (during the equinox).

relatively warm oceans, and low-pressure centers (cyclones) are over the hotter continents. In winter, low-pressure centers are over the cool oceans, and high-pressure centers are over the colder continents.

These monsoon circulations represent average conditions over a season. The actual weather on any given day can be variable, and can deviate from these seasonal averages.

Our Earth has a complex arrangement of continents and oceans. As a result, seasonally-varying monsoonal circulations are superimposed on the seasonally-varying planetary-scale circulation to yield a complex and varying global-circulation pattern.

At this point, you have a descriptive understanding of the global circulation. But what drives it?

11.3. RADIATIVE DIFFERENTIAL HEATING

The general circulation is driven by differential heating. Incoming solar radiation (**insolation**) nearly balances the outgoing infrared (IR) radiation when averaged over the whole globe. However, at different latitudes are significant imbalances (Fig. 11.6), which cause the differential heating.

Recall from the Solar & Infrared Radiation chapter that the flux of solar radiation incident on the top of the atmosphere depends more or less on the cosine of the latitude, as shown in Fig. 11.7. The component of the incident ray of sunlight that is perpendicular to the Earth’s surface is small in polar regions, but larger toward the equator (grey dashed arrows in Figs. 11.6 and 11.7). The incoming energy adds heat to the Earth-atmosphere-ocean system.

Heat is lost due to infrared (IR) radiation emitted from the Earth-ocean-atmosphere system to space. Since all locations near the surface in the Earth-ocean-atmosphere system are relatively warm compared to absolute zero, the Stefan-Boltzmann law from the Solar & Infrared Radiation chapter tells us that the emission rates are also more or less uniform around the Earth. This is sketched by the solid black arrows in Fig. 11.6.

Thus, at low latitudes, more solar radiation is absorbed than leaves as IR, causing net warming. At high latitudes, the opposite is true: IR radiative losses exceed solar heating, causing net cooling. This differential heating drives the global circulation.

The general circulation can’t instantly eliminate all the global north-south temperature differences. What remains is a meridional temperature gradient — the focus of the next subsection.

11.3.1. North-South Temperature Gradient

To create a first-order toy model, neglect monthly variations, monsoonal variations and mountains. Instead, focus on surface temperatures averaged around separate latitude belts and over one year. Those latitude belts near the equator are warmer, and those near the poles are colder (Fig. 11.8a). One equation that roughly approximates the variation of zonally-averaged surface temperature T with latitude ϕ is:

$$T \approx a + b \cdot \left[\cos^3 \phi \cdot \left(1 + \frac{3}{2} \cdot \sin^2 \phi \right) \right] \quad (11.1)$$

where $a \approx -12^\circ\text{C}$ is an offset and $b \approx 40^\circ\text{C}$ is a temperature difference between equator and pole.

The equation above applies only to the surface. At higher altitudes the north-south temperature difference is smaller, and even becomes negative in the stratosphere (i.e., warm over the poles and cold over the tropics). To account for this altitude variation, b cannot be a constant. Instead, use:

$$b \approx b_1 \cdot \left(1 - \frac{z}{z_T} \right) \quad (11.2)$$

where average tropospheric depth is $z_T \approx 11 \text{ km}$, parameter $b_1 = 40^\circ\text{C}$, and z is height above the surface.

A similarly crude but useful generalization of parameter a can be made so that it too changes with altitude z above sea level:

$$a \approx a_1 - \gamma \cdot z \quad (11.3)$$

where $a_1 = -12^\circ\text{C}$ and $\gamma = 3.14 \text{ }^\circ\text{C km}^{-1}$.

In Fig. 11.8a, the temperature curve looks like a flattened cosine wave. The flattened curve indicates somewhat uniformly warm temperatures between $\pm 30^\circ$ latitude, caused the strong mixing and heat transport by the Hadley circulations.

With uniform tropical temperatures, the remaining change to colder temperature is pushed to the mid-latitude belts. The slope of the Fig. 11.8a curve is plotted in Fig. 11.8b. This slope is the north-south (**meridional**) temperature gradient:

$$\frac{\Delta T}{\Delta y} \approx -b \cdot c \cdot \cos^2 \phi \cdot \sin^3 \phi \quad (11.4)$$

where y is distance in the north-south direction, $c = 1.18 \times 10^{-3} \text{ km}^{-1}$ is a constant valid at all heights, and b is given by eq. (11.2) which causes the gradient to change sign at higher altitudes (e.g., at $z = 15 \text{ km}$).

Because the meridional temperature gradient results from the interplay of differential radiative heating and advection by the global circulation, let us now look at radiative forcings in more detail.

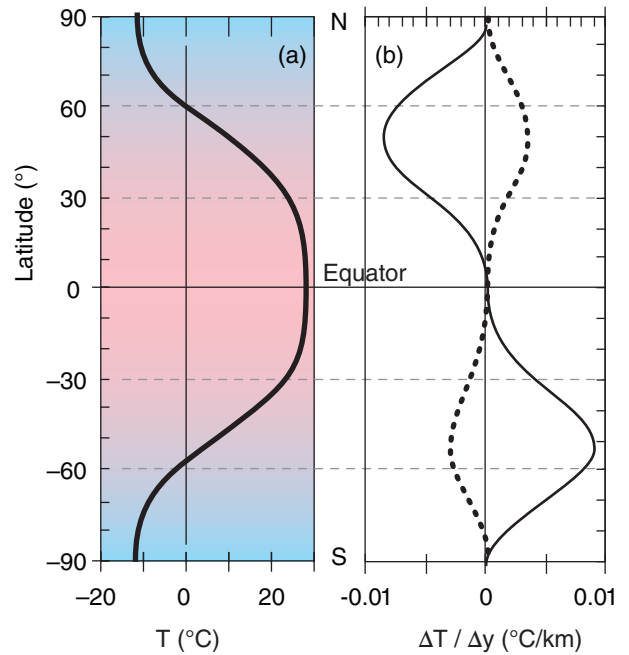


Figure 11.8
Idealized variation of annual-average temperature (a) and meridional temperature gradient (b) with latitude, averaged around latitude belts (i.e., zonal averages). Solid curve represents Earth's surface (= sea-level because the toy model neglects terrain) and dotted curve is for 15 km altitude above sea level.

Sample Application

What is the value of annual zonal average temperature and meridional temperature gradient at 50°S latitude for the surface and for $z = 15 \text{ km}$.

Find the Answer

Given: $\phi = -50^\circ$, (a) $z = 0$ (surface), and (b) $z = 15 \text{ km}$
Find: $T_{sfc} = ? \text{ }^\circ\text{C}$, $\Delta T/\Delta y = ? \text{ }^\circ\text{C km}^{-1}$

a) $z = 0$. Apply eq. (11.2): $b = (40^\circ\text{C}) \cdot (1 - 0) = 40^\circ\text{C}$.
Apply eq. (11.3): $a = (-12^\circ\text{C}) - 0^\circ\text{C} = -12^\circ\text{C}$.
Apply eq. (11.1):
 $T_o \approx -12^\circ\text{C} + (40^\circ\text{C}) \cdot \left[\cos^3(-50^\circ) \cdot \left(1 + \frac{3}{2} \cdot \sin^2(-50^\circ) \right) \right] = \underline{7.97 \text{ }^\circ\text{C}}$

Apply eq. (11.4):
 $\frac{\Delta T}{\Delta y} \approx -(40^\circ\text{C}) \cdot (1.18 \times 10^{-3}) \cdot \cos^2(-50^\circ) \cdot \sin^3(-50^\circ) = \underline{0.0087 \text{ }^\circ\text{C km}^{-1}}$

b) $z = 15 \text{ km}$.
Apply eq. (11.2): $b = (40^\circ\text{C}) \cdot [1 - (15/11)] = -14.55^\circ\text{C}$.
Apply (11.3): $a = (-12^\circ\text{C}) - (3.14^\circ\text{C/km}) \cdot (15 \text{ km}) = -59.1^\circ\text{C}$.
Apply eq. (11.1):
 $T_{15 \text{ km}} \approx -59.1^\circ\text{C} - 14.6^\circ\text{C} \cdot \left[\cos^3(-50^\circ) \cdot \left(1 + \frac{3}{2} \cdot \sin^2(-50^\circ) \right) \right] = \underline{-66.4 \text{ }^\circ\text{C}}$

Apply eq. (11.4) at $z = 15 \text{ km}$:
 $\frac{\Delta T}{\Delta y} \approx +(14.55^\circ\text{C}) \cdot (1.18 \times 10^{-3}) \cdot \cos^2(-50^\circ) \cdot \sin^3(-50^\circ) = \underline{-0.0032 \text{ }^\circ\text{C km}^{-1}}$

Check: Phys. & units reasonable. Agrees with Fig. 11.8 for Southern Hemisphere.

Exposition: Cold at $z = 15 \text{ km}$ even though warm at $z = 0$. Gradient signs would be opposite in N. Hem.

HIGHER MATH • Derivation of the North-South Temperature Gradient

The goal is to find $\partial T/\partial y$ for the toy model.

a) First, expand the derivative: $\frac{\partial T}{\partial y} = \frac{\partial T}{\partial \phi} \cdot \frac{\partial \phi}{\partial y}$ (a)

We will look at factors $\partial T/\partial \phi$ and $\partial \phi/\partial y$ separately:

b) Factor $\partial \phi/\partial y$ describes the meridional gradient of latitude. Consider a circumference of the Earth that passes through both poles. The total latitude change around this circle is $\Delta \phi = 2\pi$ radians. The total circumference of this circle is $\Delta y = 2\pi R$ for average Earth radius of $R = 6371$ km. Hence:

$$\frac{\partial \phi}{\partial y} = \frac{\Delta \phi}{\Delta y} = \frac{2\pi}{2\pi \cdot R} = \frac{1}{R} \quad (b)$$

c) For factor $\partial T/\partial \phi$, start with eq. (11.1) for the toy model:

$$T \approx a + b \cdot \left[\cos^3 \phi \cdot \left(1 + \frac{3}{2} \cdot \sin^2 \phi \right) \right] \quad (11.1)$$

and take its derivative vs. latitude: $\frac{\partial T}{\partial \phi} = b \cdot \left(\frac{3}{2} \right) \cdot$

$$\left[(2 \sin \phi \cdot \cos \phi) \cos^3 \phi - 3 \left(\frac{2}{3} + \sin^2 \phi \right) \cos^2 \phi \cdot \sin \phi \right]$$

Next, take the common term ($\sin \phi \cdot \cos^2 \phi$) out of []:

$$\frac{\partial T}{\partial \phi} = b \left(\frac{3}{2} \right) \sin \phi \cdot \cos^2 \phi \cdot \left[2 \cos^2 \phi - 2 - 3 \sin^2 \phi \right]$$

Use the trig. identity: $\cos^2 \phi = 1 - \sin^2 \phi$.
Hence: $2 \cos^2 \phi = 2 - 2 \sin^2 \phi$. Substituting this in into the previous full-line equation gives:

$$\frac{\partial T}{\partial \phi} = b \left(\frac{3}{2} \right) \sin \phi \cdot \cos^2 \phi \cdot \left[-5 \sin^2 \phi \right] \quad (c)$$

d) Plug equations (b) and (c) back into eq. (a):

$$\frac{\partial T}{\partial y} = -b \cdot \left(\frac{15}{2} \cdot \frac{1}{R} \right) \cdot \sin^3 \phi \cdot \cos^2 \phi \quad (d)$$

Define: $c = \left(\frac{15}{2} \cdot \frac{1}{R} \right) = \left(\frac{15}{2} \cdot \frac{1}{6371 \text{ km}} \right) = 1.177 \times 10^{-3} \text{ km}^{-1}$

Thus, the final answer is:

$$\frac{\Delta T}{\Delta y} \approx \frac{\partial T}{\partial y} = -b \cdot c \cdot \sin^3 \phi \cdot \cos^2 \phi \quad (11.4)$$

Check: Fig. 11.8 shows the curves that were calculated from eqs. (11.1) and (11.4). The fact that the sign and shape of the curve for $\Delta T/\Delta y$ is consistent with the curve for $T(y)$ suggests the answer is reasonable.

Alert: Eqs. (11.4) and (11.1) are based on a highly idealized “toy model” of the real atmosphere. They were designed only to illustrate first-order effects.

11.3.2. Global Radiation Budgets

11.3.2.1. Incoming Solar Radiation

Because of the tilt of the Earth’s axis and the change of seasons, the actual flux of incoming solar radiation is not as simple as was sketched in Fig. 11.6. But this complication was already discussed in the Solar & Infrared Radiation chapter, where we saw an equation to calculate the incoming solar radiation (**insolation**) as a function of latitude and day. The resulting insolation figure is reproduced below (Fig. 11.9a).

If you take the spreadsheet data from the Solar & Infrared Radiation chapter that was used to make this figure, and average rows of data (i.e., average over all months for any one latitude), you can find the annual average insolation E_{insol} for each latitude (Fig. 11.9b). Insolation in polar regions is not small.

The curve in Fig. 11.9b is simple, and in the spirit of a toy model can be nicely approximated by:

$$E_{insol} = E_0 + E_1 \cdot \cos(2\phi) \quad (11.5)$$

where the empirical parameters are $E_0 = 298 \text{ W m}^{-2}$, $E_1 = 123 \text{ W m}^{-2}$, and ϕ is latitude. This curve and the data points it approximates are plotted in Fig. 11.10.

But not all the radiation incident on the top of the atmosphere is absorbed by the Earth-ocean-atmosphere system. Some is reflected back into space from snow and ice on the surface, from the oceans, and from light-colored land. Some is reflected from cloud top. Some is scattered off of air molecules.

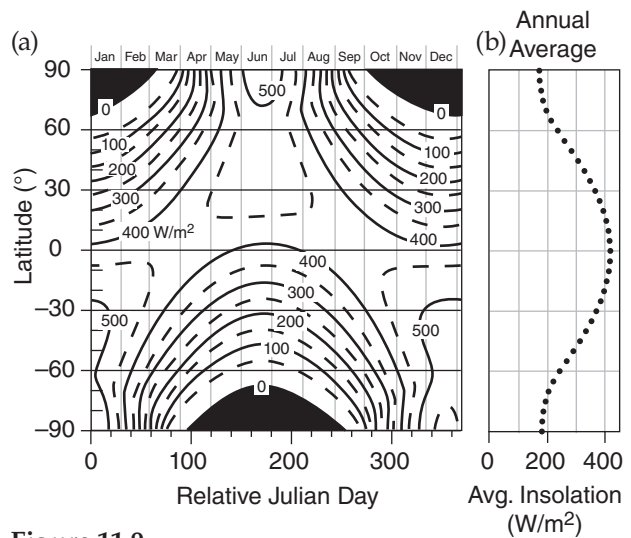


Figure 11.9
(a) Solar radiation (W m^{-2}) incident on the top of the atmosphere for different latitudes and months (copied from the Solar & Infrared Radiation chapter). The slight asymmetry about the equator is because Earth’s orbit is closer to the sun during S. Hemisphere summer. (b) Meridional variation of insolation, found by averaging the data from the left figure over all months for each separate latitude (i.e., averages for each row of data).

The amount of insolation that is NOT absorbed is surprisingly constant with latitude at about $E_2 \approx 110 \text{ W m}^{-2}$. Thus, the amount that IS absorbed is:

$$E_{in} = E_{insol} - E_2 \quad (11.6)$$

where E_{in} is the incoming flux (W m^{-2}) of solar radiation absorbed into the Earth-ocean-atmosphere system (Fig. 11.10). This absorbed radiation causes heating.

11.3.2.2. Outgoing Terrestrial Radiation

As you learned in the Satellites & Radar chapter, infrared radiation emission and absorption in the atmosphere are very complex. At some wavelengths the atmosphere is mostly transparent, while at others it is mostly opaque. Thus, some of the IR emissions to space are from the Earth’s surface, some from cloud top, and some from air at middle altitudes in the atmosphere.

In the spirit of a toy model, suppose that the net IR emissions are characteristic of the absolute temperature T_m near the middle of the troposphere (at about $z_m = 5.5 \text{ km}$). Approximate the outbound flux of radiation E_{out} (averaged over a year and averaged around latitude belts) by the Stefan-Boltzmann law (see the Solar & Infrared Radiation chapter):

$$E_{out} \approx \epsilon \cdot \sigma_{SB} \cdot T_m^4 \quad (11.7)$$

where the effective emissivity is $\epsilon \approx 0.9$ (see the Climate chapter), and the Stefan-Boltzmann constant is $\sigma_{SB} = 5.67 \times 10^{-8} \text{ W} \cdot \text{m}^{-2} \cdot \text{K}^{-4}$. When you use $z = z_m = 5.5 \text{ km}$ in eqs. (11.1 - 11.3) to get T_m vs. latitude for use in eq. (11.7), the result is E_{out} vs. ϕ , as plotted in Fig. 11.10.

11.3.2.3. Net Radiation

For an air column over any square meter of the Earth’s surface, the radiative input minus output gives the net radiative flux:

$$E_{net} = E_{in} - E_{out} \quad (11.8)$$

which is plotted in Fig. 11.10 for our toy model.

Sample Application

Estimate the annual average solar energy absorbed at the latitude of the Eiffel Tower in Paris, France.

Find the Answer

Given: $\phi = 48.8590^\circ$ (at the Eiffel tower)

Find: $E_{in} = ? \text{ W m}^{-2}$

Use eq. (11.5):

$$E_{insol} = (298 \text{ W m}^{-2}) + (123 \text{ W m}^{-2}) \cdot \cos(2 \cdot 48.8590^\circ) \\ = (298 \text{ W m}^{-2}) - (16.5 \text{ W m}^{-2}) = 281.5 \text{ W m}^{-2}$$

Use eq. (11.6):

$$E_{in} = 281.5 \text{ W m}^{-2} - 110.0 \text{ W m}^{-2} = \underline{171.5 \text{ W m}^{-2}}$$

Check: Units OK. Agrees with Fig. 11.10.

Exposition: The actual annual average E_{in} at the Eiffel Tower would probably differ from this zonal avg.

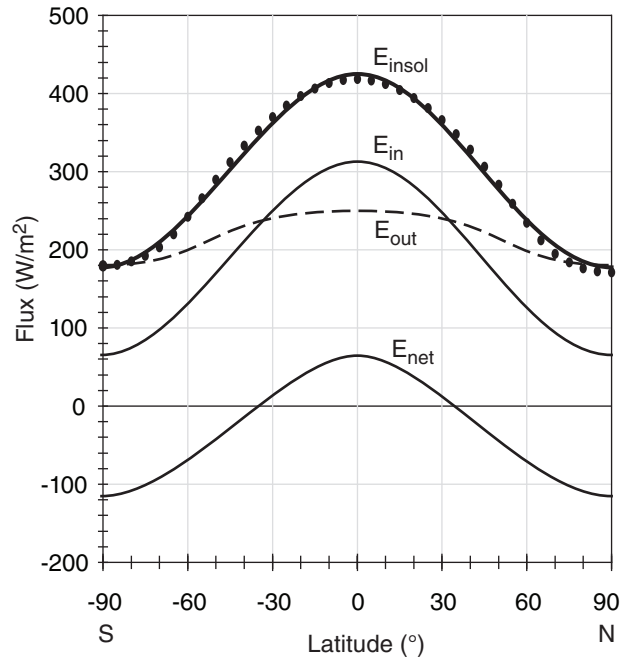


Figure 11.10

Data points are insolation vs. latitude from Fig. 11.9b. Eq. 11.5 approximates this insolation E_{insol} (thick black line). E_{in} is the solar radiation that is absorbed (thin solid line, from eq. 11.6). E_{out} is outgoing terrestrial (IR) radiation (dashed; from eq. 11.7). Net flux $E_{net} = E_{in} - E_{out}$. Positive E_{net} causes heating; negative causes cooling.

Sample Application. What is E_{net} at the Eiffel Tower latitude?

Find the Answer. Given: $\phi = 48.8590^\circ, z = 5.5 \text{ km}, E_{in} = 171.5 \text{ W m}^{-2}$ from previous Sample Application

Find: $E_{net} = ? \text{ W m}^{-2}$

Apply eq. (11.2): $b = (40^\circ\text{C}) \cdot [1 - (5.5 \text{ km}/11 \text{ km})] = 20^\circ\text{C}$

Apply eq. (11.3): $a = (-12^\circ\text{C}) - (3.14^\circ\text{C km}^{-1}) \cdot (5.5 \text{ km}) = -29.27^\circ\text{C}$

Apply eq. (11.1): $T_m = -18.73^\circ\text{C} = 254.5 \text{ K}$

Apply eq. (11.7): $E_{out} = (0.9) \cdot (5.67 \times 10^{-8} \text{ W} \cdot \text{m}^{-2} \cdot \text{K}^{-4}) \cdot (254.5 \text{ K})^4 = 213.8 \text{ W m}^{-2}$

Apply eq. (11.8): $E_{net} = (171.5 \text{ W m}^{-2}) - (213.8 \text{ W m}^{-2}) = \underline{-42.3 \text{ W m}^{-2}}$

Check: Units OK. Agrees with Fig. 11.10

Exposition: The net radiative heat loss at Paris latitude must be compensated by winds blowing heat in.

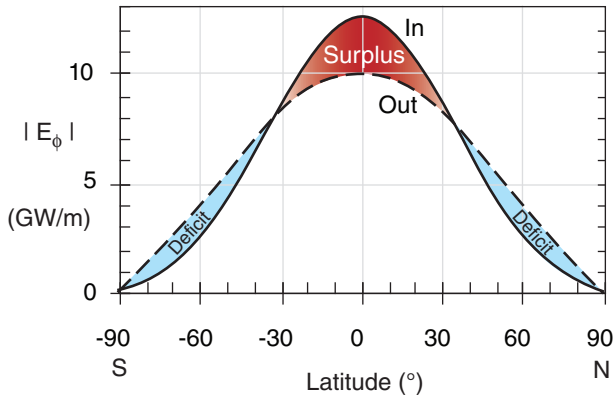


Figure 11.11
Zonally-integrated radiative forcings for absorbed incoming solar radiation (solid line) and emitted net outgoing terrestrial (IR) radiation (dashed line). The surplus balances the deficit.

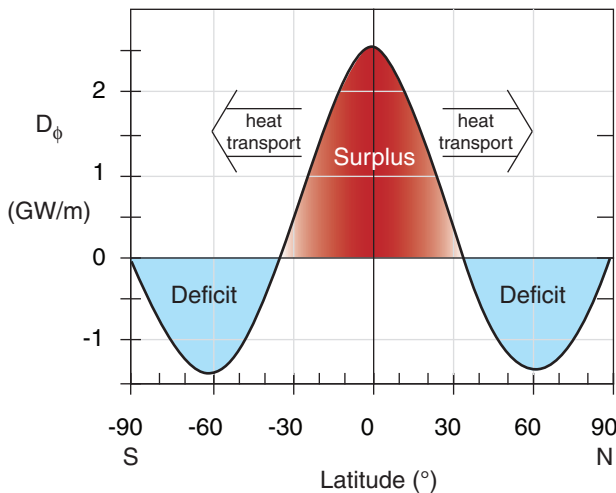


Figure 11.12
Net (incoming minus outgoing) zonally-integrated radiative forcings on the Earth. Surplus balances deficits. This differential heating imposed on the Earth must be compensated by heat transport by the global circulation; otherwise, the tropics would keep getting hotter and the polar regions colder.

Sample Application
From the previous Sample Application, find the zonally-integrated differential heating at $\phi = 48.859^\circ$.

Find the Answer
Given: $E_{net} = -42.3 \text{ W m}^{-2}$, $\phi = 48.859^\circ$ at Eiffel Tower
Find: $D_\phi = ? \text{ GW m}^{-1}$

Combine eqs. (11.8-11.10): $D_\phi = 2\pi R_{Earth} \cdot \cos(\phi) \cdot E_{net}$
 $= 2(3.14159) \cdot (6.357 \times 10^6 \text{ m}) \cdot \cos(48.859^\circ) \cdot (-42.3 \text{ W m}^{-2})$
 $= -1.11 \times 10^9 \text{ W m}^{-1} = \underline{\underline{-1.11 \text{ GW m}^{-1}}}$

Check: Units OK. Agrees with Fig. 11.12.
Exposition: Net radiative heat loss at this latitude is compensated by warm Gulf stream and warm winds.

11.3.3. Radiative Forcing by Latitude Belt

Do you notice anything unreasonable about E_{net} in Fig. 11.10? It appears that the negative area under the curve is much greater than the positive area, which would cause the Earth to get colder and colder — an effect that is not observed.

Don't despair. Eq. (11.8) is correct, but we must remember that the circumference $[2\pi \cdot R_{Earth} \cdot \cos(\phi)]$ of a parallel (a constant latitude circle) is smaller near the poles than near the equator. ϕ is latitude and the average Earth radius R_{Earth} is 6371 km.

The solution is to multiply eqs. (11.6 - 11.8) by the circumference of a parallel. The result

$$E_\phi = 2\pi \cdot R_{Earth} \cdot \cos(\phi) \cdot E \quad (11.9)$$

can be applied for $E = E_{in}$, or $E = E_{out}$, or $E = E_{net}$. This converts from E in units of W m^{-2} to E_ϕ in units of W m^{-1} , where the distance is north-south distance. You can interpret E_ϕ as the power being transferred to/from a one-meter-wide sidewalk that encircles the Earth along a parallel.

Figs. (11.11) and (11.12) show the resulting incoming, outgoing, and net radiative forcings vs. latitude. At most latitudes there is nonzero net radiation. We can define E_{net} as **differential heating** D_ϕ :

$$D_\phi = E_{\phi \text{ net}} = E_{\phi \text{ in}} - E_{\phi \text{ out}} \quad (11.10)$$

Our despair is now quelled, because the surplus and deficit areas in Figs. 11.11 and 11.12 are almost exactly equal in magnitude to each other. Hence, we anticipate that Earth's climate should be relatively steady (neglecting global warming for now).

11.3.4. General Circulation Heat Transport

Nonetheless, the imbalance of net radiation between equator and poles in Fig. 11.12 drives atmospheric and oceanic circulations. These circulations act to undo the imbalance by removing the excess heat from the equator and depositing it near the poles (as per Le Chatelier's Principle). First, we can use the radiative differential heating to find how much global-circulation heat transport is needed. Then, we can examine the actual heat transport by atmospheric and oceanic circulations.

11.3.4.1. The Amount of Transport Required

Meridional transport at each pole is zero, because the pole is a singularity where all meridians converge. If we sum D_ϕ from Fig. 11.12 over all latitude belts from the North Pole to any other latitude ϕ , we can find the total transport Tr required for the global circulation to compensate all the radiative imbalances north of that latitude:

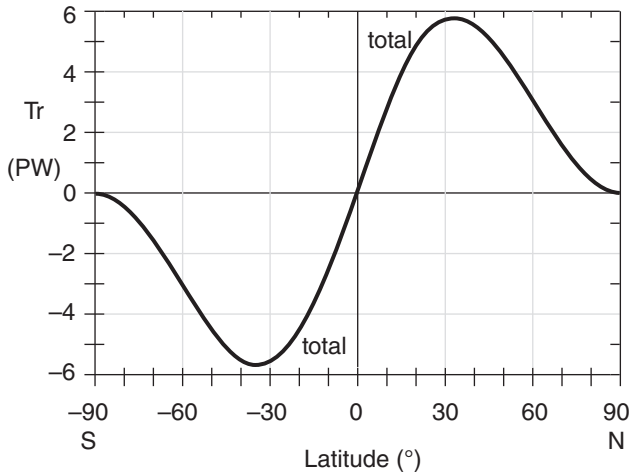


Figure 11.13
 Required heat transport Tr by the global circulation to compensate radiative differential heating, based on a simple “toy model”. Agrees very well with actual achieved transport in Fig. 11.14.

$$Tr(\phi) = \sum_{\phi_0=90^\circ}^{\phi} (-D_\phi) \cdot \Delta y \quad (11.11)$$

where the width of any latitude belt is Δy .
 [Meridional distance Δy is related to latitude change $\Delta\phi$ by: $\Delta y(\text{km}) = (111 \text{ km}/^\circ) \cdot \Delta\phi (^\circ)$.]
 The resulting “needed transport” is shown in Fig. 11.13, based on the simple “toy model” temperature and radiation curves of the past few sections. The magnitude of this curve peaks at about 5.6 PW (1 petawatt equals 10^{15} W) at latitudes of about 35° North and South (positive Tr means northward transport).

11.3.4.2. Transport Achieved

Satellite observations of radiation to and from the Earth, estimates of heat fluxes to/from the ocean based on satellite observations of sea-surface temperature, and in-situ measurements of the atmosphere provide some of the transport data needed. Numerical forecast models are then used to tie the observations together and fill in the missing pieces. The resulting estimate of heat transport achieved by the atmosphere and ocean is plotted in Fig. 11.14.

Ocean currents dominate the total heat transport only at latitudes 0 to 17°, and remain important up to latitudes of $\pm 40^\circ$. Asymmetry of the ocean curve across the equator is due to the different ocean basin shapes and currents. In the atmosphere, the Hadley circulation is a dominant contributor in the tropics and subtropics, while the Rossby waves dominate atmospheric transport at mid-latitudes.

Knowing that global circulations undo the heating imbalance raises another question. How does the differential heating in the atmosphere drive the winds in those circulations? That is the subject of the next three sections.

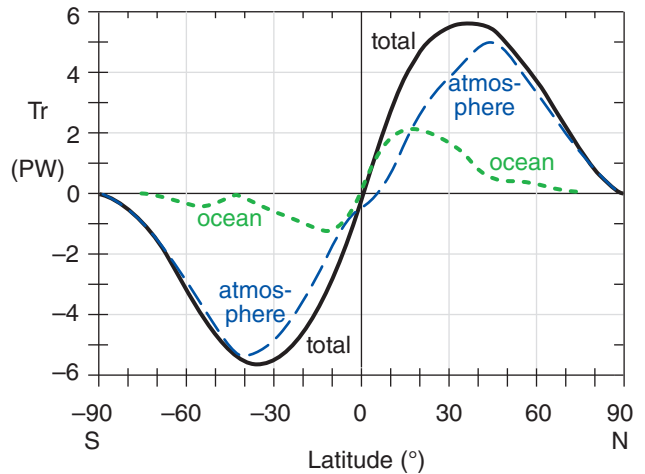


Figure 11.14
 Meridional heat transports: Satellite-observed total (solid line) & ocean estimates (dotted). Atmospheric (dashed) is found as a residual. 1 PW = 1 petawatt = 10^{15} W. [Data from K. E. Trenberth and J. M. Caron, 2001: “J. Climate”, **14**, 3433-3443.]

Sample Application

What total heat transports by the atmosphere and ocean circulations are needed at 50°N latitude to compensate for all the net radiative cooling between that latitude and the North Pole? The differential heating as a function of latitude is given in the following table (based on the toy model):

Lat (°)	D_ϕ (GW m ⁻¹)	Lat (°)	D_ϕ (GW m ⁻¹)
90	0	65	-1.380
85	-0.396	60	-1.403
80	-0.755	55	-1.331
75	-1.049	50	-1.164
70	-1.261	45	-0.905

Find the Answer

Given: $\phi = 50^\circ\text{N}$. D_ϕ data in table above.
 Find: $Tr = ?$ PW

Use eq. (11.11). Use sidewalks (latitude belts) each of width $\Delta\phi = 5^\circ$. Thus, Δy (m) = $(111,000 \text{ m}/^\circ) \cdot (5^\circ) = 555,000$ m is the sidewalk width. If one sidewalk spans 85 - 90°, and the next spans 80 - 85° etc, then the values in the table above give D_ϕ along the edges of the sidewalk, not along the middle. A better approximation is to average the D_ϕ values from each edge to get a value representative of the whole sidewalk. Using a bit of algebra, this works out to:

$$Tr = -(555000 \text{ m}) \cdot [(0.5) \cdot 0.0 - 0.396 - 0.755 - 1.049 - 1.261 - 1.38 - 1.403 - 1.331 - (0.5) \cdot 1.164] \text{ (GW m}^{-1}\text{)}$$

$$Tr = (555000 \text{ m}) \cdot [8.157 \text{ GW m}^{-1}] = \mathbf{4.527 \text{ PW}}$$

Check: Units OK (10^6 GW = 1 PW). Agrees with Fig. 11.14. **Exposition:** This northward heat transport warms all latitudes north of 50°N, not just one sidewalk. The warming per sidewalk is $\Delta Tr/\Delta\phi$.

A SCIENTIFIC PERSPECTIVE • Residuals

If something you cannot measure contributes to things you can measure, then you can estimate the unknown as the **residual** (i.e., difference) from all the knowns. This is a valid scientific approach. It was used in Fig. 11.14 to estimate the atmospheric portion of global heat transport.

CAUTION: When using this approach, your residual not only includes the desired signal, but it also includes the sums of all the errors from the items you measured. These errors can easily accumulate to cause a “noise” that is larger than the signal you are trying to estimate. For this reason, **error estimation** and **error propagation** (see Appendix A) should always be done when using the method of residuals.

11.4. PRESSURE PROFILES

The following fundamental concepts can help you understand how the global circulation works:

- non-hydrostatic pressure couplets caused by horizontal winds and vertical buoyancy,
- hydrostatic thermal circulations,
- geostrophic adjustment, and
- the thermal wind.

The first two concepts are discussed in this section. The last two are discussed in subsequent sections.

11.4.1. Non-hydrostatic Pressure Couplets

Consider a background reference environment with no vertical acceleration (i.e., **hydrostatic**). Namely, the pressure-decrease with height causes an upward pressure-gradient force that exactly balances the downward pull of gravity, causing zero net vertical force on the air (see Fig. 1.12 and eq. 1.25).

Next, suppose that immersed in this environment is a column of air that might experience a different pressure decrease (Fig. 11.15); i.e., **non-hydrostatic pressures**. At any height, let $p' = P_{column} - P_{hydrostatic}$ be the deviation of the actual pressure in the column from the theoretical hydrostatic pressure in the environment. Often a positive p' in one part of the atmospheric column is associated with negative p' elsewhere. Taken together, the positive and negative p' 's form a **pressure couplet**.

Non-hydrostatic p' profiles are often associated with non-hydrostatic vertical motions through Newton's second law. These non-hydrostatic motions can be driven by horizontal convergence and divergence, or by buoyancy (a vertical force). These two effects create opposite pressure couplets, even though both can be associated with upward motion, as explained next.

11.4.1.1. Horizontal Convergence/Divergence

If external forcings cause air near the ground to converge horizontally, then air molecules accumulate. As density ρ increases according to eq. (10.60), the ideal gas law tells us that p' will also become positive (Fig. 11.16a). Non-zero p' implies that a pressure gradient exists, which will drive winds.

Positive p' does two things: it (1) decelerates the air that was converging horizontally, and (2) accelerates air vertically in the column. Thus, the pressure perturbation causes **mass continuity** (horizontal inflow near the ground balances vertical outflow).

Similarly, an externally imposed horizontal divergence at the top of the troposphere would lower the air density and cause negative p' , which would also accelerate air in the column upward. Hence, we

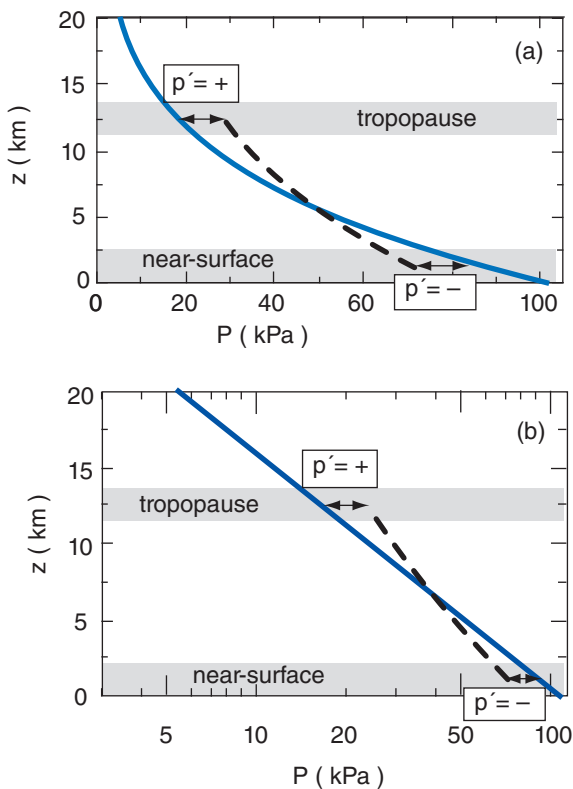


Figure 11.15 Background hydrostatic pressure (solid line), and non-hydrostatic column of air (dashed line) with pressure perturbation p' that deviates from the hydrostatic pressure $P_{hydrostatic}$ at most heights z . In this example, even though p' is positive (+) near the tropopause, the total pressure in the column ($P_{column} = P_{hydrostatic} + p'$) at the tropopause is still less than the surface pressure. The same curve is plotted as (a) linear and as (b) semilog.

expect upward motion ($W = \text{positive}$) to be driven by a p' couplet, as shown in Fig. 11.16a.

11.4.1.2. Buoyant Forcings

For a different scenario, suppose air in a column is positively buoyant, such as in a thunderstorm where water-vapor condensation releases lots of latent heat. This vertical buoyant force creates upward motion (i.e., warm air rises, as in Fig. 11.16b).

As air in the thunderstorm column moves away from the ground, it removes air molecules and lowers the density and the pressure; hence, p' is negative near the ground. This suction under the updraft causes air near the ground to horizontally converge, thereby conserving mass.

Conversely, at the top of the troposphere where the thunderstorm updraft encounters the even warmer environmental air in the stratosphere, the upward motion rapidly decelerates, causing air molecules to accumulate, making p' positive. This pressure perturbation drives air to diverge horizontally near the tropopause, causing the outflow in the anvil-shaped tops of thunderstorms.

The resulting pressure-perturbation p' couplet in Fig. 11.16b is opposite that in Fig. 11.16a, yet both are associated with upward vertical motion. The reason for this pressure-couplet difference is the difference in driving mechanism: imposed horizontal convergence/divergence vs. imposed vertical buoyancy.

Similar arguments can be made for downward motions. For either upward or downward motions, the pressure couplets that form depend on the type of forcing. We will use this process to help explain the pressure patterns at the top and bottom of the troposphere.

11.4.2. Hydrostatic Thermal Circulations

Cold columns of air tend to have high surface pressures, while warm columns have low surface pressures. Figs. 11.17 illustrate how this happens.

Consider initial conditions (Fig. 11.17i) of two equal columns of air at the same temperature and with the same number of air molecules in each column. Since pressure is related to the mass of air above, this means that both columns A and B have the same initial pressure (100 kPa) at the surface.

Next, suppose that some process heats one column relative to the other (Fig. 11.17ii). Perhaps condensation in a thunderstorm cloud causes latent heating of column B, or infrared radiation cools column A. After both columns have finished expanding or contracting due to the temperature change, they will reach new hydrostatic equilibria for their respective temperatures.

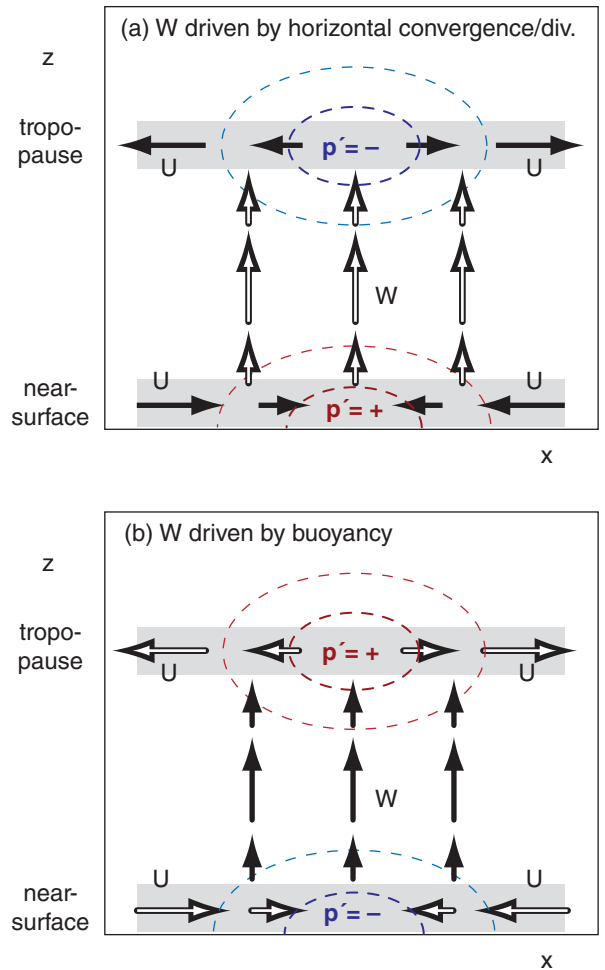


Figure 11.16

(a) Vertical motions driven by pressure gradients caused by horizontal convergence or divergence. (b) Vertical motions driven by buoyancy. In both figures, black arrows indicate the cause (the driving force), and white arrows are the effect (the response). p' is the pressure perturbation (deviation from hydrostatic), and thin dashed lines are isobars of p' . U and W are horizontal and vertical velocities. In both figures, the responding flow (white arrows) is driven down the pressure-perturbation gradient, away from positive p' and toward negative p' .

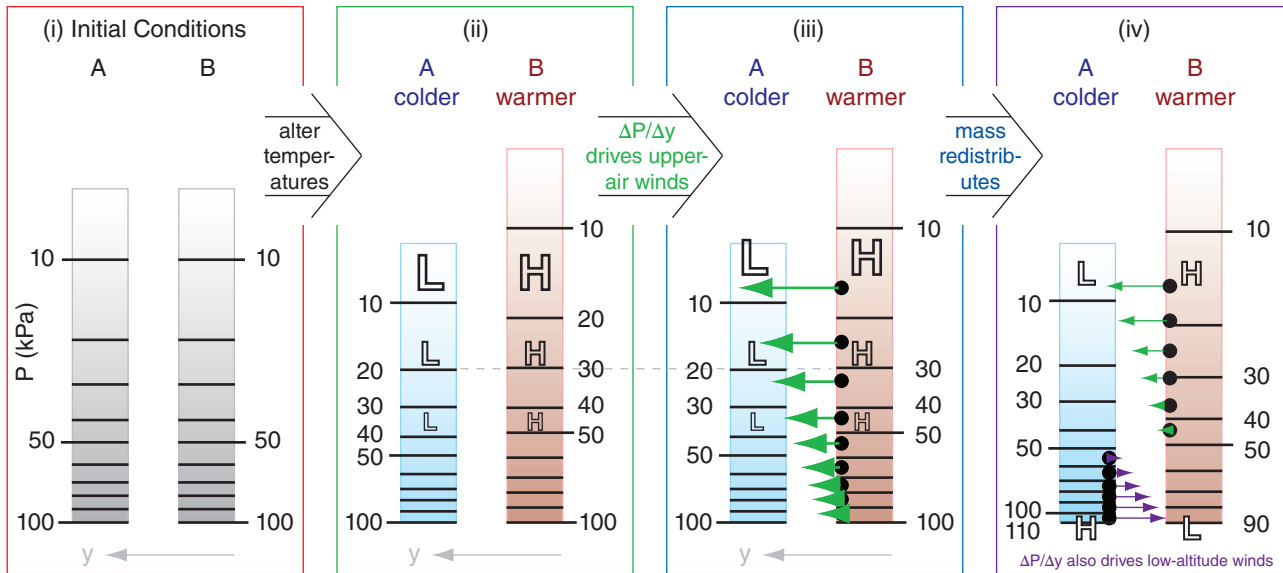


Figure 11.17

Formation of a thermal circulation. The response of two columns of air that are heated differently is that the warmer air column develops a low pressure perturbation at the surface and a high pressure perturbation aloft. Response of the cold column is the opposite. Notation: H = high pressure perturbation (i.e., relative to the average pressure at that altitude). L = low pressure perturbation (relative to the average pressure at that same altitude). Black dots represent air parcels. Thin arrows are winds (i.e., movement of air parcels).

The hypsometric equation (see Chapter 1) says that pressure decreases more rapidly with height in cold air than in warm air. Thus, although both columns have the same surface pressure because they contain the same number of molecules, the higher you go above the surface, the greater is the pressure difference between warm and cold air. In Fig. 11.17ii, the printed size of the “H” and “L” indicate the relative magnitudes of the high- and low-pressure perturbations p' .

The horizontal pressure gradient $\Delta P/\Delta y$ aloft between the warm and cold air columns drives horizontal winds from high toward low pressure (Fig. 11.17iii). Since winds are the movement of air molecules, this means that molecules leave the regions of high pressure-perturbation and accumulate in the regions of low. Namely, they leave the warm column, and move into the cold column.

Since there are now more molecules (i.e., more mass) in the cold column, it means that the surface pressure must be greater (H) in the cold column (Fig. 11.17iv). Similarly, mass lost from the warm column results in lower (L) surface pressure. This is called a **thermal low**.

A result (Fig. 11.17iv) is that, near the surface, high pressure in the cold air drives winds toward the low pressure in warm air. Aloft, high pressure-perturbation in the warm air drives winds towards low pressure-perturbation in the cold air. The resulting **thermal circulation** causes each column to

gain as many air molecules as they lose; hence, they are in mass equilibrium.

This equilibrium circulation also transports heat. Air from the warm air column mixes into the cold column, and vice versa. This intermixing reduces the temperature contrast between the two columns, causing the corresponding equilibrium circulations to weaken. Continued destabilization (more latent heating or radiative cooling) would be needed to maintain the circulation.

The circulations and mass exchange described above can be realized at the equator. At other latitudes, the exchange of mass is often slower (near the surface) or incomplete (aloft) because Coriolis force turns the winds to some angle away from the pressure-gradient direction. This added complication, due to geostrophic wind and geostrophic adjustment, is described next.

11.5. GEOSTROPHIC WIND & GEOSTROPHIC ADJUSTMENT

11.5.1. Ageostrophic Winds at the Equator

Air at the equator can move directly from high (H) to low (L) pressure (Fig. 11.18 - center part) under the influence of pressure-gradient force. Zero Coriolis force at the equator implies infinite geostrophic winds. But actual winds have finite speed, and are thus **ageostrophic** (not geostrophic).

Because such flows can happen very easily and quickly, equatorial air tends to quickly flow out of highs into lows, causing the pressure centers to neutralize each other. Indeed, weather maps at the equator show very little pressure variations zonally. One exception is at continent-ocean boundaries, where continental-scale differential heating can continually regenerate pressure gradients to compensate the pressure-equalizing action of the wind. Thus, very small pressure gradients can cause continental-scale (5000 km) monsoon circulations near the equator. Tropical forecasters focus on winds, not pressure.

If the large-scale pressure is uniform in the horizontal near the equator (away from monsoon circulations), then the horizontal pressure gradients disappear. With no horizontal pressure-gradient force, no large-scale winds can be driven there. However, winds can exist at the equator due to inertia — if the winds were first created geostrophically at nonzero latitude and then coast across the equator.

But at most other places on Earth, Coriolis force deflects the air and causes the wind to approach geostrophic or gradient values (see the Forces & Winds chapter). Non-accelerating geostrophic and gradient winds do not cross isobars, so they cannot transfer mass from highs to lows. Thus, significant pressure patterns (e.g., strong high and low centers, Fig. 11.18) can be maintained for long periods at mid-latitudes in the global circulation.

11.5.2. Definitions

A **temperature field** is a map showing how temperatures are spatially distributed. A **wind field** is a map showing how winds are distributed. A **mass field** represents how air mass is spatially distributed. But we don't routinely measure air mass.

In the first Chapter, we saw how pressure at any one altitude depends on (is a measure of) all the air mass above that altitude. So we can use the **pressure field** at a fixed altitude as a surrogate for the mass field. Similarly, the **height field** on a map of constant pressure is another surrogate.

But the temperature and mass fields are coupled via the hypsometric equation (see Chapter 1).

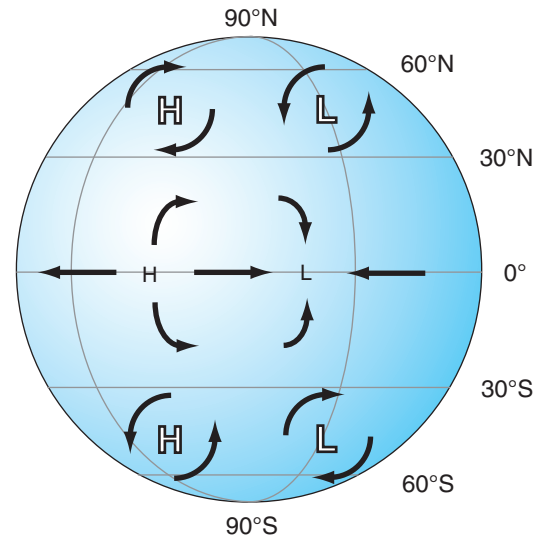


Figure 11.18

At the equator, winds flow directly from high (H) to low (L) pressure centers. At other latitudes, Coriolis force causes the winds to circulate around highs and lows. Smaller size font for H and L at the equator indicate weaker pressure gradients at that latitude.

A SCIENTIFIC PERSPECTIVE • The Scientific Method Revisited

"Like other exploratory processes, [the scientific method] can be resolved into a dialogue between fact and fancy, the actual and the possible; between what could be true and what is in fact the case. The purpose of scientific enquiry is not to compile an inventory of factual information, nor to build up a totalitarian world picture of Natural Laws in which every event that is not compulsory is forbidden. We should think of it rather as a logically articulated structure of justifiable beliefs about a Possible World — a story which we invent and criticize and modify as we go along, so that it ends by being, as nearly as we can make it, a story about real life."

- by Nobel Laureate Sir Peter Medawar (1982) *Pluto's Republic*. Oxford Univ. Press.

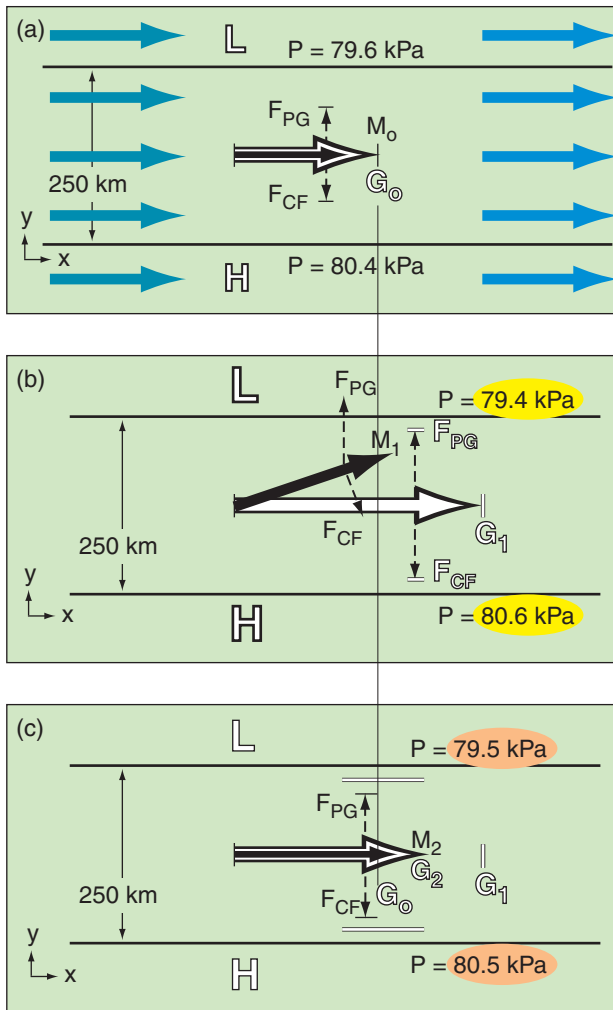


Figure 11.19
 Example of geostrophic adjustment in the N. Hemisphere (not at equator). (a) Initial conditions, with the actual wind M (thick black arrow) in equilibrium with (equal to) the theoretical geostrophic value G (white arrow with black outline). (b) Transition. (c) End result at a new equilibrium. Dashed lines indicate forces F . Each frame focuses on the region of disturbance. Note that both the wind AND the pressure gradient have adjusted.

Sample Application
 Find the internal Rossby radius of deformation in a standard atmosphere at 45°N .

Find the Answer
 Given: $\phi = 45^\circ$. Standard atmosphere from Chapter 1:
 $T(z = Z_T = 11 \text{ km}) = -56.5^\circ\text{C}$, $T(z = 0) = 15^\circ\text{C}$.
 Find: $\lambda_R = ? \text{ km}$

First, find $f_c = (1.458 \times 10^{-4} \text{ s}^{-1}) \cdot \sin(45^\circ) = 1.031 \times 10^{-4} \text{ s}^{-1}$
 Next, find the average temperature and temperature difference across the depth of the troposphere:
 $T_{avg} = 0.5 \cdot (-56.5 + 15.0)^\circ\text{C} = -20.8^\circ\text{C} = 252 \text{ K}$
 $\Delta T = (-56.5 - 15.0)^\circ\text{C} = -71.5^\circ\text{C}$ across $\Delta z = 11 \text{ km}$
 (continued on next page)

Namely, if the temperature changes in the horizontal (defined as a **baroclinic** atmosphere), then pressures at any fixed altitude must also change in the horizontal. Later in this chapter, we will also see how the wind and temperature fields are coupled (via the thermal wind relationship).

11.5.3. Geostrophic Adjustment - Part 1

The tendency of non-equatorial winds to approach geostrophic values (or gradient values for curved isobars) is a very strong process in the Earth’s atmosphere. If the actual winds are not in geostrophic balance with the pressure patterns, then both the winds and the pressure patterns tend to change to bring the winds back to geostrophic (another example of Le Chatelier’s Principle). **Geostrophic adjustment** is the name for this process.

Picture a wind field (grey arrows in Fig. 11.19a) initially in geostrophic equilibrium ($M_0 = G_0$) at altitude 2 km above sea level (thus, no drag on ground). We will focus on just one of those arrows (the black arrow in the center), but all the wind vectors will march together, performing the same maneuvers.

Next, suppose an external process increases the horizontal pressure gradient to the value shown in Fig. 11.19b, with the associated faster theoretical geostrophic wind speed G_1 . Inertia prevents instantaneous response of the actual wind M . During this transition, pressure-gradient force F_{PG} is greater than Coriolis force F_{CF} . This force imbalance turns the wind M_1 slightly toward low pressure and accelerates the air (Fig. 11.19b).

The component of wind M_1 from high to low pressure horizontally moves air molecules, weakening the pressure field and thereby reducing the theoretical geostrophic wind speed G_1 . Namely, **the wind field changed the mass (i.e., pressure) field**. Simultaneously the actual wind accelerates to M_2 . Thus, **the mass field also changed the wind field**. After both fields have adjusted, the result is $M_2 > M_0$ and $G_2 < G_1$, with $M_2 = G_2$. These changes are called **geostrophic adjustments**.

Define a “disturbance” as the region that was initially forced out of equilibrium. As you move further away from the disturbance, the amount of geostrophic adjustment diminished. The e-folding distance for this reduction is

$$\lambda_R = \frac{N_{BV} \cdot Z_T}{f_c} \quad \bullet(11.12)$$

where λ_R is known as the **internal Rossby deformation radius**. The Coriolis parameter is f_c , tropospheric depth is Z_T , and the Brunt-Väisälä frequency is N_{BV} (see eq. on page 372). λ_R is roughly 1300 km.

For a given wavelength λ of the initial disturbance, eq. (11.12) can be used as follows. For large

Sample Application (continuation)

Find the Brunt-Väisälä frequency (see the Atmos. Stability chapter). $N_{BV} = \sqrt{\frac{(9.8\text{m/s})}{252\text{K}} \left[\frac{-71.5\text{K}}{11000\text{m}} + 0.0098 \frac{\text{K}}{\text{m}} \right]} = 0.0113\text{s}^{-1}$ where the temperature differences in square brackets can be expressed in either °C or Kelvin.

Finally, use eq. (11.12): $\lambda_R = (0.0113 \text{ s}^{-1}) \cdot (11 \text{ km}) / (1.031 \times 10^{-4} \text{ s}^{-1}) = \mathbf{1206 \text{ km}}$

Check: Physics, units & magnitude are reasonable.

Exposition: When a cold-front over the Pacific approaches the steep mountains of western Canada, the front feels the influence of the mountains 1200 to 1300 km before reaching the coast, and begins to slow down.

disturbances ($\lambda > \lambda_R$), the wind field experiences the greatest adjustment. For smaller λ , the pressure and temperature fields have the greatest adjustment.

11.6. THERMAL WIND EFFECT

Recall that horizontal temperature gradients cause vertically varying horizontal pressure gradients (Fig. 11.17), and that horizontal pressure gradients drive geostrophic winds. We can combine those concepts to see how horizontal temperature gradients drive vertically varying geostrophic winds. This is called the **thermal wind effect**.

This effect can be pictured via the slopes of isobaric surfaces (Fig. 11.20). The hypsometric equation from Chapter 1 describes how there is greater thickness between any two isobaric (constant pressure) surfaces in warm air than in cold air. This causes the tilt of the isobaric surfaces to change with altitude. But as described by eq. (10.29), tilting isobaric surface imply a pressure-gradient force that can drive the geostrophic wind (U_g, V_g).

The relationship between the horizontal temperature gradient and the changing geostrophic wind with altitude is known as the **thermal wind effect**. After a bit of manipulation (see the Higher Math box on the next page), one finds that:

$$\frac{\Delta U_g}{\Delta z} \approx \frac{-|g|}{T_v \cdot f_c} \cdot \frac{\Delta T_v}{\Delta y} \quad \bullet(11.13a)$$

$$\frac{\Delta V_g}{\Delta z} \approx \frac{|g|}{T_v \cdot f_c} \cdot \frac{\Delta T_v}{\Delta x} \quad \bullet(11.13b)$$

where the Coriolis parameter is f_c , virtual absolute temperature is T_v and gravitational acceleration magnitude is $|g| = 9.8 \text{ m}\cdot\text{s}^{-2}$. Thus, the meridional temperature gradient causes the zonal geostrophic winds to change with altitude, and the zonal temperature gradient causes the meridional geostrophic winds to change with altitude.

Above the atmospheric boundary layer, actual winds are nearly equal to geostrophic or gradient winds. Thus, eqs. (11.13) provide a first-order estimate of the variation of actual winds with altitude.

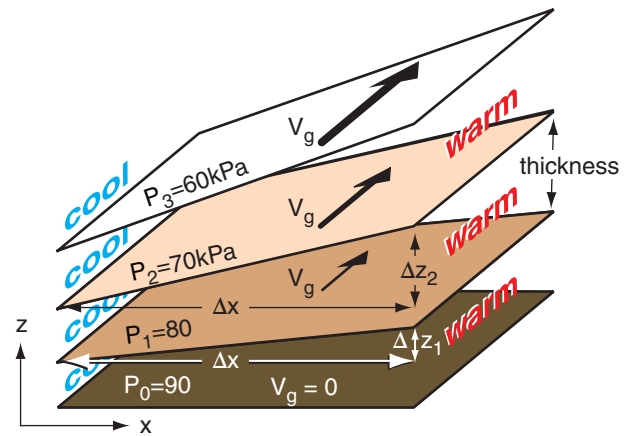


Figure 11.20

Isobaric surfaces are shaded brown. A zonal (west-east) temperature gradient causes the isobaric surfaces to tilt more and more with increasing altitude. Greater tilt causes stronger geostrophic winds (V_g) meridionally (south-north), as plotted with the black vectors for the N. Hemisphere. Geostrophic winds are reversed in S. Hemisphere.

Sample Application

While driving north a distance of 500 km, your car thermometer shows the outside air temperature decreasing from 20°C to 10°C. How does the theoretical geostrophic wind change with altitude?

Find the Answer

Given: $\Delta y = 500 \text{ km}$, $\Delta T = 10^\circ\text{C} - 20^\circ\text{C} = -10^\circ\text{C}$, average $T = 0.5 \cdot (10 + 20^\circ\text{C}) = 15^\circ\text{C} = 288 \text{ K}$.

Find: $\Delta U_g / \Delta z = ? (\text{m s}^{-1}) / \text{km}$

Given lack of other data, for simplicity assume: $f_c = 10^{-4} \text{ s}^{-1}$, and $T_v = T$ (i.e., air is dry).

Apply eq. (11.13a):

$$\frac{\Delta U_g}{\Delta z} \approx \frac{-(9.8\text{m/s}^2)}{(288\text{K}) \cdot (10^{-4}\text{s}^{-1})} \cdot \frac{(-10^\circ\text{C})}{(500\text{km})} = 6.81 (\text{m s}^{-1}) / \text{km}$$

Check: Physics & units reasonable. Agrees with Fig.

Exposition: Even if the wind were zero at the ground, the answer indicates that a west wind will increase in speed by 6.81 m s^{-1} for each 1 km of altitude gained.

Given no info about temperature change in the x direction, assume uniform temperature, which implies $\Delta V_g / \Delta z = 0$ from eq. (11.13b). Namely, the south wind is constant with altitude.

HIGHER MATH • Thermal Wind Effect

Problem: Derive Thermal Wind eq. (11.13a).

Find the Answer: Start with the definitions of geostrophic wind (10.26a) and hydrostatic balance (1.25b):

$$U_g = -\frac{1}{\rho \cdot f_c} \frac{\partial P}{\partial y} \quad \text{and} \quad \rho \cdot |g| = -\frac{\partial P}{\partial z}$$

Replace the density in both eqs using the ideal gas law (1.20). Thus:

$$\frac{U_g \cdot f_c}{T_v} = -\frac{\mathfrak{R}_d}{P} \frac{\partial P}{\partial y} \quad \text{and} \quad \frac{|g|}{T_v} = -\frac{\mathfrak{R}_d}{P} \frac{\partial P}{\partial z}$$

Use $(1/P) \cdot \partial P = \partial \ln(P)$ from calculus to rewrite both:

$$\frac{U_g \cdot f_c}{T_v} = -\mathfrak{R}_d \frac{\partial \ln(P)}{\partial y} \quad \text{and} \quad \frac{|g|}{T_v} = -\mathfrak{R}_d \frac{\partial \ln(P)}{\partial z}$$

Differentiate the left eq. with respect to z :

$$\frac{\partial}{\partial z} \left(\frac{U_g \cdot f_c}{T_v} \right) = -\mathfrak{R}_d \frac{\partial \ln(P)}{\partial y \partial z}$$

and the right eq. with respect to y :

$$\frac{\partial}{\partial y} \left(\frac{|g|}{T_v} \right) = -\mathfrak{R}_d \frac{\partial \ln(P)}{\partial y \partial z}$$

But the right side of both eqs are identical, thus we can equate the left sides to each other:

$$\frac{\partial}{\partial z} \left(\frac{U_g \cdot f_c}{T_v} \right) = \frac{\partial}{\partial y} \left(\frac{|g|}{T_v} \right)$$

Next, do the indicated differentiations, and rearrange to get the exact relationship for thermal wind:

$$\frac{\partial U_g}{\partial z} = -\frac{|g|}{T_v \cdot f_c} \frac{\partial T_v}{\partial y} + \frac{U_g}{T_v} \left(\frac{\partial T_v}{\partial z} \right)$$

The last term depends on the geostrophic wind speed and the lapse rate, and has magnitude of 0 to 30% of the first term on the right. If we neglect the last term, we get the approximate thermal wind relationship:

$$\frac{\partial U_g}{\partial z} \approx -\frac{|g|}{T_v \cdot f_c} \frac{\partial T_v}{\partial y} \tag{11.13a}$$

Exposition: A **barotropic** atmosphere is when the geostrophic wind does not vary with height. Using the exact equation above, we see that this is possible only when the two terms on the right balance.

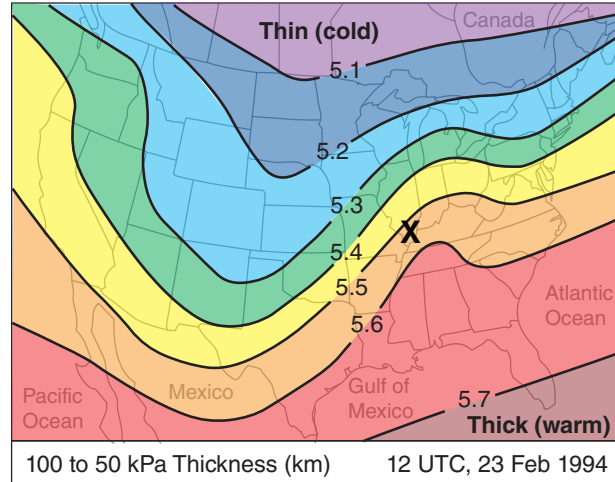


Figure 11.21
Thickness chart based on a US National Weather Service 24-hour forecast. The surface cyclone center is at the “X”.

11.6.1. Definition of Thickness

In Fig. 11.20, focus on two isobaric surfaces, such as $P = 90$ kPa (dark brown in that figure), and $P = 80$ kPa (medium brown). These two surfaces are at different altitudes z , and the altitude difference is called the “thickness”. For our example, we focused on the “90 to 80 kPa thickness”. For any two isobaric surfaces P_1 and P_2 having altitudes z_{P1} and z_{P2} , the thickness is defined as

$$TH = z_{P2} - z_{P1} \tag{11.14}$$

The hypsometric equation from Chapter 1 tells us that the thickness is proportional to the average absolute virtual-temperature within that layer. Colder air has thinner thickness. Thus, horizontal changes in temperature must cause horizontal changes in thickness.

Weather maps of “100 to 50 kPa thickness” such as Fig. 11.21 are often created by forecast centers. Larger thickness on this map indicates warmer air within the lowest 5 km of the atmosphere.

11.6.2. Thermal-wind Components

Suppose that we use thickness TH as a surrogate for absolute virtual temperature. Then we can combine eqs. (11.14) and (10.29) to yield:

$$U_{TH} = U_{G2} - U_{G1} = -\frac{|g|}{f_c} \frac{\Delta TH}{\Delta y} \tag{11.15a}$$

$$V_{TH} = V_{G2} - V_{G1} = +\frac{|g|}{f_c} \frac{\Delta TH}{\Delta x} \tag{11.15b}$$

where U_{TH} and V_{TH} are **components of the thermal wind**, $|g|$ = magnitude of gravitational-acceleration, f_c = Coriolis parameter, (U_{G1}, V_{G1}) are geostrophic-wind components on the P_1 isobaric surface, and (U_{G2}, V_{G2}) are geostrophic-wind components on the P_2 isobaric surface.

The horizontal vector defined by (U_{TH}, V_{TH}) is the difference between the geostrophic wind vector on the P_2 surface and the geostrophic wind vector on the P_1 surface, as Fig. 11.22 demonstrates. The corresponding **magnitude of the thermal wind** M_{TH} is:

$$M_{TH} = \sqrt{U_{TH}^2 + V_{TH}^2} \quad (11.16)$$

To illustrate this, consider two isobaric surfaces $P_2 = 50$ kPa (shaded blue in Figure 11.22) and $P_1 = 100$ kPa (shaded red). The P_1 surface has higher height to the east (toward the back of this sketch). If you conceptually roll a ball bearing down this red surface to find the direction of the pressure gradient, and then recall that the geostrophic wind in the N. Hemisphere is 90° to the right of that direction, then you would anticipate a geostrophic wind G_1 direction as shown by the red arrow. Namely, it is parallel to a constant height contour (dotted red line) pointing in a direction such that low heights are to the vector's left.

Suppose cold air in the north (left side of this sketch) causes a small thickness of only 4 km between the red and blue surfaces. Warm air to the south causes a larger thickness of 5 km between the two isobaric surfaces. Adding those thicknesses to the heights of the P_1 surface (red) give the heights of the P_2 surface (blue). The blue P_2 surface tilts more steeply than the red P_1 surface, hence the geostrophic wind G_2 is faster (blue arrow) and is parallel to a constant height contour (blue dotted line).

Projecting the G_1 and G_2 vectors to the ground (green in Fig. 11.22), the vector difference is shown in yellow, and is labeled as the thermal wind M_{TH} . It is parallel to the contours of thickness (i.e., perpendicular to the temperature gradient between cold and warm air) pointing in a direction with cold air (thin thicknesses) to its left (Fig. 11.23).

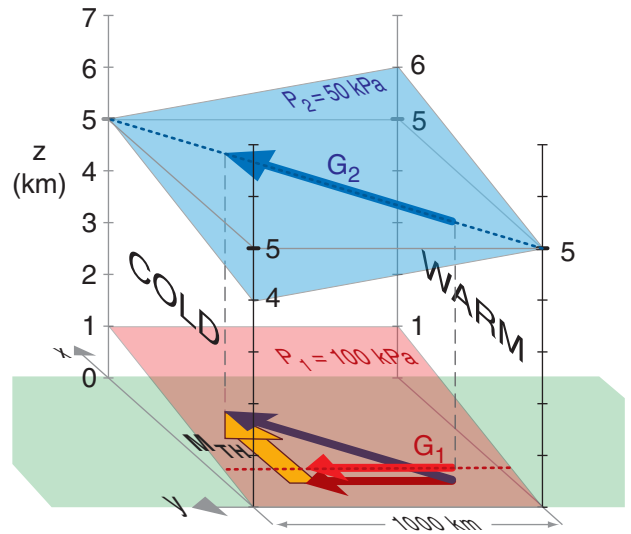


Figure 11.22
Relationship between the thermal wind M_{TH} and the geostrophic winds G on isobaric surfaces P . View is from the west north-west, in the Northern Hemisphere.

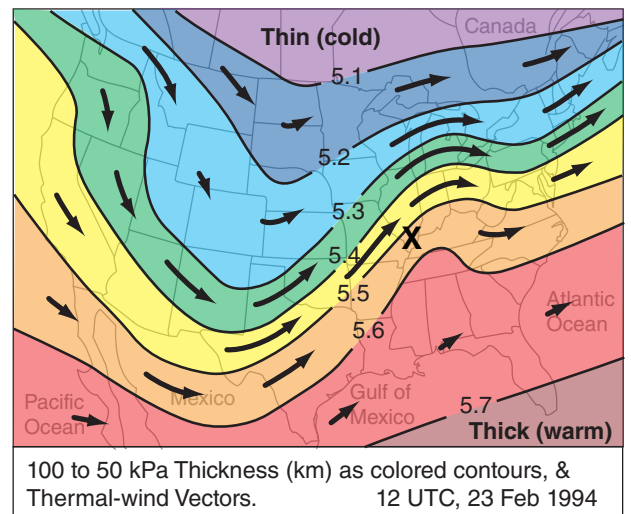


Figure 11.23
Arrows indicate thermal-wind vectors, where longer arrows indicate thermal winds that are stronger. Colored contours are 100 to 50 kPa thicknesses.

Sample Application. For Fig. 11.22, what are the thermal-wind components. Assume $f_c = 1.1 \times 10^{-4} \text{ s}^{-1}$.

Find the Answer. Given: $TH_2 = 4 \text{ km}$, $TH_1 = 5 \text{ km}$, $\Delta y = 1000 \text{ km}$ from the figure, $f_c = 1.1 \times 10^{-4} \text{ s}^{-1}$.
Find: $U_{TH} = ? \text{ m s}^{-1}$, $V_{TH} = ? \text{ m s}^{-1}$

Apply eq. (11.15a):
$$U_{TH} = \frac{-|g| \Delta TH}{f_c \Delta y} = \frac{-(9.8 \text{ ms}^{-2}) \cdot (4 - 5) \text{ km}}{(1.1 \times 10^{-4} \text{ s}^{-1}) \cdot (5000 \text{ km})} = \underline{17.8 \text{ m s}^{-1}}$$

Check: Physics & units are reasonable. Positive sign for U_{TH} indicates wind toward positive x direction, as in Fig.

Exposition: With no east-to-west temperature gradient, and hence no east-to-west thickness gradient, we would expect zero north-south thermal wind, hence, $V_{TH} = 0$.

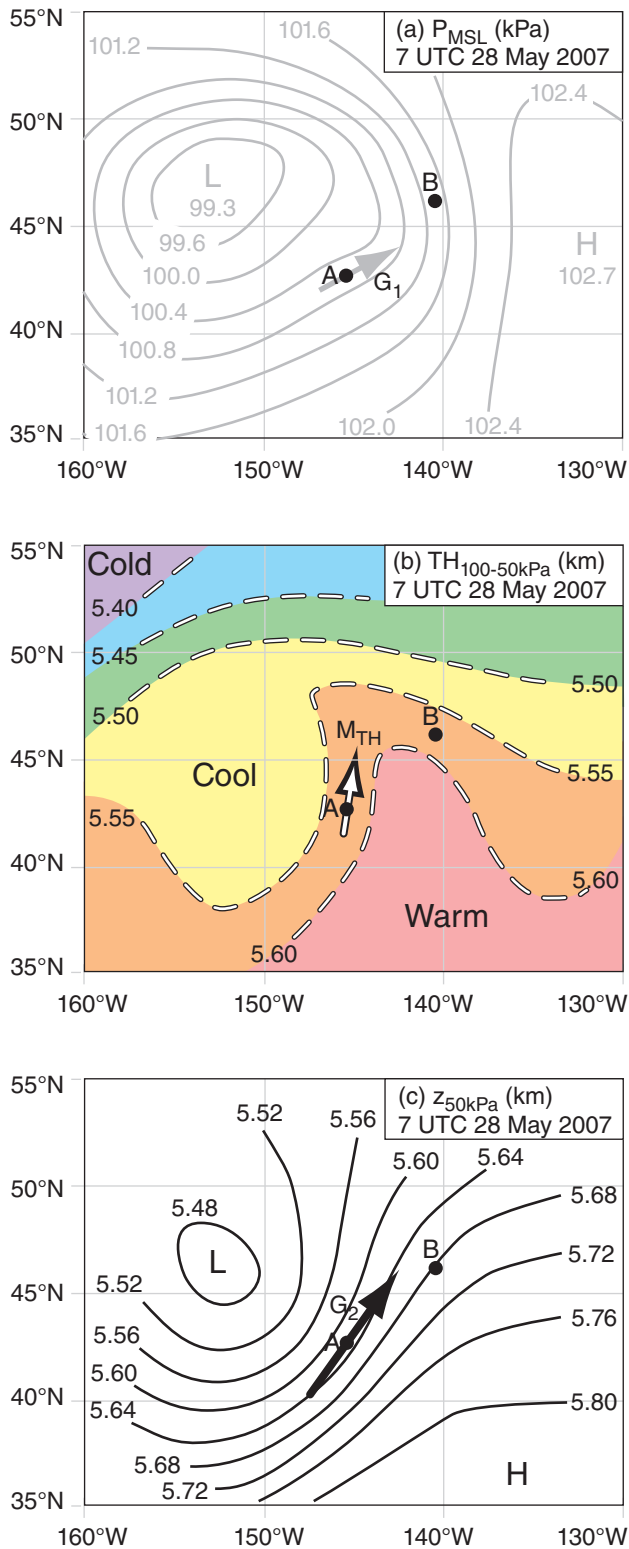


Figure 11.24
 Weather maps for a thermal-wind case-study. (a) Mean sea-level pressure (kPa), as a surrogate for height of the 100 kPa surface. (b) Thickness (km) of the layer between 100 kPa to 50 kPa isobaric surfaces. (c) Geopotential heights (km) of the 50 kPa isobaric surface.

Thermal-wind magnitude is stronger where the thickness gradient is greater. Thus, regions on a weather map (Fig. 11.23) where thickness contours are closer together (i.e., have **tighter packing**) indicates faster thermal winds. The relationship between thermal winds and thickness contours is analogous to the relationship between geostrophic winds and height contours. But never forget that no physically realistic wind can equal the thermal wind, because the thermal wind represents the difference or shear between two geostrophic winds.

Nonetheless, you will find the thermal-wind concept useful because it helps you anticipate how geostrophic wind will change with altitude. Actual winds tend towards being geostrophic above the atmospheric boundary layer, hence the thermal-wind concept allows you to anticipate real wind shears.

11.6.3. Case Study

Figs. 11.24 show how geostrophic winds and thermal winds can be found on weather maps, and how to interpret the results. These maps may be copied onto transparencies and overlain.

Fig. 11.24a is a weather map of pressure at sea level in the N. Hemisphere, at a location over the northeast Pacific Ocean. As usual, L and H indicate low- and high-pressure centers. At point A, we can qualitatively draw an arrow (grey) showing the theoretical geostrophic (G_1) wind direction; namely, it is parallel to the isobars with low pressure to its left.

Recall that pressures on a constant height surface (such as at height $z = 0$ at sea level) are closely related to geopotential heights on a constant pressure surface. So we can be confident that a map of 100 kPa heights would look very similar to Fig. 11.24a.

Fig. 11.24b shows the 100 - 50 kPa thickness map, valid at the same time and place. The thickness between the 100 and the 50 kPa isobaric surfaces is about 5.6 km in the warm air, and only 5.4 km in the cold air. The white arrow qualitatively shows the thermal wind M_{TH} , as being parallel to the thickness lines with cold temperatures to its left.

Fig. 11.24c is a weather map of geopotential heights of the 50 kPa isobaric surface. L and H indicate low and high heights. The black arrow at A shows the geostrophic wind (G_2), drawn parallel to the height contours with low heights to its left.

If we wished, we could have calculated quantitative values for G_1 , G_2 , and M_{TH} utilizing the scale that 5° of latitude equals 555 km. [ALERT: This scale does not apply to longitude, because the meridians get closer together as they approach the poles. However, once you have determined the scale (map mm : real km) based on latitude, you can use it to good approximation in any direction on the map.]

Back to the thermal wind: if you add the geostrophic vector from Fig. 11.24a with the thermal wind vector from Fig. 11.24b, the result should equal the geostrophic wind vector in Fig. 11.24c. This is shown in the Sample Application.

Although we will study much more about weather maps and fronts in the next few chapters, I will interpret these maps for you now.

Point A on the maps is near a cold front. From the thickness chart, we see cold air west and northwest of point A. Also, knowing that winds rotate counterclockwise around lows in the N. Hemisphere (see Fig. 11.24a), I can anticipate that the cool air will advance toward point A. Hence, this is a region of **cold-air advection**. Associated with this cold-air advection is **backing of the wind** (i.e., turning counterclockwise with increasing height), which we saw was fully explained by the thermal wind.

Point B is near a warm front. I inferred this from the weather maps because warmer air is south of point B (see the thickness chart) and that the counterclockwise winds around lows are causing this warm air to advance toward point B. **Warm air advection** is associated with **veering of the wind** (i.e., turning clockwise with increasing height), again as given by the thermal wind relationship. I will leave it to you to draw the vectors at point B to prove this to yourself.

11.6.4. Thermal Wind & Geostrophic Adjustment - Part 2

As geostrophic winds adjust to changes in pressure gradients, they move mass to alter the pressure gradients. Eventually, an equilibrium is approached (Fig. 11.25) based on the combined effects of geostrophic adjustment and the thermal wind. This figure is much more realistic than Fig. 11.17(iv) because Coriolis force prevents the winds from flowing directly from high to low pressure.

With these concepts of:

- differential heating,
- nonhydrostatic pressure couplets due to horizontal winds and vertical buoyancy,
- hydrostatic thermal circulations,
- geostrophic adjustment, and
- the thermal wind,

we can now go back and explain why the global circulation works the way it does.

Sample Application

For Fig. 11.24, qualitatively verify that when vector M_{TH} is added to vector G_1 , the result is vector G_2 .

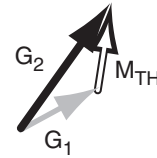
Find the Answer

Given: the arrows from Fig. 11.24 for point A.

These are copied and pasted here.

Find: The vector sum of $G_1 + M_{TH} = ?$

Recall that to do a vector sum, move the tail of the second vector (M_{TH}) to be at the arrow head of the first vector (G_1). The vector sum is then the vector drawn from the tail of the first vector to the tip (head) of the second vector.



Check: Sketch is reasonable.

Exposition: The vector sum indeed equals vector G_2 , as predicted by the thermal wind.

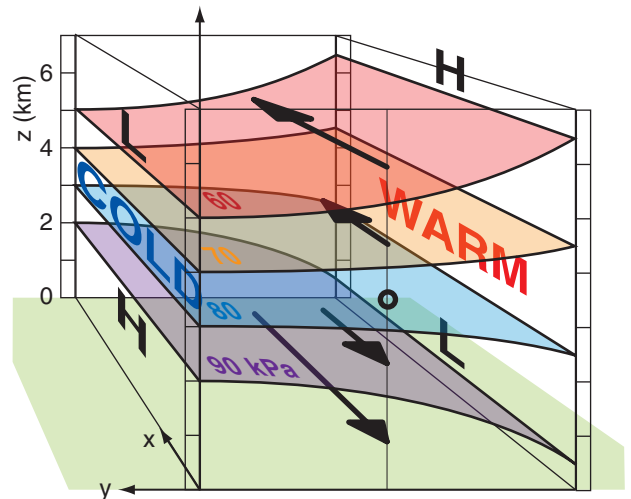


Figure 11.25

Typical equilibrium state of the pressure, temperature and wind fields after it has adjusted geostrophically. Isobaric surfaces are shaded with color, and recall that high heights of isobaric surfaces correspond to regions of high pressure on constant altitude surfaces. Black arrows give the geostrophic wind vectors.

Consider the red-shaded isobaric surface representing $P = 60$ kPa. That surface has high (H) heights to the south (to the right in this figure), and low (L) heights to the north. In the Northern Hemisphere, the geostrophic wind would be parallel to a constant height contour in a direction with lower pressure to its left. A similar interpretation can be made for the purple-shaded isobaric surface at $P = 90$ kPa. At a middle altitude in this sketch there is no net pressure gradient (i.e., zero slope of an isobaric surface), hence no geostrophic wind.

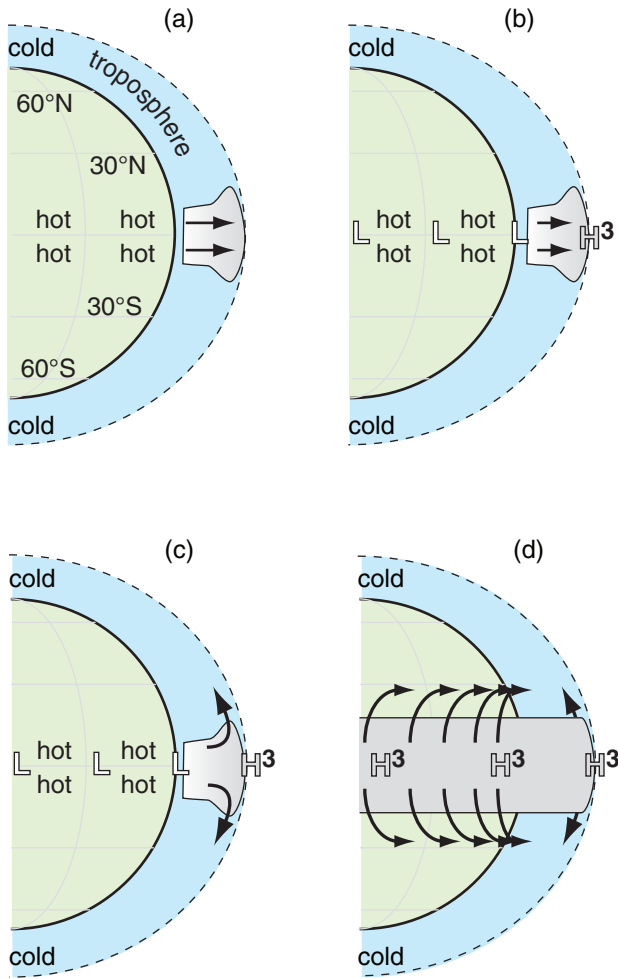


Figure 11.26
 Application of physical concepts to explain the general circulation (see text). White-filled H and L indicate surface high and low pressure regions; grey-filled H and L are pressure regions near the tropopause. (continued on next pages)

A SCIENTIFIC PERSPECTIVE • Model Sensitivity

CAUTION: Whenever you find that a model has high **sensitivity** (i.e., the output result varies by large magnitude for small changes in the input parameter), you should be especially wary of the results. Small errors in the parameter could cause large errors in the result. Also, if the real atmosphere does not share the same sensitivity, then this is a clue that the model is poorly designed, and perhaps a better model should be considered.

Models are used frequently in meteorology — for example: numerical weather prediction models (Chapter 20) or climate-change models (Chapter 21). Most researchers who utilize models will perform careful **sensitivity studies** (i.e., compute the output results for a wide range of parameter values) to help them gauge the potential weaknesses of the model.

11.7. EXPLAINING THE GENERAL CIRCULATION

11.7.1. Low Latitudes

Differential heating of the Earth's surface warms the tropics and cools the poles (Fig. 11.26a). The warm air near the equator can hold large amounts of water vapor evaporated from the oceans. Buoyancy force causes the hot humid air to rise over the equator. As the air rises, it cools and water vapor condenses, causing a belt of thick thunderstorm clouds around the equator (Fig. 11.26a) with heavy tropical precipitation.

The buoyantly forced vertical motion removes air molecules from the lower troposphere in the tropics, and deposits the air near the top of the troposphere. The result is a pressure couplet (Fig. 11.26b) of very high perturbation pressure p' (indicated with HHH or H^3 on the figures) near the tropopause, and low perturbation pressure (L in the figures) at the surface.

The belt of tropical high pressure near the tropopause forces air to diverge horizontally, forcing some air into the Northern Hemisphere and some into the Southern (Fig. 11.26c). With no Coriolis force at the equator, these winds are driven directly away from the high-pressure belt.

As these high-altitude winds move away from the equator, they are increasingly affected by Coriolis force (Fig. 11.26d). This causes winds moving into the Northern Hemisphere to turn to their right, and those moving into the Southern Hemisphere to turn to their left. Winds in both hemispheres accelerate.

But as the winds move further and further away from the equator, they are turned more and more to the east, creating the subtropical jet (Fig. 11.26e) at about 30° latitude. Coriolis force prevents these upper-level winds from getting further away from the equator than about 30° latitude (north and south), so the air accumulates and the pressure increases in those belts.

When simulations of the general circulation impose a larger Coriolis force (as if the Earth spun faster), the convergence bands occur closer to the equator. This effect is indeed found in the atmospheres of Jupiter and Saturn, as is evident by motions in their banded structures. For weaker Coriolis force, the convergence is closer to the poles. But for our Earth, the air converges at 30° latitude.

This pressure perturbation p' is labeled as HH or H^2 in Fig. 11.26e, to show that it is a positive pressure perturbation, but not as strong as the H^3 perturbation over the equator. Namely, the horizontal pressure gradient between H^3 and H^2 drives the upper-level winds to diverge away from the equator.

The excess air accumulated at 30° latitudes cannot go up into the stratosphere in the face of very strong static stability there. The air cannot go further poleward because of Coriolis force. And the air cannot move equatorward in the face of the strong upper-level winds leaving the equator. The only remaining path is downward at 30° latitude (Fig. 11.26f) as a nonhydrostatic flow. As air accumulates near the ground, it causes a high-pressure perturbation there — the belt of subtropical highs labeled with H.

The descending air at 30° latitude warms dry-adiabatically, and does not contain much moisture because it was squeezed out earlier in the thunderstorm updrafts. These are the latitudes of the subtropical deserts (Fig. 11.26h), and the source of hot airmasses near the surface.

Finally, the horizontal pressure gradient between the surface subtropical highs near 30° latitude and the equatorial lows near 0° latitude drives the surface winds toward the equator. Coriolis force turns these winds toward the west in both hemispheres (Fig. 11.26g), resulting in the easterly trade winds (winds from the east) that converge at the ITCZ.

The total vertical circulation in the tropics and subtropics we recognize as the Hadley Cell (labeled h.c. in Fig. 11.26f). This vertical circulation (a **thermally-direct circulation**) is so vigorous in its vertical mixing and heat transport that it creates a deeper troposphere in the tropics than elsewhere (Fig. 11.4). Also, the vigorous circulation spreads and horizontally mixes the radiatively warmed air somewhat uniformly between ±30° latitude, as sketched by the flattened temperature curve in Fig. 11.8a.

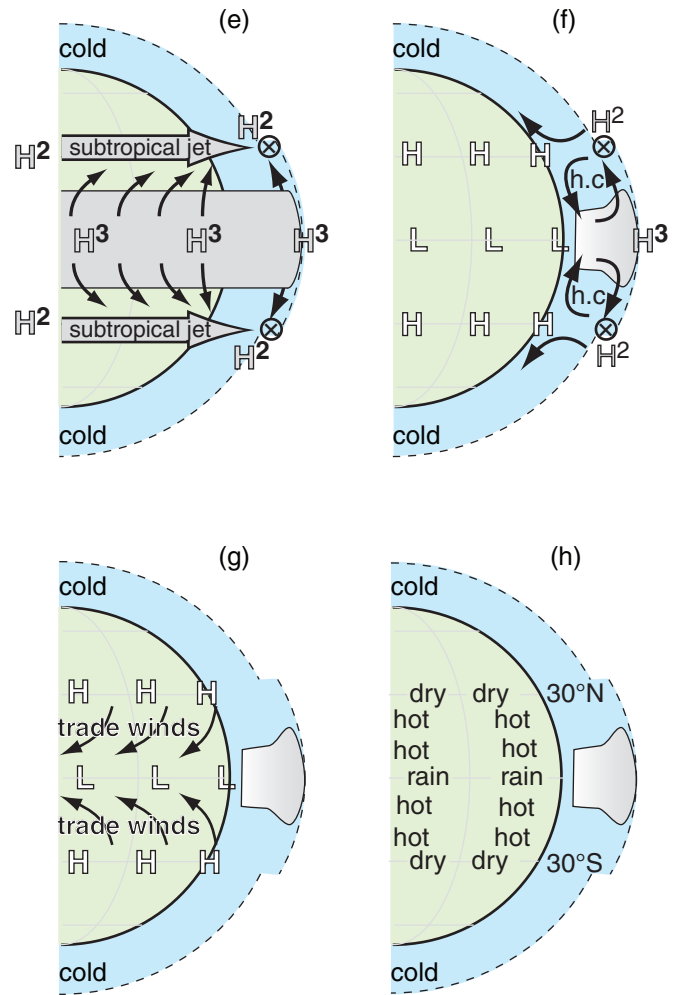


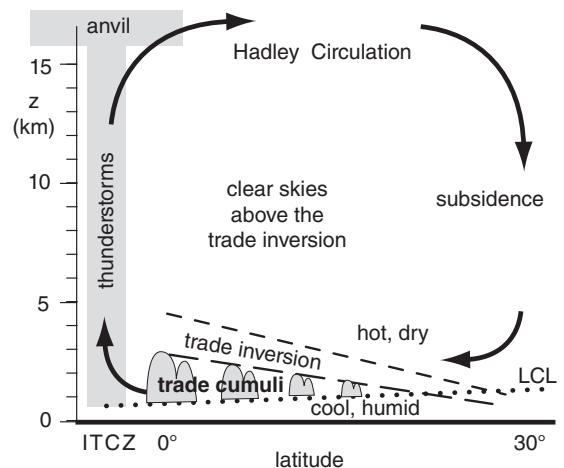
Figure 11.26 (continuation)

Explanation of low-latitude portion of the global circulation. The dashed line shows the tropopause. The “x” with a circle around it (representing the tail feathers of an arrow) indicates the axis of a jet stream that goes into the page.

INFO • The Trade Inversion

Descending air in the subtropical arm of the Hadley circulation is hot and dry. Air near the tropical sea surface is relatively cool and humid. Between these layers is a strong temperature inversion called the **trade inversion** or **passat inversion**. This statically stable layer (between the dashed lines in the Figure) creates a lid to the tropical convection below it. The inversion base is lowest (order of 500 m) in the subtropics, and is highest (order of 2,500 m) near the ITCZ. Fair-weather cumulus clouds (**trade cumuli**) between the lifting condensation level (LCL) and the trade inversion are shallowest in the subtropics and deeper closer to the ITCZ.

By capping the humid air below it, the trade inversion allows a latent-heat fuel supply to build up, which can be released in hurricanes and ITCZ thunderstorms.



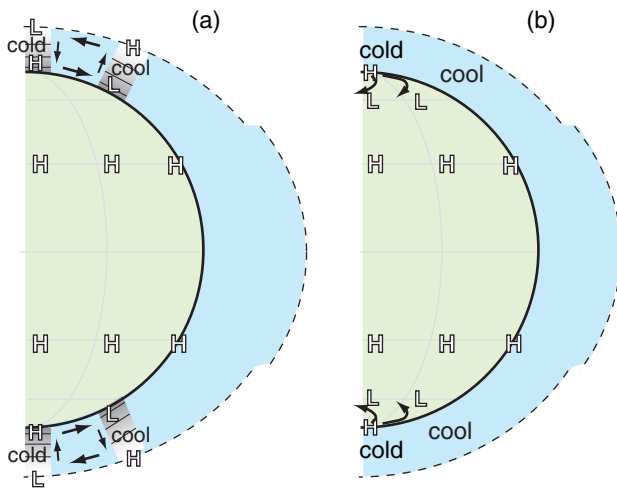


Figure 11.27
Explanation of high-latitude portion of general circulation.

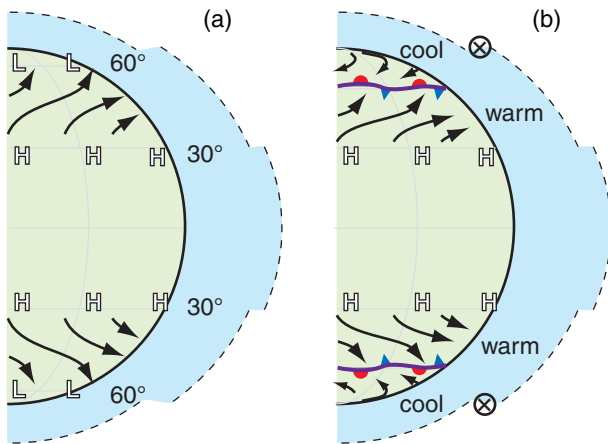


Figure 11.28
Explanation of mid-latitude flow near the Earth's surface. H and L indicate belts of high and low pressure, black arrows are average surface winds, and the polar front is shaded grey. The circle with "x" in it represents the tail feathers of the jet-stream wind vector blowing into the page.

11.7.2. High Latitudes

As sketched in Fig. 11.8a, air temperature is very cold at the poles, and is cool at 60° latitude. The temperature difference between 60° and 90° latitudes creates opposite north-south pressure gradients and winds at the top and bottom of the troposphere, due to the thermal circulation effect (Fig. 11.17). A vertical cross section of this thermal circulation (Fig. 11.27a) shows a weak polar cell. Air generally rises near 60°N and descends near the pole.

At the poles are surface high-pressure centers, and at 60° latitudes are belts of subpolar lows at the surface. This horizontal pressure gradient drives equatorward winds, which are turned toward the west in both hemispheres due to Coriolis force (Fig. 11.27b). Namely, the winds become geostrophic, and are known as **polar easterlies**.

At the top of the shallow (6 to 8 km thick) troposphere are poleward winds that are turned toward the east by Coriolis force. These result in an upper-level westerly flow that circulates around the upper-level polar low (Fig. 11.3b).

11.7.3. Mid-latitudes

Recall that the Hadley cell is unable to mix heat beyond about $\pm 30^\circ$ latitude. This leaves a very strong meridional temperature gradient in mid-latitudes (Fig. 11.8) throughout the depth of the troposphere. Namely, the temperature change between the equator (0°) and the poles (90°) has been compressed to a latitude band of about 30 to 60° in each hemisphere.

Between the subtropical high-pressure belt near 30° latitude and the subpolar low-pressure belt near 60° latitude is a weak meridional pressure gradient near the Earth's surface. This climatological-average pressure gradient drives weak boundary-layer winds from the west in both hemispheres (Fig. 11.28a), while the drag of the air against the surface causes the wind to turn slightly toward low pressure.

Near the subpolar belt of low pressure is a region of surface-air convergence, with easterly winds from the poles meeting westerly winds from mid-latitudes. The boundary between the warm subtropical air and the cool polar air at the Earth's surface is called the **polar front** (Fig. 11.28b) — a region of even stronger horizontal temperature gradient.

Recall from the hypsometric equation in Chapter 1 that the height difference (i.e., the thickness) between two isobaric surfaces increases with increasing temperature. As a result of the meridional temperature gradient, isobaric surfaces near the top of the troposphere in mid-latitudes are much more steeply sloped than near the ground (Figs. 11.29 & 11.32). This is related to the thermal-wind effect.

In the Northern Hemisphere this effect is greatest in winter (Fig. 11.32), because there is the greatest temperature contrast between pole and equator. In the Southern Hemisphere, the cold Antarctic continent maintains a strong meridional temperature contrast all year.

Larger pressure gradients at higher altitudes drive stronger winds. The core of fastest westerly winds near the tropopause (where the pressure-gradient is strongest) is called the **polar jet stream**, and is also discussed in more detail later in this chapter. Thus, the climatological average winds throughout the troposphere at mid-latitudes are from the west (Fig. 11.30a) in both hemispheres.

Although the climatological average polar-jet-stream winds are straight from west to east (as in Fig. 11.30a), the actual flow on any single day is unstable. Two factors cause this instability: the variation of Coriolis parameter with latitude (an effect that leads to **barotropic instability**), and the increase in static stability toward the poles (an effect that leads to **baroclinic instability**). Both of these instabilities are discussed in more detail later.

Air flow over a surface heterogeneity such as a mountain range can cause the initial meridional deviation of the jet stream. Once triggered, the jet stream continues to meander or oscillate north-south as it generally blows from the west (Fig. 11.30b). The meanders that form in this flow are called **Rossby waves**. Regions near the tropopause where the jet stream meanders equatorward are called **troughs**, because the lower pressure on the north side of the jet stream is brought equatorward there. Poleward meanders of the jet stream are called **ridges**, where higher pressure extends poleward. The locations of Rossby-wave troughs and ridges usually propagate toward the east with time, as will be explained in detail later in this chapter.

Recall that there is a subtropical jet at roughly 30° latitude associated with outflow from the Hadley Cell. Thus, in each hemisphere is a somewhat-steady subtropical jet and a meandering polar jet (Fig. 11.30b). Both of these jets are strongest in the winter hemisphere, where there is the greatest temperature gradient between cold poles and hot equator.

Troughs and ridges in the jet stream are crucial in creating and destroying cyclones and anticyclones near the Earth's surface. Namely, they cause the extremely large weather variability that is normal for mid-latitudes. The field of **synoptic meteorology** comprises the study and forecasting of these variable systems, as discussed in the Airmasses, Fronts, and Extratropical Cyclone chapters.

Figs. 11.31 and 11.32 show actual global pressure patterns at the bottom and top of the troposphere. The next section explains why the patterns over the oceans and continents differ.

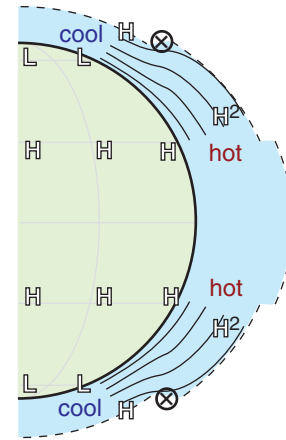


Figure 11.29

Isobaric surfaces (thin solid black lines) are spaced further apart in hot air than in cool air. Regions of steeper slope of the isobars have stronger pressure gradient, and drive faster winds. The jet-stream axis is shown with ⊗.

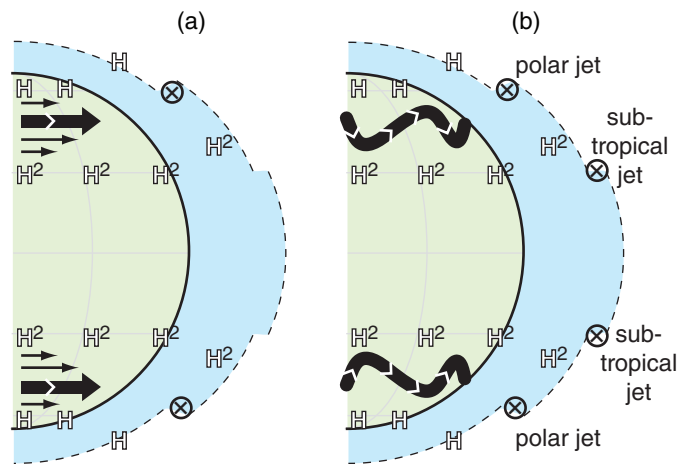


Figure 11.30

Mid-latitude flow near the top of the troposphere. The thick black arrow represents the core or axis of the jet stream: (a) average, (b) snapshot. (See caption in previous two figures for legend.)

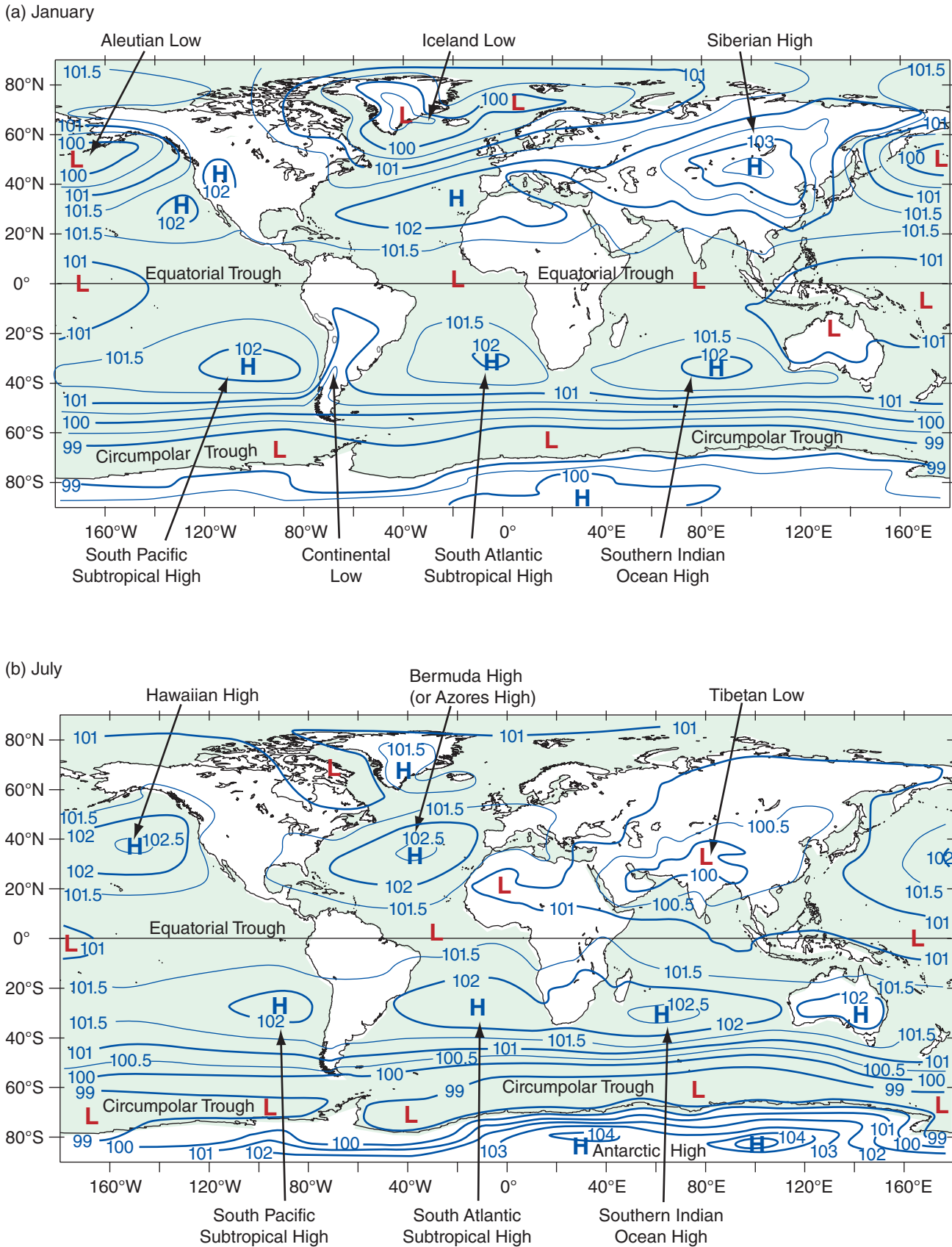
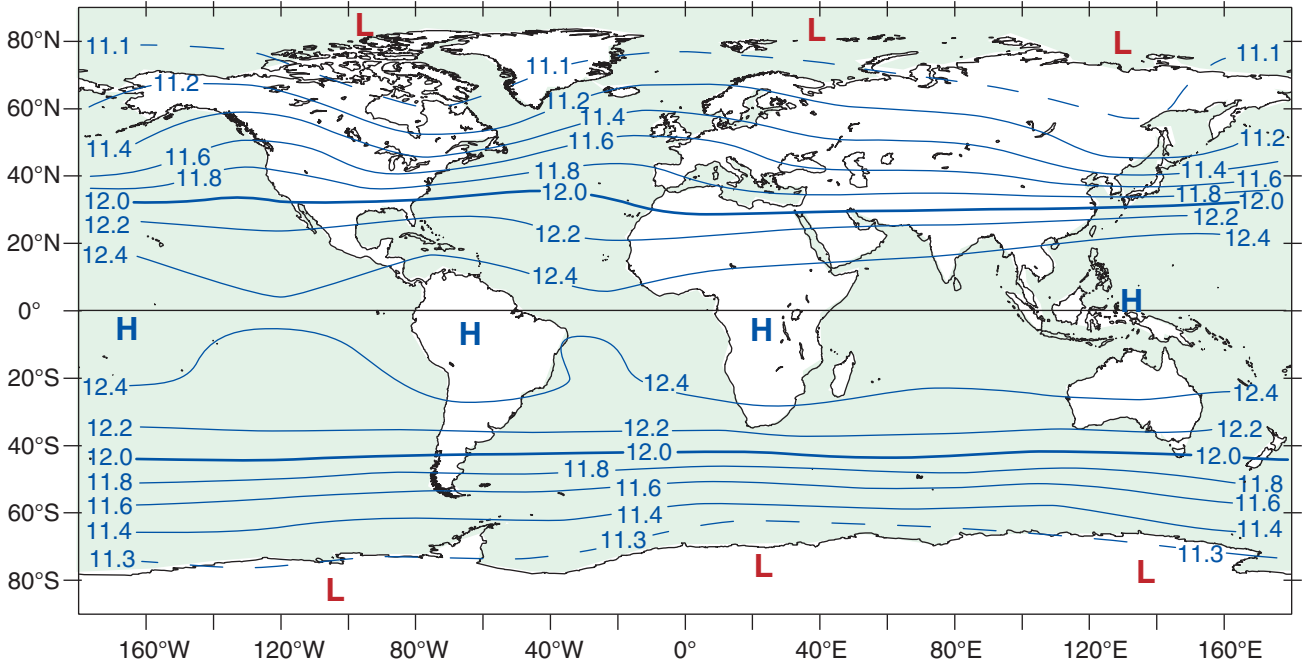


Figure 11.31
 Mean sea-level pressure (kPa) for (a) January, and (b) July, averaged over 30 years: 1981 to 2010. [NCEP/NCAR Reanalysis.]

(a) January



(b) July

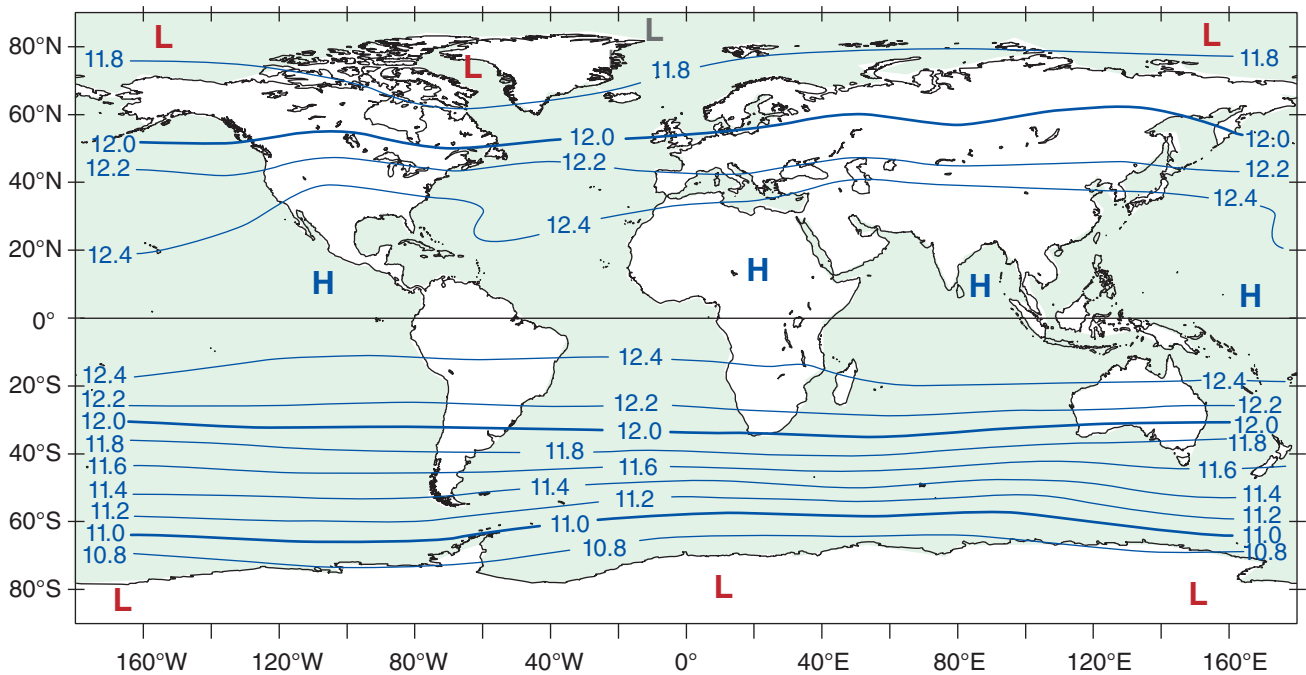


Figure 11.32
 Geopotential height (km) of the 20 kPa isobaric surface (near the tropopause) for (a) January, and (b) July, averaged over 30 years: 1981 to 2010. [NCEP/NCAR Reanalysis.]

11.7.4. Monsoon

Recall from the Heat Budgets chapter that the temperature change of an object depends on the mass of material being heated or cooled, and on the material's specific heat. If you put the same amount of heat into objects of similar material but differing mass, the smaller masses will warm the most.

Rocks and soil on continents are opaque to sunlight, and are good insulators of heat. Thus, sunlight directly striking the land surface warms only a very thin top layer (mm) of molecules, causing this thin layer to get quite warm. Similarly, longwave (infrared) radiative heat loss at night causes the very thin top layer to become very cold. Namely, there is a large **diurnal** (daily) temperature contrast. Also, because there are more daylight hours in summer and more nighttime hours in winter, continental land surfaces tend to become hot in summer and cold in winter.

Water in the oceans is partially transparent and sometimes turbulent, allowing sunlight to be absorbed and spread over a thick layer (meters to tens of meters) of molecules. Also, water has a large specific heat (see the Heat Budgets chapter), hence a large input of heat causes only a small temperature change. Thus, ocean surfaces have very small diurnal temperature changes, and have only a medium amount of seasonal temperature changes.

The net result is that during summer, continents warm faster than the oceans. During winter, continents cool faster than the oceans.

Consider a cold region next to a warm region. Over the cold surface, the near-surface air cools and develops a high-pressure center with anticyclonically rotating winds, as explained by the thermal circulation sketched in Fig. 11.17. Over warm surfaces, the thermal circulation causes near-surface air to warm and develop a low-pressure center with cyclonic winds. As already mentioned, this is called a **thermal low**.

Combining the effects from the previous two paragraphs with the strong tendency of the winds to become geostrophic (or gradient) yields the near-surface monsoonal flows shown in Fig. 11.5. Opposite pressure patterns and circulations would occur near the top of the troposphere. The regions near surface lows tend to have rising air and abundant clouds and rain. Regions near surface highs tend to have dry fair weather with few clouds.

Monsoon circulations occur over every large continent and ocean (Fig. 11.31). Some are given names. Over the Atlantic in summer, winds on the south and west sides of the monsoonal **Bermuda High** (also called the **Azores High**) steer Atlantic hurricanes northward as they near North America. Over the North Pacific in summer is the **Hawaiian**

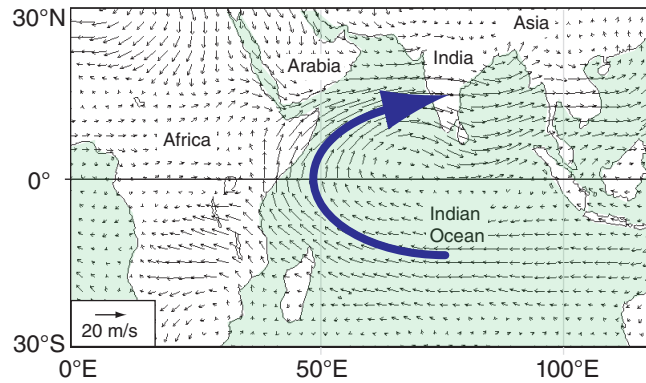


Figure 11.33

Monsoon winds near India on 85 kPa isobaric surface (at $z \approx 1.5$ km), averaged over July 2001. Thin arrow length shows wind speed (see legend). Thick arrow shows cross-equatorial flow.

High or **Pacific High** which provides cool northerly breezes and months of fair weather to the west coast of North America.

The summer low over northern India is called the **Tibetan Low**. It helps drive strong cross-equatorial flow (Fig. 11.33) that brings the much needed monsoon rains over India. Ghana in West Africa also receives a cross-equatorial monsoon flow.

Winter continental highs such as the **Siberian High** over Asia are formation locations for cold air-masses. Over the North Atlantic Ocean in winter is the **Icelandic Low**, with an average circulation on its south side that steers mid-latitude cyclones toward Great Britain and northern Europe. The south side of the winter **Aleutian Low** over the North Pacific brings strong onshore flow toward the west coast of North America, causing many days of clouds and rain.

The actual mean global circulation is a superposition of the zonally averaged flows and the monsoonal flows (Fig. 11.31). Also, a snapshot or satellite image of the Earth on any given day would likely deviate from the 30-year averages presented here. Other important aspects of the global circulation were not discussed, such as conversion between available potential energy and kinetic energy. Also, monsoons and the whole global circulation are modulated by El Niño / La Niña events and other oscillations, discussed in the Climate chapter.

In the previous sections, we have described characteristics of the global circulation in simple terms, looked at what drives these motions, and explained dynamically why they exist. Some of the phenomena we encountered deserve more complete analysis, including the jet stream, Rossby waves with their troughs and ridges, and some aspects of the ocean currents. The next sections give details about how these phenomena work.

11.8. JET STREAMS

In the winter hemisphere there are often two strong jet streams of fast west-to-east moving air near the tropopause: the **polar jet stream** and the **subtropical jet stream** (Figs. 11.34 & 11.35).

The subtropical jet is centered near 30° latitude in the winter hemisphere. This jet: (1) is very steady; (2) meanders north and south a bit; (3) is about 10° latitude wide (width ≈ 1,000 km); and (4) has seasonal-average speeds of about 45 m s⁻¹ over the Atlantic Ocean, 55 to 65 m s⁻¹ over Africa and the Indian Ocean, and 60 to 80 m s⁻¹ over the western Pacific Ocean. The **core** of fast winds near its center is at 12 km altitude (Fig. 11.35). It is driven by outflow from the top of the Hadley cell, and is affected by both Coriolis force and angular-momentum conservation.

The polar jet is centered near 50 to 60° latitude in the winter hemisphere. The polar jet: (1) is extremely variable; (2) meanders extensively north and south; (3) is about 5° latitude wide; and (4) has widely varying speeds (25 to 100 m s⁻¹) driven by varying horizontal temperature gradients. The core altitude is about 9 km. This jet forms over the polar front — driven by thermal-wind effects due to the strong horizontal temperature contrast across the front.

When meteorological data are averaged over 30 years, the subtropical jet shows up clearly in the data (e.g., Fig. 11.36) because it is so steady. However, the polar jet disappears because it meanders and shifts so extensively that it is washed out by the long-term average. Nonetheless, these transient meanders of the polar jet (troughs and ridges in the Rossby waves) are extremely important for mid-latitude cyclone formation and evolution (see the Extratropical Cyclone chapter).

In the summer hemisphere, the jets from the west have merged (Figs. 11.35b and 11.36), and the winds are slower because of the weaker temperature contrast between the equator and the warm pole. Core wind speeds in the jet are 0 to 10 m s⁻¹ in N. Hemisphere summer, and 5 to 45 m s⁻¹ in S. Hemisphere summer. This core shifts poleward to be centered near 40° to 45° latitude. A weak jet from the east is centered at roughly 10° latitude in the summer hemisphere.

INFO • Jet Stream Aspect Ratio

Jet streams in the real atmosphere look very much like the thin ribbons of fast-moving air, as sketched in Fig. 11.34. Jet vertical thickness (order of 5 to 10 km) is much smaller than their horizontal width (order of 1000 to 2000 km). Namely, their aspect ratio (width/thickness) is large. Figures such as 11.35 are intentionally distorted to show vertical variations better.

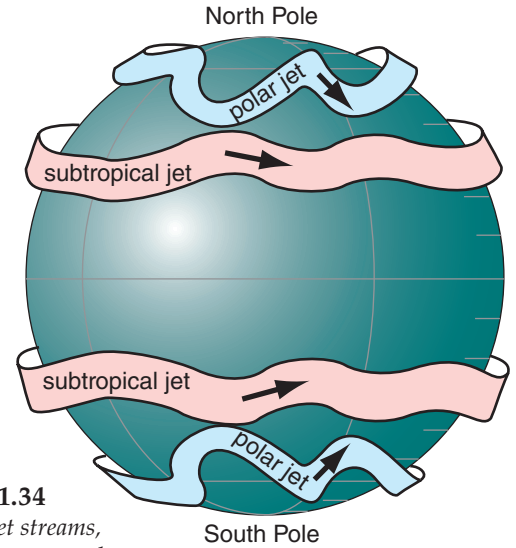


Figure 11.34
Sketch of jet streams, representing a snapshot.

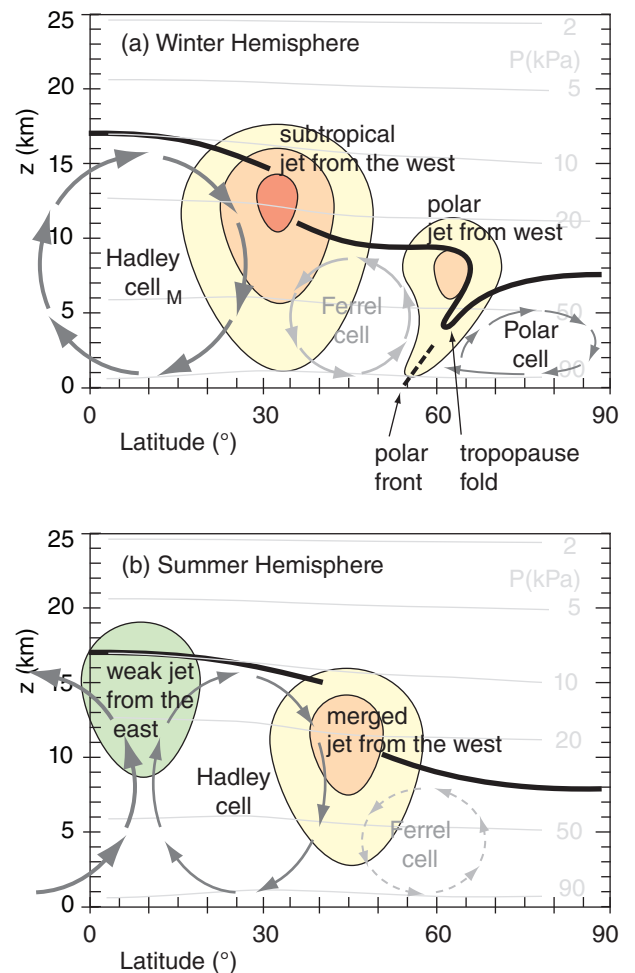
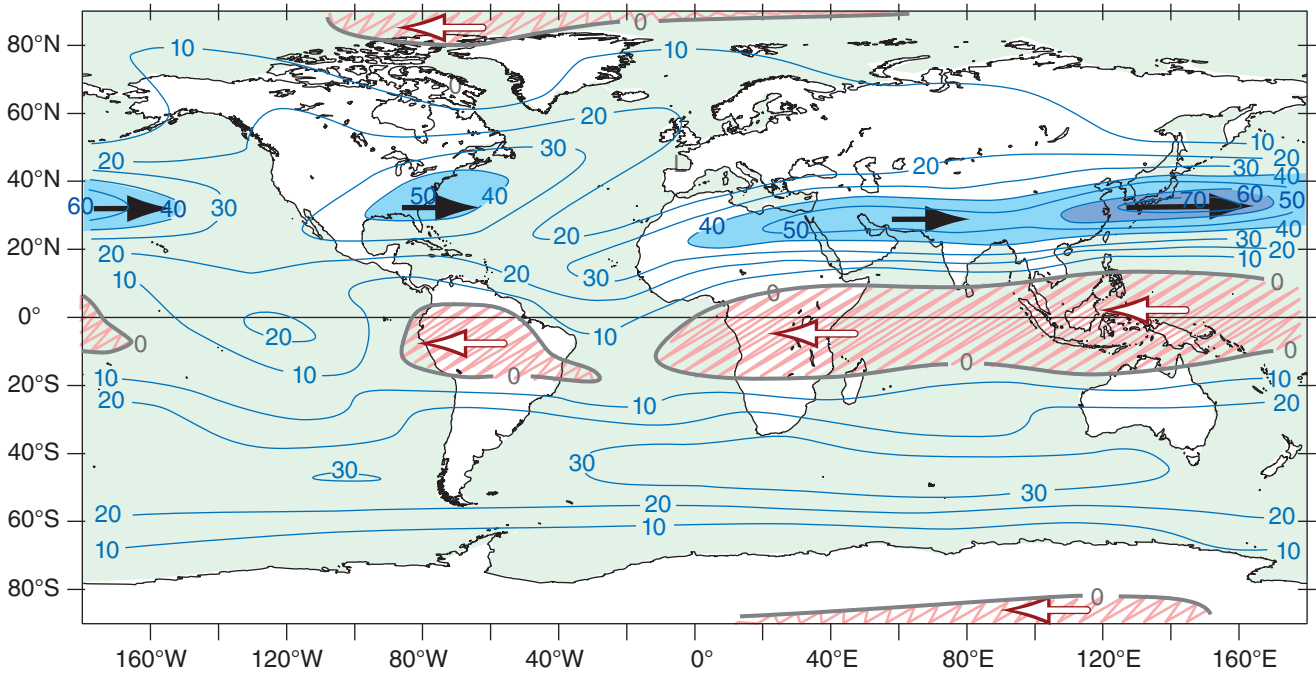


Figure 11.35
Simplified vertical cross-section. Thick solid line is the tropopause. Darker shading indicates faster winds (perpendicular to the page). This is a snapshot, not a climatological average; hence, the polar jet and polar front can be seen.

(a) January



(b) July

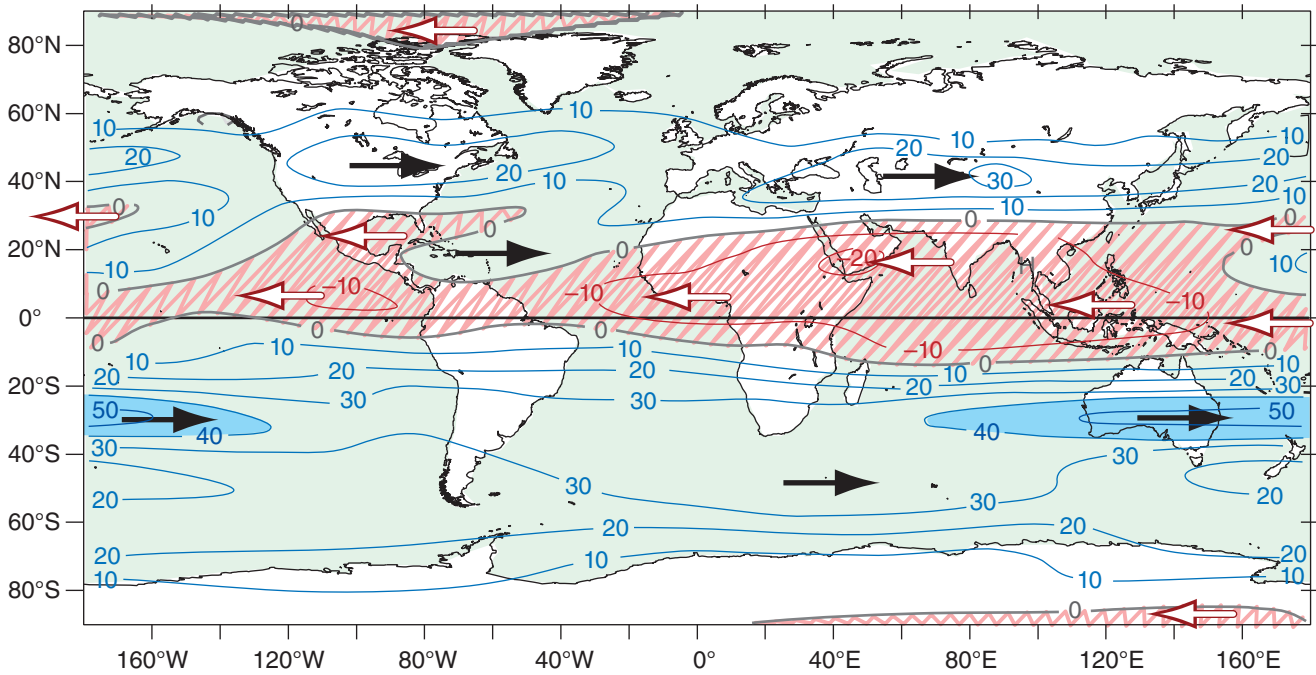


Figure 11.36
 Zonal (U) component of winds ($m s^{-1}$) at 20 kPa isobaric surface (near the tropopause) for (a) January, and (b) July, averaged over the 30 years of 1981 to 2010. Contour interval is $10 m s^{-1}$. All negative (east) winds are lightly hatched in red, and are indicated with white arrows. Positive (west) winds are indicated with black arrows, and are shaded in blue with isotachs at 40 and $60 m s^{-1}$. In polar regions, the tropopause is relatively low (at about 8 km altitude, where $P \approx 35 kPa$; see Table 6-1 in Chapter 6), so 20 kPa is well above the tropopause (compare the 20 kPa winds here with tropopause winds sketched in Fig. 11.3b). [NCAR/NCEP Reanalysis.]

11.8.1. Baroclinicity & the Polar Jet

First, consider how temperature varies with height and latitude (Fig. 11.37a). At any altitude in the troposphere you will find a horizontal temperature gradient between colder poles and warmer equator. According to the hypsometric relationship, the thickness between two isobaric surfaces is smaller in the colder (polar) air and greater in the warmer (equatorial) air (Fig. 11.37b). Hence, isobaric surfaces tilt in the horizontal, which drives a geostrophic wind (Fig. 11.37c).

The greatest tilt is near 30° latitude at the tropopause, and the associated pressure gradient drives the fastest winds (**jet-stream core**) there, as expected due to the thermal wind. Because the isobars cross the isotherms (and isobars also cross the isopycnics — lines of equal density), the atmosphere is said to be **baroclinic**. It is this **baroclinicity** associated with the meridional temperature gradient that creates the west winds of the jet stream.

Notice that the troposphere is deeper near the equator than near the poles. Thus, the typical lapse rate in the troposphere, applied over the greater depth, causes colder temperatures at the tropopause over the equator than over the poles (Fig. 11.37a). In the stratosphere above the equatorial tropopause, the air is initially isothermal, but at higher altitudes the air gets warmer. Meanwhile, further north in the stratosphere, such as at latitude 60°, the air is isothermal over a very large depth. Thus, the meridional temperature gradient reverses in the bottom of the stratosphere, with warmer air over 60° latitude and colder equatorial air.

The associated north-south thickness changes between isobaric surfaces cause the meridional pressure gradient to decrease, which you can see in Fig. 11.37b as reductions in slopes of the isobars. The reduced pressure gradient in the lower stratosphere causes wind speeds to decrease with increasing altitude (Fig. 11.37c), leaving the **jet max** at the tropopause. Near the jet core is a region where the tropopause has a break or a fold, as is covered in the Fronts and Extratropical Cyclone chapters.

You can apply the concepts described above to the toy model of eq. (11.1) and Fig. 11.8. Using that model with eqs. (11.2, 11.4 & 11.13) gives

$$U_{jet} \approx \frac{|g| \cdot c \cdot b_1}{2\Omega \cdot T_v} \cdot z \cdot \left(1 - \frac{z}{2 \cdot z_T}\right) \cdot \cos^2(\phi) \cdot \sin^2(\phi) \tag{11.17}$$

where ϕ is latitude, $|g| = 9.8 \text{ m s}^{-2}$, U_g has been relabeled as U_{jet} , T_v is average absolute virtual temperature, $b_1 \approx 40 \text{ K}$, $c = 1.18 \times 10^{-3} \text{ km}^{-1}$, $z_T \approx 11 \text{ km}$ is average depth of the troposphere, and assuming $U_{jet} = 0$ at $z = 0$. The factor $2 \cdot \Omega = 1.458 \times 10^{-4} \text{ s}^{-1}$ comes from the Coriolis-parameter definition $f_c = 2 \cdot \Omega \cdot \sin\phi$.

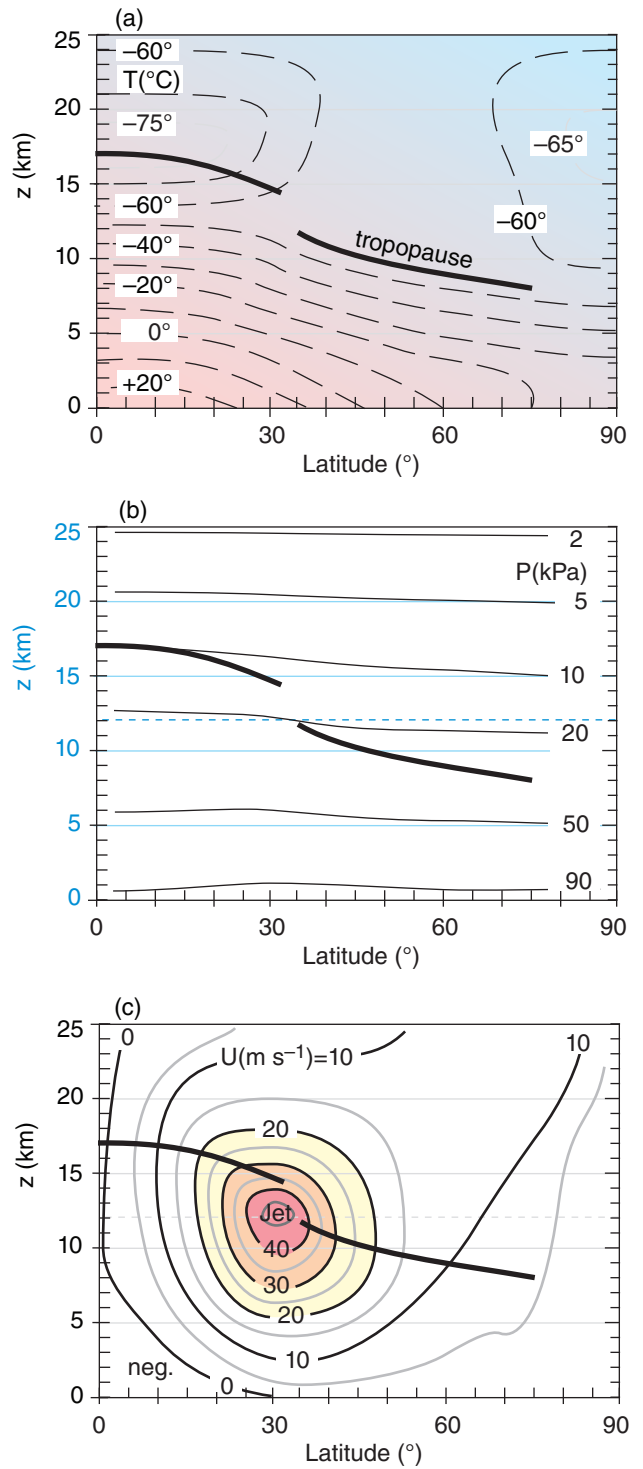


Figure 11.37 Vertical cross sections through the atmosphere on January 2003. (a) isotherms T ($^{\circ}\text{C}$), (b) isobars P (kPa), (c) isotachs of the zonal wind U (m s^{-1}). The tropopause is indicated by a heavy solid line. For this Northern Hemisphere case, the jet-stream winds in (c) are from the west (i.e., toward the reader). In Fig. b, height contours are light blue (dashed and thin solid), and isobars are black. You can superimpose copies of these three figures to see the relationship between the **temperature field**, **mass field** (i.e., pressures), and **wind field**.

Sample Application

Use the toy-model temperature eqs. (11.1 & 11.4) to estimate the speed of the geostrophic wind for latitude 60° at the top of the troposphere. Assume $T_0 = -5^\circ\text{C}$.

Find the Answer

Given: $\phi = 60^\circ$, $T_0 = 268\text{ K}$, $z = z_T$.

Find: $U_{jet} = ?\text{ m s}^{-1}$

From Fig. 11.39 estimate troposphere top $z_T \approx 9\text{ km}$. Apply eq. (11.17), which already incorporates toy model eq. (11.4).

$$U_{jet} \approx \frac{(9.8\text{ m}\cdot\text{s}^{-2}) \cdot (1.18 \times 10^{-3}\text{ km}^{-1}) \cdot (40\text{ K})}{(1.458 \times 10^{-4}\text{ s}^{-1}) \cdot (268\text{ K})}$$

$$(9\text{ km}) \cdot (1 - (1/2)) \cdot \cos^2(60^\circ) \cdot \sin^2(60^\circ)$$

$$= \underline{10.1\text{ m s}^{-1}}$$

Check: Physics & units are reasonable.

Exposition: Agrees with Fig. 11.37c. During winter the poles are colder relative to the equator, driving faster jet-stream winds than summer. Peak winds in the jet core can reach 100 m s^{-1} , although 3-month-average speeds are typically 40 m s^{-1} .

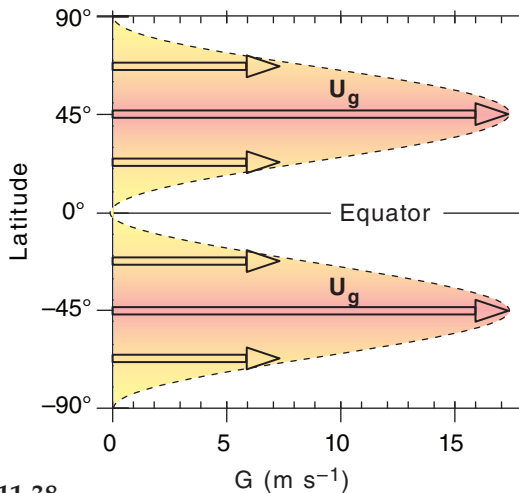


Figure 11.38
Idealized profile of 11 km altitude jet-stream winds vs. latitude.

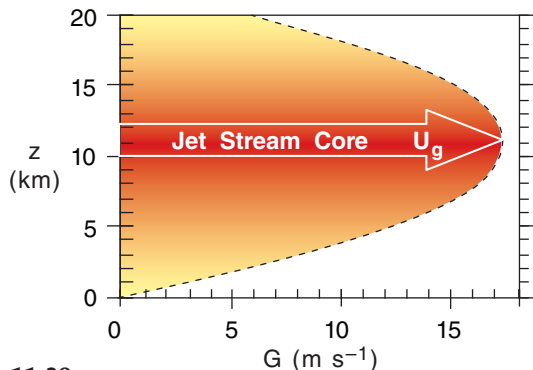


Figure 11.39
Idealized profile of 45°N latitude jet-stream winds vs. altitude.

The thermal-wind relationship tells us that the meridional variation of temperature between the cold poles and warm equator will drive westerly jet-stream winds in both hemispheres. Namely, the opposite Coriolis-parameter signs in the two hemispheres are canceled by the opposite meridional temperature-gradient signs, yielding positive values for U_g in the two hemispheres.

Although Fig. 11.8 indicates the largest meridional temperature gradients are at roughly 50° latitude (north & south) in our toy model, the meridional variation of the Coriolis parameter conspires to make the fastest jet-stream winds at 45° latitude (north & south) according to eq. (11.17). Solving eq. (11.27) for a tropopause height of $z_T = 11\text{ km}$ with an average virtual temperature of -20°C in the troposphere gives peak jet-stream wind speeds (Figs. 11.38 & 11.39) of about 17.25 m s^{-1} .

While our simple toy model is insightful because it mimics the main features of the global circulation and allows an analytical solution that you can solve on a spreadsheet, it is too simple. Compared to Fig. 11.37, the toy jet-stream speeds are too slow, are located too far poleward, and don't give fast-enough winds near the ground. Also, actual locations in both hemispheres shift a bit to the (north, south) in northern hemisphere (summer, winter).

11.8.2. Angular Momentum & Subtropical Jet

Angular momentum can influence the subtropical jet, and is defined as mass times velocity times radius of curvature. Suppose that initially there is air moving at some zonal velocity U_s relative to the Earth's surface at some initial (source) latitude ϕ_s . Because the Earth is rotating, the Earth's surface at the source latitude is moving toward the east at velocity U_{Es} . Thus, the total eastward speed of the air parcel relative to the Earth's axis is $(U_s + U_{Es})$.

As sketched in Fig. 11.40, suppose some disturbance such as a meandering jet stream moves the air to some other (destination) latitude ϕ_d , assuming that no other forces are applied. Conservation of angular momentum requires:

$$m \cdot (U_s + U_{Es}) \cdot R_s = m \cdot (U_d + U_{Ed}) \cdot R_d \quad \bullet(11.18)$$

where U_d represents the new zonal air velocity relative to the Earth's surface at the destination latitude, U_{Ed} is the tangential velocity of the Earth's surface at the destination, and m is air mass.

For latitude ϕ at either the source or destination, the radius is R_s or $R_d = R_E \cdot \cos(\phi)$, where average Earth radius is $R_E = 6371\text{ km}$. Similarly, tangential velocities at either the source or destination are U_s or $U_d = \Omega \cdot R_\phi = \Omega \cdot R_E \cdot \cos(\phi)$, for an Earth angular velocity of $\Omega = 0.729 \times 10^{-4}\text{ s}^{-1}$.

Solving these equations for the destination air velocity U_d relative to Earth's surface gives:

$$U_d = [\Omega \cdot R_E \cdot \cos(\phi_s) + U_s] \cdot \frac{\cos(\phi_s)}{\cos(\phi_d)} - \Omega \cdot R_E \cdot \cos(\phi_d) \tag{11.19}$$

As we already discussed, winds at the top of the Hadley cell diverge away from the equator, but cannot move beyond 30° latitude because Coriolis force turns the wind. When we use eq. (11.19) to predict the zonal wind speed for typical trade-wind air that starts at the equator with $U_s = -7 \text{ m s}^{-1}$ and ends at 30° latitude, we find unrealistically large wind speeds (125 m s^{-1}) for the subtropical jet (Fig. 11.41). Actual typical wind speeds in the subtropical jet are of order 40 to 80 m s^{-1} in the winter hemisphere, and slower in the summer hemisphere.

The discrepancy is because in the real atmosphere there is no conservation of angular momentum due to forces acting on the air. Coriolis force turns the wind, causing air to accumulate and create a pressure-gradient force to oppose poleward motion in the Hadley cell. Drag due to turbulence slows the wind a small amount. Also, the jet streams meander north and south, which helps to transport slow angular momentum southward and fast angular momentum northward. Namely, these meanders or synoptic-scale eddies cause mixing of zonal momentum.

Next, the concept of vorticity is discussed, which will be useful for explaining how troughs and ridges develop in the jet stream. Then, we will introduce a way to quantify circulation, to help understand the global wind patterns.

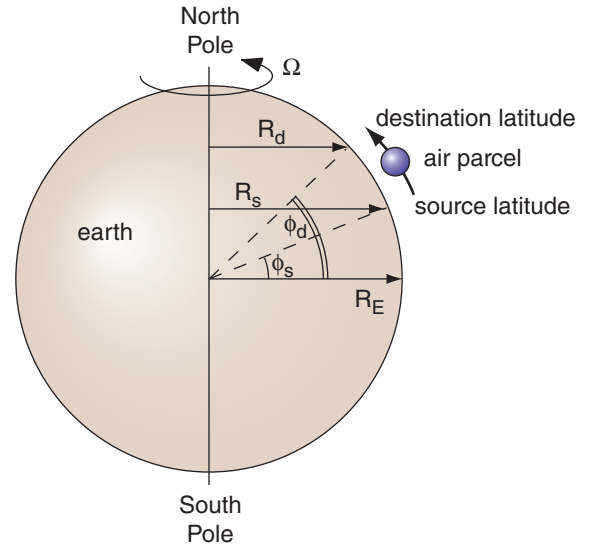


Figure 11.40
Geometry for angular-momentum calculations affecting an air parcel that moves toward the north.

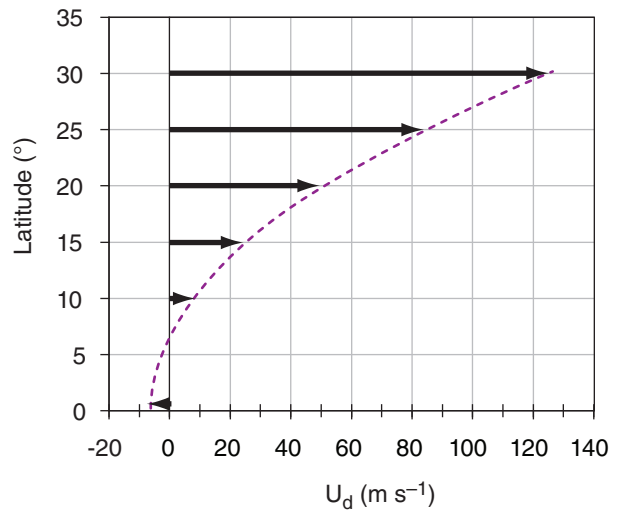


Figure 11.41
Computed zonal wind speed U_d at various destination latitudes for typical trade-wind air that starts at the equator with $U_s = -7 \text{ m s}^{-1}$, for the unrealistic case of conservation of angular momentum. Actual zonal winds are not this fast at 30° latitude.

Sample Application

For air starting at the equatorial tropopause, what would be its zonal velocity at 20°N if angular momentum were conserved?

Find the Answer

Given: $\phi_d = 20^\circ\text{N}$, $\phi_s = 0^\circ$, $\Omega \cdot R_E = 463 \text{ m s}^{-1}$
Find: $U_d = ? \text{ m s}^{-1}$
Assume: no turbulence; $U_s = -7 \text{ m s}^{-1}$ easterlies.

Use eq. (11.19): $U_d =$

$$[(463\text{m/s})\cos(0^\circ) + U_s] \frac{\cos(0^\circ)}{\cos(20^\circ)} - (463\text{m/s})\cos(20^\circ)$$

$$U_d = = \underline{50.2} \text{ m s}^{-1}$$

Check: Physics & units are reasonable. Agrees with Fig. 11.41

Exposition: Actual winds are usually slower, because of turbulent drag and other forces..

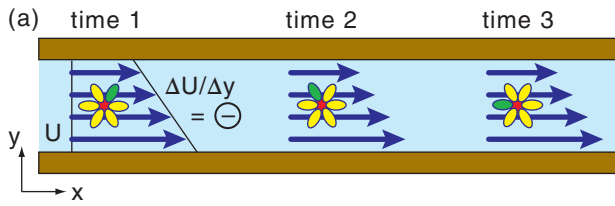


Figure 11.42
Flower blossoms dropped into a river illustrate positive relative vorticity (counterclockwise rotation) caused by river-current shear as the blossoms translate downstream.

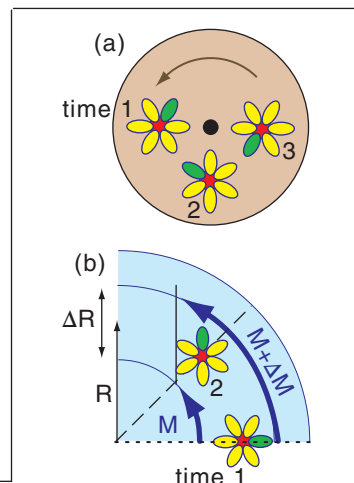
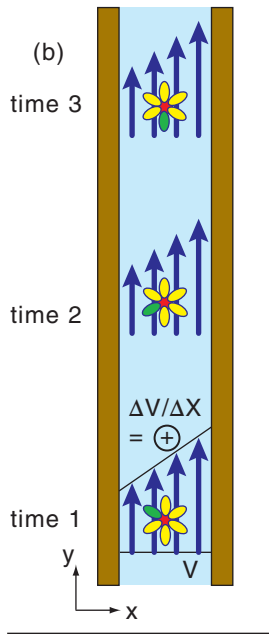


Figure 11.43

(a) Vorticity associated with solid-body rotation, illustrated with a flower blossom glued to a solid turntable at time 1.
(b) Vorticity caused by radial shear of tangential velocity M .

11.9. TYPES OF VORTICITY

11.9.1. Relative-vorticity Definition

Counterclockwise rotation about a local vertical axis defines positive vorticity. One type of vorticity ζ_r , called **relative vorticity**, is measured relative to both the location of the object and to the surface of the Earth (also see the Forces & Winds chapter).

Picture a flower blossom dropped onto a straight river, where the river current has shear (Fig. 11.42). As the floating blossom drifts (translates) downstream, it also spins due to the velocity shear of the current. Both Figs. 11.42a & b show counterclockwise rotation, giving positive relative vorticity as defined by:

$$\zeta_r = \frac{\Delta V}{\Delta x} - \frac{\Delta U}{\Delta y} \quad \bullet(11.20)$$

for (U, V) positive in the local (x, y) directions.

Next, consider a flower blossom glued to a solid turntable, as sketched in Fig. 11.43a. As the table turns, so does the orientation of the flower petals relative to the center of the flower. This is shown in Fig. 11.43b. Solid-body rotation requires vectors that start on the dotted line and end on the dashed line. But in a river (or atmosphere), currents can have additional radial shear of the tangential velocity M . Thus, relative vorticity can also be defined as:

$$\zeta_r = \frac{\Delta M}{\Delta R} + \frac{M}{R} \quad \bullet(11.21)$$

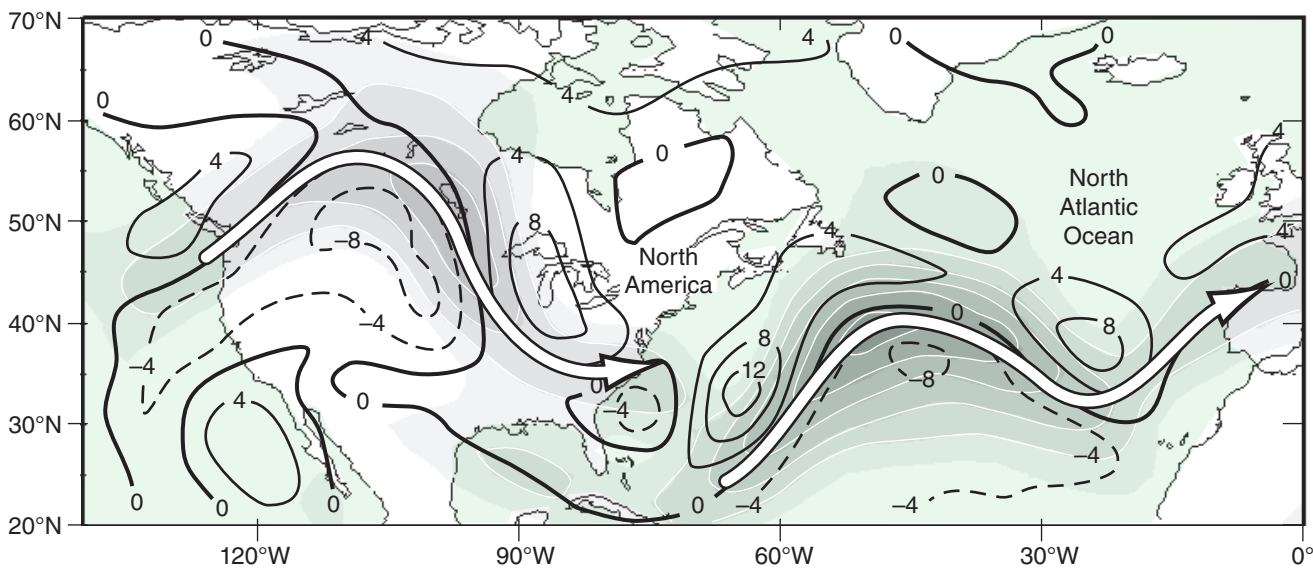


Figure 11.44

Weather map example of relative vorticity (contour lines, with units of 10^{-5} s^{-1}) near the tropopause (at the 20 kPa isobaric surface) at 12 UTC on 5 January 2001. White arrows show jet stream axis of fastest winds over North America and the Atlantic Ocean. Shading gives wind speeds every 10 m s^{-1} from 30 m s^{-1} (lightest grey) to over 80 m s^{-1} (darkest grey). (Based on NCEP/NCAR 40-year reanalysis data, utilizing the plotting tool by Christopher Godfrey, the Univ. of Oklahoma School of Meteorology.)

INFO • Solid Body Relative Vorticity

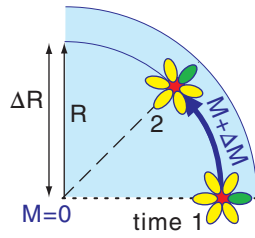
To get eq. (11.22) you can begin with eq. (11.21):

$$\zeta_r = \frac{\Delta M}{\Delta R} + \frac{M}{R}$$

For solid-body rotation, $\Delta M/\Delta R$ exactly equals M/R , as is illustrated in the figure at right. Hence:

$$\zeta_r = \frac{(M-0)}{R} + \frac{M}{R} = \frac{2M}{R}$$

which is eq. (11.22).



For pure solid-body rotation (where the tangential current- or wind-vectors do indeed start at the same dotted line and end at the same dashed line in Fig. 11.43b), eq. (11.21) can be rewritten as

$$\zeta_r = \frac{2M}{R} \quad \bullet(11.22)$$

Relative vorticity has units of s^{-1} . A quick way to determine the sign of the vorticity is to curl the fingers of your right hand in the direction of rotation. If your thumb points up, then vorticity is positive. This is the **right-hand rule**. Fig. 11.44 shows relative vorticity of various signs, where vorticity was created by both shear and curvature.

11.9.2. Absolute-vorticity Definition

Define an absolute vorticity ζ_a as the sum of the vorticity relative to the Earth plus the rotation of the Earth relative to the so-called fixed stars:

$$\zeta_a = \zeta_r + f_c \quad \bullet(11.23)$$

where $f_c = 2\Omega \cdot \sin(\phi)$ is the Coriolis parameter, $2\Omega = 1.458 \times 10^{-4} s^{-1}$ is the angular velocity of the Earth relative to the fixed stars, and latitude is ϕ . Absolute vorticity has units of s^{-1} .

11.9.3. Potential-vorticity Definition

Define a potential vorticity ζ_p as absolute vorticity per unit depth Δz of the rotating air column:

$$\zeta_p = \frac{\zeta_r + f_c}{\Delta z} = \text{constant} \quad \bullet(11.24)$$

This is the most important measure of vorticity because it is constant (i.e., is conserved) for flows having no latent or radiative heating, and no turbulent drag. Potential vorticity units are $m^{-1} s^{-1}$.

Sample Application

At $50^\circ N$ is a west wind of $100 m s^{-1}$. At $46^\circ N$ is a west wind of $50 m s^{-1}$. Find the (a) relative, & (b) absolute vorticity.

Find the Answer

Given: $U_2 = 100 m s^{-1}$, $U_1 = 50 m s^{-1}$, $\Delta\phi = 4^\circ \text{lat}$. $V = 0$
Find: $\zeta_r = ? s^{-1}$, $\zeta_a = ? s^{-1}$

(a) Use eq. (11.20): Appendix A: $1^\circ \text{latitude} = 111 \text{ km}$
 $\zeta_r = -(100 - 50 m s^{-1}) / (4.4 \times 10^5 m) = -1.14 \times 10^{-4} s^{-1}$

(b) Average $\phi = 48^\circ N$. Thus, $f_c = (1.458 \times 10^{-4} s^{-1}) \cdot \sin(48^\circ)$
 $f_c = 1.08 \times 10^{-4} s^{-1}$. then, use eq. (11.23):
 $\zeta_a = (-1.14 \times 10^{-4}) + (1.08 \times 10^{-4}) = -6 \times 10^{-6} s^{-1}$.

Check: Physics and units are reasonable.

Exposition: Shear vorticity from a strong jet stream, but its vorticity is opposite to the Earth's rotation.

Sample Application

Given a N. Hemisphere high-pressure center with tangential winds of $5 m s^{-1}$ at radius 500 km . What is the value of relative vorticity?

Find the Answer

Given: $|M| = 5 m s^{-1}$ (anti-cyclonic), $R = 500,000 m$.
Find: $\zeta_r = ? s^{-1}$

In the N. Hem., anti-cyclonic winds turn clockwise, so using the right-hand rule means your thumb points down, so vorticity will be negative. Apply eq. (11.22):

$$\zeta_r = -2 \cdot (5 m s^{-1}) / (5 \times 10^5 m) = -2 \times 10^{-5} s^{-1}$$

Check: Physics and units are reasonable.

Exposition: Anticyclones often have smaller magnitudes of relative vorticity than cyclones (Fig. 11.44).

Sample Application

A hurricane at latitude $20^\circ N$ has tangential winds of $50 m s^{-1}$ at radius 50 km from the center averaged over a 15 km depth. Find potential vorticity, assuming solid-body rotation for simplicity.

Find the Answer

Assume the shear is in the cyclonic direction.
Given: $\Delta z = 15,000 m$, $\phi = 20^\circ N$, $M = 50 m s^{-1}$,
 $\Delta R = 50,000 m$.
Find: $\zeta_p = ? m^{-1} \cdot s^{-1}$

Apply eqs. (11.22) with (11.24):

$$\zeta_p = \frac{2 \cdot (50 m/s) + (1.458 \times 10^{-4} s^{-1}) \cdot \sin(20^\circ)}{5 \times 10^4 m}$$

$$= (2 \times 10^{-3} + 5 \times 10^{-5}) / 15000 m = 1.37 \times 10^{-7} m^{-1} \cdot s^{-1}$$

Check: Physics & units are reasonable.

Exposition: Positive sign due to cyclonic rotation.

Sample Application

If $\zeta_a = 1.5 \times 10^{-4} \text{ s}^{-1}$, $\rho = 0.7 \text{ kg m}^{-3}$ and $\Delta\theta/\Delta z = 4 \text{ K km}^{-1}$, find the isentropic potential vorticity in PVU.

Find the Answer

Given: $\zeta_a = 1.5 \times 10^{-4} \text{ s}^{-1}$, $\rho = 0.7 \text{ kg m}^{-3}$,
 $\Delta\theta/\Delta z = 4 \text{ K km}^{-1}$

Find: $\zeta_{IPV} = ? \text{ PVU}$

Apply eq. (11.26):

$$\zeta_{IPV} = \frac{(1.5 \times 10^{-4} \text{ s}^{-1})}{(0.7 \text{ kg} \cdot \text{m}^{-3})} \cdot (4 \text{ K} \cdot \text{km}^{-1})$$

$$= 8.57 \times 10^{-7} \text{ K} \cdot \text{m}^2 \cdot \text{s}^{-1} \cdot \text{kg}^{-1} = \underline{0.857 \text{ PVU}}$$

Check: Physics & units are reasonable.

Exposition: As expected for tropospheric air, the answer has magnitude less than 1.5 PVU.

Rewrite the potential vorticity using eqs. (11.24 & 11.21):

$$\frac{\Delta M}{\Delta R} + \frac{M}{R} + f_c = \zeta_p \cdot \Delta z \quad \bullet(11.25)$$

shear curvature planetary stretching

The initial values of absolute vorticity and rotating-air depth determine the value for the constant ζ_p . In order to preserve the equality in the equation above while preserving the constant value of ζ_p , any increase of depth Δz of the rotating layer of air must be associated with greater relative vorticity (air spins faster) or larger f_c (rotating air moves poleward).

11.9.4. Isentropic Potential Vorticity Definition

By definition, an isentropic surface connects locations of equal entropy. But non-changing entropy corresponds to non-changing potential temperature θ in the atmosphere (i.e., adiabatic conditions). If you calculate the absolute vorticity ($\zeta_r + f_c$) on such a surface, then it can be used to define an isentropic potential vorticity (IPV):

$$\zeta_{IPV} = \frac{\zeta_r + f_c}{\rho} \cdot \left(\frac{\Delta\theta}{\Delta z} \right) = \zeta_a \cdot \left(\frac{\Delta\theta}{\Delta z} \right) \quad (11.26)$$

or

$$\zeta_{IPV} = -|g| \cdot (\zeta_r + f_c) \cdot \frac{\Delta\theta}{\Delta p} \quad (11.27)$$

where air pressure is p , air density is ρ , gravitational acceleration magnitude is $|g|$, and $\Delta\theta/\Delta z$ indicates the static stability.

Define a **potential vorticity unit (PVU)** such that $1 \text{ PVU} = 10^{-6} \text{ K} \cdot \text{m}^2 \cdot \text{s}^{-1} \cdot \text{kg}^{-1}$. The stratosphere has lower density and greater static stability than the troposphere, hence stratospheric air has IPV values that are typically 100 times larger than for tropospheric air. Typically, $\zeta_{IPV} > 1.5 \text{ PVU}$ for stratospheric air (a good atmospheric cross-section example is shown in the Extratropical Cyclone chapter).

For idealized situations where the air moves adiabatically without friction while following a constant θ surface (i.e., isentropic motion), then ζ_{IPV} is conserved, which means you can use it to track air motion. Also, stratospheric air does not instantly lose its large IPV upon being mixed downward into the troposphere.

Thus, IPV is useful for finding tropopause folds and the accompanying intrusions of stratospheric air into the troposphere (Fig. 11.45), which can bring down toward the ground the higher ozone concentrations and **radionuclides** (radioactive atoms from former atomic-bomb tests) from the stratosphere.

Because isentropic potential vorticity is conserved, if static stability ($\Delta\theta/\Delta z$) weakens, then eq. (11.26) says absolute vorticity must increase to maintain constant IPV. For example, Fig. 11.46 shows isentropes for flow from west to east across the

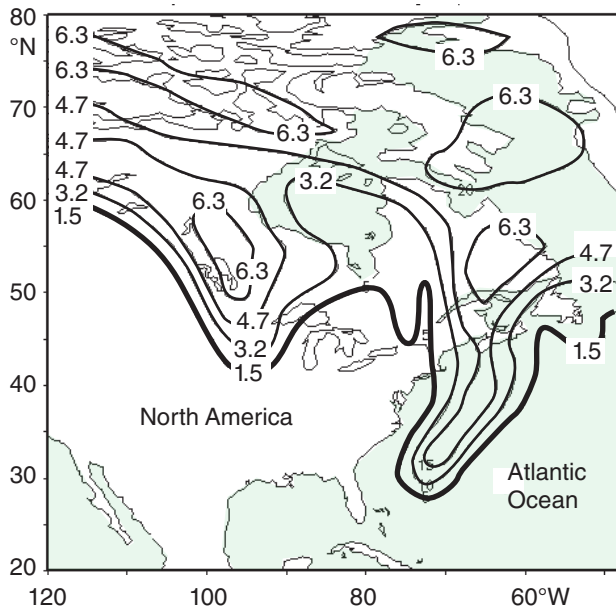


Figure 11.45

Example of isentropic potential vorticity on the 315 K isentropic surface, at 00 UTC on 5 January 2001. Units are PVU. Values greater than 1.5 are in stratospheric air. Because the tropopause is at lower altitude near the poles than at the equator, the 315 K potential temperature surface crosses the tropopause; so it is within the troposphere in the southern part of the figure and in the stratosphere in the northern part. Tropopause folds are evident by the high PVU values just west of the Great Lakes, and just east of the North American coastline. (Based on NCEP/NCAR 40-year reanalysis data, with initial plots produced using the plotting tool by Christopher Godfrey, the University of Oklahoma School of Meteorology.)

Rocky Mountains. Where isentropes are spread far apart, static stability is low. Because air tends to follow isentropes (for frictionless adiabatic flow), a column of air between two isentropes over the crest of the Rockies will remain between the same two isentropes as the air continues eastward.

Thus, the column of air shown in Fig. 11.46 becomes stretched on the lee side of the Rockies and its static stability decreases (same $\Delta\theta$, but spread over a larger Δz). Thus, absolute vorticity in the stretched region must increase. Such increased cyclonic vorticity encourages formation of low-pressure systems (extratropical cyclones) to the lee of the Rockies — a process called **lee cyclogenesis**.

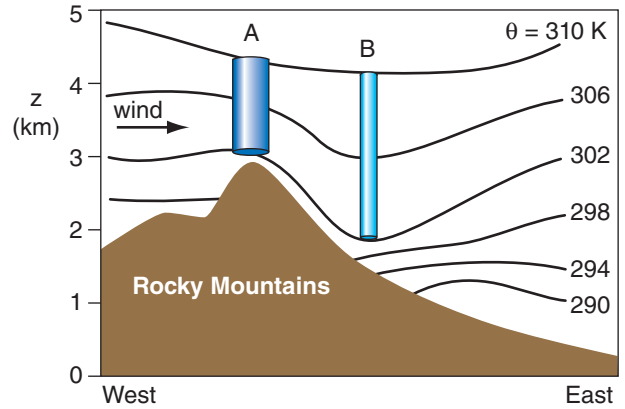


Figure 11.46
Wind blowing from west to east (A) over the Rocky Mountains creates mountain waves and downslope winds, which cause greater separation (B) between the 302 and 310 K isentropes to the lee of the mountains. This greater separation implies reduced static stability and vertical stretching.

11.10. HORIZONTAL CIRCULATION

Consider a closed shape of finite area (Fig. 11.47a). Pick any starting point on the perimeter, and hypothetically travel counterclockwise around the perimeter until you return to the starting point. As you travel each increment of distance Δl , observe the local winds along that increment, and get the average tangential component of wind velocity M_t .

The horizontal **circulation** C is defined as the product of this tangential velocity times distance increment, summed over all the increments around the whole perimeter:

$$C = \sum_{i=1}^n (M_t \cdot \Delta l)_i \quad (11.28)$$

where i is the index of each increment, and n is the number of increments needed to complete one circuit around the perimeter. Take care that the sign of M_t is such that it is positive if the tangential wind is in the same direction as you are traveling, and negative if opposite. The units of circulation are $\text{m}^2 \cdot \text{s}^{-1}$.

If we approximate the perimeter by Cartesian line segments (Fig. 11.47b), then eq. (11.28) becomes:

$$C = \sum_{i=1}^n (U \cdot \Delta x + V \cdot \Delta y)_i \quad (11.29)$$

The sign of Δx is (+) if you travel in the positive x -direction (toward the East), and (–) if opposite. Similar rules apply for Δy (+ toward North).

To better understand circulation, consider idealized cases (Figs. 11.48a & b). For winds of tangential velocity M_t rotating counterclockwise around a circle of radius R , the circulation is $C = 2\pi R \cdot M_t$. For clockwise circular rotation, the circulation is $C = -2\pi R \cdot M_t$, namely, the circulation value is negative. From these two equations, we see that a fast speed around a small circle (such as a tornado) can give

Sample Application

Given Fig. 11.46. (a) Estimate $\Delta\theta/\Delta z$ at A and B. (b) if the initial absolute vorticity at A is 10^{-4} s^{-1} , find the absolute vorticity at B.

Find the Answer

Given: $\zeta_a = 10^{-4} \text{ s}^{-1}$ at A, $\theta_{top} = 310 \text{ K}$, $\theta_{bottom} = 302 \text{ K}$.
Find: (a) $\Delta\theta/\Delta z = ? \text{ K km}^{-1}$ at A and B.
(b) $\zeta_a = ? \text{ s}^{-1}$ at B.

$\Delta\theta = 310 \text{ K} - 302 \text{ K} = 8 \text{ K}$ at A & B. Estimate the altitudes at the top and bottom of the cylinders in Fig. 11.46.

A: $z_{top} = 4.4 \text{ km}$, $z_{bottom} = 3.1 \text{ km}$. Thus $\Delta z_A = 1.3 \text{ km}$.

B: $z_{top} = 4.2 \text{ km}$, $z_{bottom} = 1.9 \text{ km}$. Thus $\Delta z_B = 2.3 \text{ km}$.

(a) $\Delta\theta/\Delta z = 8 \text{ K} / 1.3 \text{ km} = \mathbf{6.15 \text{ K km}^{-1}}$ at A.

$\Delta\theta/\Delta z = 8 \text{ K} / 2.3 \text{ km} = \mathbf{3.48 \text{ K km}^{-1}}$ at B.

(b) If initial (A) and final (B) IPV are equal, then rearranging eq. (11.26) and substituting $(\zeta_r + f_c) = \zeta_a$ gives:

$$\begin{aligned} \zeta_{aB} &= \zeta_{aA} \cdot (\Delta z_B / \Delta z_A) \\ &= (10^{-4} \text{ s}^{-1}) \cdot [(2.3 \text{ km}) / (1.3 \text{ km})] = \mathbf{1.77 \times 10^{-4} \text{ s}^{-1}} \end{aligned}$$

Check: Sign, magnitude & units are reasonable.

Exposition: Static stability $\Delta\theta/\Delta z$ is much weaker at B than A. Thus absolute vorticity at B is much greater than at A. If the air flow directly from west to east and if the initial relative vorticity were zero, then the final relative vorticity is $\zeta_r = 0.77 \times 10^{-4} \text{ s}^{-1}$. Namely, to the lee of the mountains, cyclonic rotation forms in the air where none existed upwind. Namely, this implies cyclogenesis (birth of cyclones) to the lee (downwind) of the Rocky Mountains.

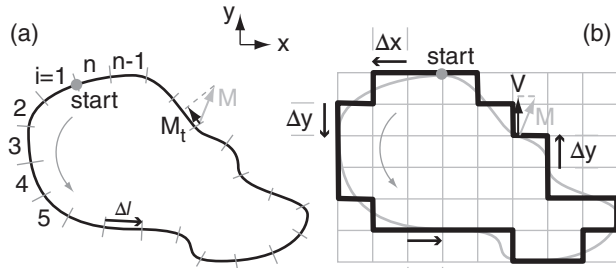


Figure 11.47
Method for finding the circulation. M is the wind vector. M_t and V are projections onto the perimeter. (a) Stepping in increments of Δl around an arbitrary shape. (b) Stepping around a Cartesian (gridded) approximation to the shape in (a).

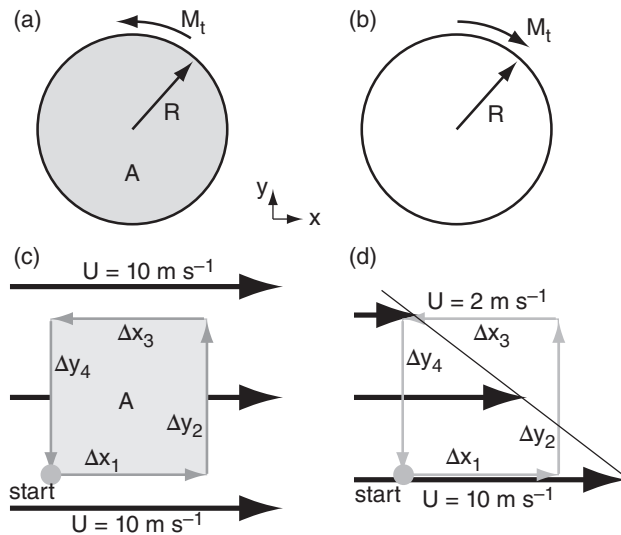


Figure 11.48
Circulation examples. (a) Counterclockwise rotation around a circle. (b) Clockwise rotation around a circle. (c) Uniform wind. (d) Uniform shear. Area A enclosed by circulation is shaded.

Sample Application
Find the horizontal circulation for Fig. 11.48d. Assume $\Delta x = \Delta y = 1 \text{ km}$. Relate to shear and rel. vorticity.

Find the Answer
Given: $U_{\text{bottom}} = 10 \text{ m s}^{-1}$, $U_{\text{top}} = 2 \text{ m s}^{-1}$, $V = 0$,
 $\Delta x = \Delta y = 1 \text{ km}$. Find: $C = ? \text{ m}^2 \text{ s}^{-1}$, $\zeta_r = ? \text{ s}^{-1}$

Use eq. (11.29) from start point:
 $C = (U \cdot \Delta x)_1 + (V \cdot \Delta y)_2 + (U \cdot \Delta x)_3 + (V \cdot \Delta x)_4$
 $(10 \text{ m s}^{-1}) \cdot (1 \text{ km}) + 0 + (2 \text{ m s}^{-1}) \cdot (-1 \text{ km}) + 0$
 $C = 8 \text{ (m s}^{-1}) \cdot \text{km} = \mathbf{8000 \text{ m}^2 \text{ s}^{-1}}$

Use eq. (11.30): with area $A = \Delta x \cdot \Delta y = 1 \text{ km}^2$
 $U_{\text{shear}} = \Delta U / \Delta y = (U_{\text{top}} - U_{\text{bottom}}) / \Delta y$
 $= [(2 - 10 \text{ m s}^{-1}) / (1 \text{ km})] = -8 \text{ (m s}^{-1}) / \text{km}$
 $C = [0 - U_{\text{shear}}] \cdot A = -[-8 \text{ (m s}^{-1}) / \text{km}] \cdot (1 \text{ km}^2)$
 $= 8 \text{ (m s}^{-1}) \cdot \text{km} = \mathbf{8000 \text{ m}^2 \text{ s}^{-1}}$

Use eq. (11.31): $\zeta_r = C / A = 8 \text{ (m s}^{-1}) / \text{km} = \mathbf{0.008 \text{ s}^{-1}}$.

Check: Physics, magnitude & units are reasonable.
Exposition: Strong shear. Large circ. Large vorticity.

the same circulation magnitude as a slower speed around a larger circle (e.g., a mid-latitude cyclone).

Consider two more cases (Figs. 11.48c & d). For a circuit in a constant wind field of any speed, the circulation is $C = 0$. For a circuit within a region of uniform shear such as $\Delta U / \Delta y$, the circulation is $C = -(\Delta U / \Delta y) \cdot (\Delta y \cdot \Delta x)$. Comparing these last two cases, we see that the wind speed is irrelevant for the circulation, but the wind shear is very important.

In the last equation above, $(\Delta y \cdot \Delta x) = A$ is the area enclosed by the circulation of Fig. 11.48d. In general, for uniform U and V shear across a region, the horizontal circulation is:

$$C = \left(\frac{\Delta V}{\Delta x} - \frac{\Delta U}{\Delta y} \right) \cdot A \quad (11.30)$$

But the term in parentheses is the relative vorticity ζ_r . This gives an important relationship between horizontal circulation and vorticity:

$$C = \zeta_r \cdot A \quad (11.31)$$

Vorticity is defined at any one point in a fluid, while circulation is defined around a finite-size area. Thus, eq. (11.31) is valid only in the limit as A becomes small, or for the special case of a fluid having uniform vorticity within the whole circulation area.

The horizontal circulation C defined by eq. (11.30 & 11.31) is also known as the **relative circulation** C_r . An **absolute circulation** C_a can be defined as

$$C_a = (\zeta_r + f_c) \cdot A \quad (11.32)$$

where f_c is the Coriolis parameter. The absolute circulation is the circulation that would be seen from a fixed point in space looking down on the atmosphere rotating with the Earth.

For the special case of a frictionless **barotropic atmosphere** (where isopycnics are parallel to isobars), **Kelvin's circulation theorem** states that C_a is constant with time.

For a more realistic **baroclinic atmosphere** containing horizontal temperature gradients, the **Bjerknes circulation theorem**:

$$\frac{\Delta C_r}{\Delta t} = - \sum_{i=1}^n \left(\frac{\Delta P}{\rho} \right)_i - f_c \cdot \frac{\Delta A}{\Delta t} \quad (11.33)$$

says relative circulation varies with the torque applied to the fluid (via the component of pressure forces in the direction of travel, summed around the perimeter of the circulation area) minus the Earth's rotation effects in a changing circulation area. The units of $\Delta P / \rho$ are J kg^{-1} , which are equivalent to the $\text{m}^2 \cdot \text{s}^{-2}$ units of $\Delta C_r / \Delta t$. The pressure term in eq. (11.33) is called the **solenoid term**.

11.11. EXTRATROPICAL RIDGES & TROUGHS (ROSSBY WAVES)

The atmosphere is generally warm near the equator and cool near the poles. This meridional temperature gradient drives a west-to-east wind having increasing speed with increasing altitude within the troposphere, as described by the thermal-wind effect. The resulting fast wind near the tropopause is called the jet stream. To first order, we would expect this jet stream to encircle the globe (Fig. 11.49a) along the zone between the warm and cool airmasses, at roughly 50 to 60° latitude in winter.

However, this flow is unstable, allowing small disturbances (e.g., flow over mountain ranges) to grow into large north-south meanders (Fig. 11.49b) of the jet stream. These meanders are called **Rossby waves** or **planetary waves**. Typical wavelengths are 3 - 4 Mm. Given the circumference of a parallel at those latitudes, one typically finds 3 to 13 waves around the globe, with a normal **zonal wavenumber** of 7 to 8 waves.

The equatorward region of any meander is called a **trough** (pronounced like “troff”) and is associated with low pressure or low geopotential height. The poleward portion of a meander is called a **ridge**, and has high pressure or height. The turning of winds around troughs and ridges are analogous to the turning around closed lows and highs, respectively. The trough center or **trough axis** is labeled with a dashed line, while the **ridge axis** is labeled with a zig-zag symbol (Fig. 11.49b).

Like many waves or oscillations in nature, Rossby waves result from the interplay between inertia (trying to make the jet stream continue in the direction it was deflected) and a restoring force (acting opposite to the deflection). For Rossby waves, the restoring force can be explained by the conservation of potential vorticity, which depends on both the Coriolis parameter and the layer thickness (related to layer static stability). **Baroclinic instability** considers both restoring factors, while **barotropic instability** is a simpler approximation that considers only the Coriolis effect.

11.11.1. Barotropic Instability

Consider tropospheric air of constant depth Δz (≈ 11 km). For this situation, the conservation of potential vorticity can be written as

$$\left[\frac{M}{R} + f_c \right]_{initial} = \left[\frac{M}{R} + f_c \right]_{later} \quad (11.34)$$

where jet-stream wind speed M divided by radius of

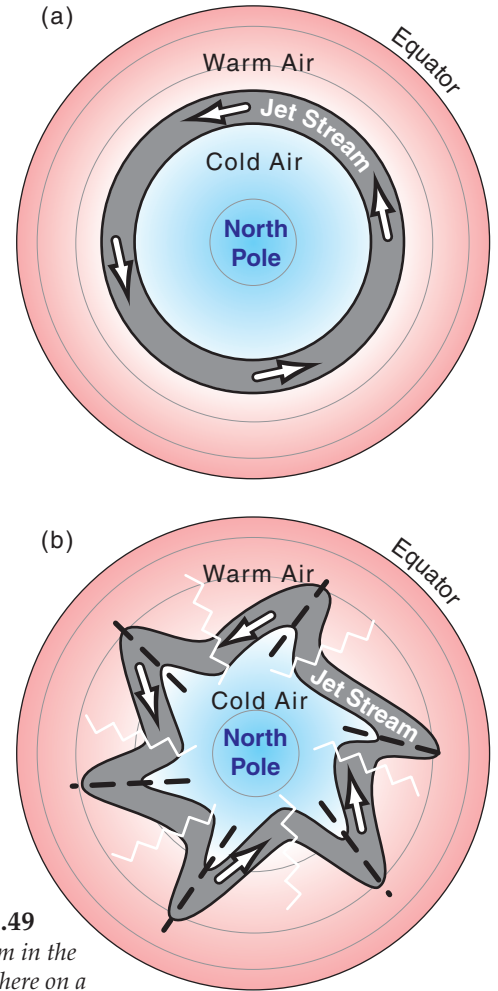


Figure 11.49
 (a) Jet stream in the N. Hemisphere on a world with no instabilities. (b) Jet stream with barotropic or baroclinic instabilities, creating a meandering jet. Troughs are marked with a black dashed line, and ridges with a white zig-zag line.

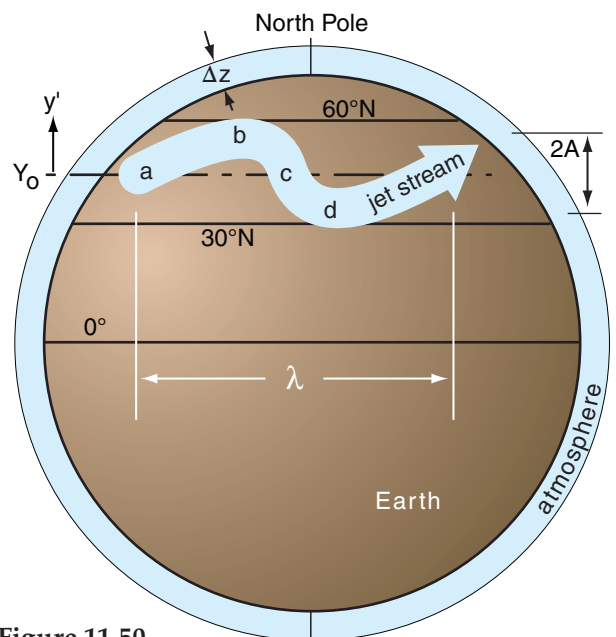


Figure 11.50
 Illustration of barotropic instability.

HIGHER MATH • Planetary-wave Vorticity

Suppose the jet-stream axis oscillates north or south some distance y relative to an arbitrary reference latitude as the air flows toward the east (x):

$$y = A \cdot \sin(2\pi \cdot x / \lambda) \tag{a}$$

where the wavelength is λ and the meridional amplitude of the wave is A . The jet speed along this wave is M , and the associated wind components (U, V) depend on the local slope s of the wave at location x . From geometry: $U^2 + V^2 = M^2$ and $s = V/U$, thus:

$$U = M \cdot (1 + s^2)^{-1/2} \quad \& \quad V = M \cdot s \cdot (1 + s^2)^{-1/2} \tag{b}$$

To find slope s from eq. (a), take the derivative of y :

$$s = \partial y / \partial x = (2\pi A / \lambda) \cdot \cos(2\pi \cdot x / \lambda) \tag{c}$$

Next, change eq. (11.20) from finite difference to partial derivatives:

$$\zeta_r = \partial V / \partial x - \partial U / \partial y \tag{d}$$

But you can expand the last term as follows:

$$\zeta_r = \partial V / \partial x - (\partial U / \partial x) \cdot (\partial x / \partial y)$$

where the last factor is just one over the slope:

$$\zeta_r = \partial V / \partial x - (\partial U / \partial x) \cdot (1 / s) \tag{e}$$

Combine eqs. (e, c, & b) to get the desired relative vorticity:

$$\zeta_r = \frac{-2 \cdot M \cdot A \cdot \left(\frac{2\pi}{\lambda}\right)^2 \cdot \sin\left(\frac{2\pi x}{\lambda}\right)}{\left[1 + \left(\frac{2\pi A}{\lambda}\right)^2 \cdot \cos^2\left(\frac{2\pi x}{\lambda}\right)\right]^{3/2}} \tag{f}$$

Fig. 11.a illustrates this for a wave with $A = 1500$ km, $\lambda = 6000$ km, & $M = 40$ m s⁻¹.

Exposition: Some calculus books give equations for the sine-wave radius of curvature R . Using that in $|\zeta_r| = 2M/R$ would give a similar equation for vorticity. The largest vorticities are concentrated near the wave crest and trough, allowing meteorologists to use positive vorticity to help find troughs.

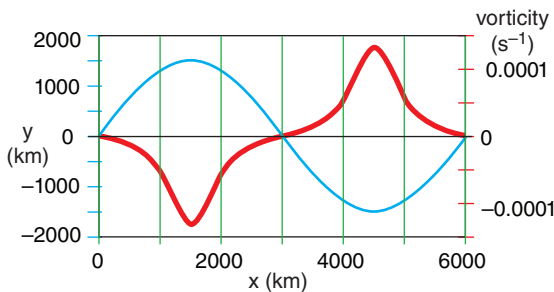


Figure 11.a. Jet-stream path (blue) and associated vorticity (thick red).

curvature R gives the relative vorticity, and f_c is the Coriolis parameter (which is a function of latitude).

(Location **a** in Fig. 11.50) Consider a jet stream at initial latitude Y_0 moving in a straight line from the southwest. At that latitude it has a certain value of the Coriolis parameter, but no relative vorticity ($M/R = 0$, because $R = \infty$ for a straight line). But f_c increases as the air moves poleward, thus the M/R term on the right side of eq. (11.34) must become smaller than its initial value (i.e., it becomes negative) so that the sum on the right side still equals the initial value on the left side.

(Location **b**) We interpret negative curvature as anticyclonic (clockwise turning in the N. Hemisphere). This points the jet stream equatorward.

(Location **c**) As the air approaches its starting latitude, its Coriolis parameter decreases toward its starting value. This allows the flow to become a straight line again at location c. But now the wind is blowing from the northwest, not the southwest.

(Location **d**) As the air overshoots equatorward, f_c gets smaller, requiring a positive M/R (cyclonic curvature) to maintain constant potential vorticity. This turns the jet stream back toward its starting latitude, where the cycle repeats. The flow is said to be **barotropically unstable**, because even pure, non-meandering zonal flow, if perturbed just a little bit from its starting latitude, will respond by meandering north and south.

This north-south (meridional) oscillation of the west-to-east jet stream creates the wavy flow pattern we call a **Rossby wave** or a **planetary wave**. Because the restoring force was related to the change of Coriolis parameter with latitude, it is useful to define a beta parameter as

$$\beta = \frac{\Delta f_c}{\Delta y} = \frac{2 \cdot \Omega}{R_{Earth}} \cdot \cos \phi \tag{11.35}$$

where the average radius of the Earth is $R_{Earth} = 6371$ km. For $2 \cdot \Omega / R_{Earth} = 2.29 \times 10^{-11} \text{ m}^{-1} \cdot \text{s}^{-1}$, one finds that β is roughly $(1.5 \text{ to } 2) \times 10^{-11} \text{ m}^{-1} \cdot \text{s}^{-1}$.

The wave path in Fig. 11.50 can be approximated with a simple cosine function:

$$y' \approx A \cdot \cos \left[2\pi \cdot \left(\frac{x' - c \cdot t}{\lambda} \right) \right] \tag{11.36}$$

where the displacement distance of the Rossby wave from Y_0 (its starting latitude) is y' . Let x' be the eastward distance from the start of the wave. The position of the wave crests move at phase speed c with respect to the Earth. The wavelength is λ and its amplitude is A (see Fig. 11.50). The primes indicate the deviations from a mean background state.

Barotropic Rossby waves of the jet stream have wavelengths of about $\lambda \approx 6000$ km and amplitudes

of about $A \approx 1665$ km, although a wide range of both is possible. Typically 4 to 5 of these waves can fit around the earth at mid-latitudes (where the circumference of a latitude circle is $2\pi R_{Earth} \cos\phi$, and ϕ is latitude).

The waves move through the air at **intrinsic phase speed** c_o :

$$c_o = -\beta \cdot \left(\frac{\lambda}{2\pi}\right)^2 \quad \bullet(11.37a)$$

The negative sign means that the wave crests propagate toward the west relative to the air.

However, the air in which the wave is embedded is itself moving toward the east at wind speed U_o . Thus, relative to the ground, the **phase speed** c is:

$$c = U_o + c_o \quad \bullet(11.37b)$$

Given typical values for U_o , the total phase speed c relative to the ground is positive. Such movement toward the east is indeed observed on weather maps.

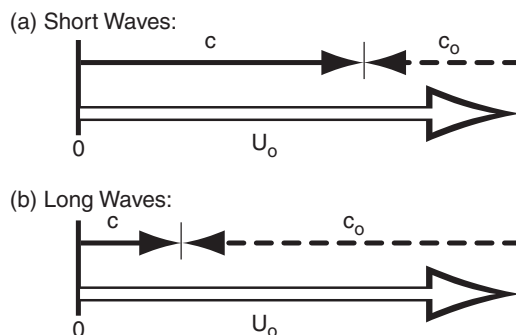
Barotropic Rossby waves can have a range of different wavelengths. But eq. (11.37a) says that different wavelength waves move at different intrinsic phase speeds. Thus, the different waves tend to move apart from each other, which is why eq. (11.37a) is known as a **dispersion relationship**.

Short waves have slower intrinsic phase speed toward the west, causing the background wind to blow them rapidly toward the east. **Long waves**, with their faster intrinsic phase speed westbound end up moving more slowly toward the east relative to the ground, as illustrated in Fig. 11.51. The net effect is that short waves move through long waves (see the 3rd Sample Application on the next page).

The speed that Rossby waves transport energy is called the **group velocity**, c_g :

$$c_g = +\beta \cdot \left(\frac{\lambda}{2\pi}\right)^2 \quad (11.38)$$

which differs in sign from eq. (11.37a). This causes **teleconnections** in storminess that moves faster toward the east than the phase speed of the waves.



HIGHER MATH • The Beta Plane

Here is how you can get β using the definition of the Coriolis parameter f_c (eq. 10.16):

$$f_c = 2 \Omega \sin \phi$$

where ϕ is latitude.

Since y is the distance along the perimeter of a circle of radius R_{Earth} , recall from geometry that

$$y = R_{Earth} \cdot \phi$$

for ϕ in radians.

Rearrange this to solve for ϕ , and then plug into the first equation to give:

$$f_c = 2 \Omega \sin(y/R_{Earth})$$

By definition of β , take the derivative to find

$$\beta = \frac{\partial f_c}{\partial y} = \frac{2 \cdot \Omega}{R_{earth}} \cdot \cos\left(\frac{y}{R_{earth}}\right)$$

Finally, use the second equation above to give:

$$\beta = \frac{2 \cdot \Omega}{R_{earth}} \cdot \cos \phi \quad \bullet(11.35)$$

For a small range of latitudes, β is nearly constant. Some theoretical derivations assume constant beta, which has the same effect as assuming that the earth is shaped like a cone. The name for this lamp-shade shaped surface is the **beta plane**.

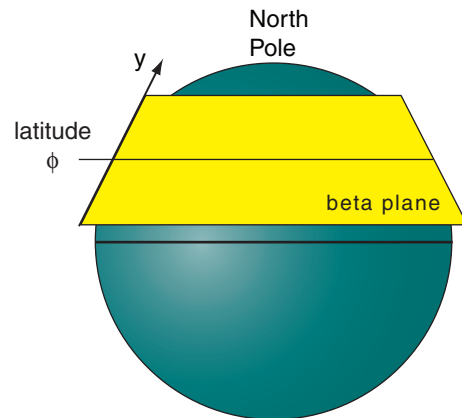


Figure 11.51 (at left)
Sum of a large background west wind U_o with a smaller intrinsic Rossby-wave phase speed c_o from the east gives the resulting propagation speed c of Rossby waves relative to the ground.

Sample Application (§)

The jet stream meanders north and south with barotropic wavelength of 8000 km and amplitude of 1200 km relative to reference latitude 50°N. Winds in this jet are 40 m s⁻¹. Calculate the following for a barotropic wave: beta parameter, phase speeds, and wave translation distance in 12 h. Also, plot the initial and final wave streamlines y'(x') for x' of 0 to 11,000 km.

Find the Answer

Given: U₀ = 40 m s⁻¹, φ = 50°, A = 1200 km, λ = 8000 km, for t = 0 to 12 h

Find: β = ? m⁻¹·s⁻¹, c₀ = ? m s⁻¹, c = ? m s⁻¹, D = cΔt ? km translation distance, y'(x') = ? km.

Apply eq. (11.35):

$$\beta = 2.29 \times 10^{-11} \cdot \cos(50^\circ) = \underline{1.47 \times 10^{-11}} \text{ m}^{-1} \cdot \text{s}^{-1}.$$

Next, apply eq. (11.37a):

$$c_0 = -(1.47 \times 10^{-11} \text{ m}^{-1} \cdot \text{s}^{-1}) \left(\frac{8 \times 10^6 \text{ m}}{2\pi} \right)^2 = \underline{-23.9} \text{ m s}^{-1}$$

Then apply eq. (11.37b):

$$c = (50 - 23.9) \text{ m s}^{-1} = \underline{16.1} \text{ m s}^{-1}$$

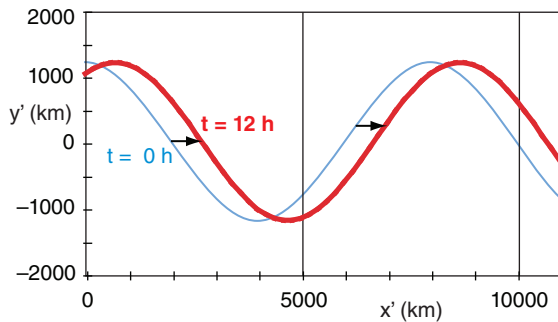
Wave crest translation distance in 12 h is

$$D = c\Delta t = (16.1 \text{ m s}^{-1}) \cdot (12 \text{ h} \cdot 3600 \text{ s/h}) = \underline{697.1} \text{ km}$$

Finally solve & plot eq. (11.36) for t = 0 to 12 h:

$$y' \approx (1200 \text{ km}) \cdot \cos \left[2\pi \cdot \left(\frac{x' - (16.1 \text{ m/s}) \cdot t}{8 \times 10^6 \text{ m}} \right) \right]$$

with conversions between m & km, and for s & h.



Check: Physics & units are reasonable.

Exposition: The thin blue streamlines plotted above show the path of the 40 m s⁻¹ jet stream, but this path gradually shifts toward the east (thick red streamlines).

Although this Rossby-wave phase speed is much slower than a jet airliner, the wave does not need to land and refuel. Thus, during 24 hours, this long wave could travel about 1,400 km — roughly half the distance between San Francisco, CA & Chicago, IL, USA. Even longer waves can be stationary, and some extremely long waves can **retrograde** (move in a direction opposite to the background jet-stream flow; namely, move toward the west).

Sample Application (§)

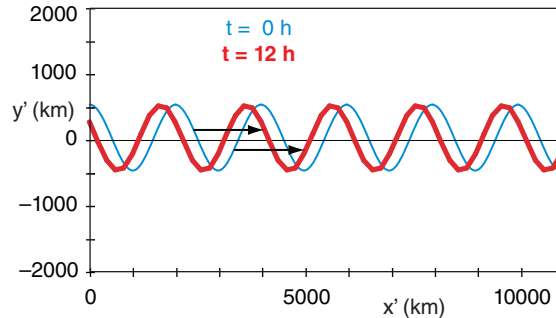
Similar to the previous Sample, but for a short wave with 500 km amplitude and 2000 km wavelength.

Find the Answer

Given: Same, but λ = 2000 km, A = 500 km.

Apply similar equations (not shown here) as before, yielding: β = 1.47 × 10⁻¹¹ m⁻¹·s⁻¹, c₀ = -1.5 m s⁻¹, c = 38.5 m s⁻¹, and D = 1664 km.

The short-wave streamline plot:



Check: Physics & units reasonable.

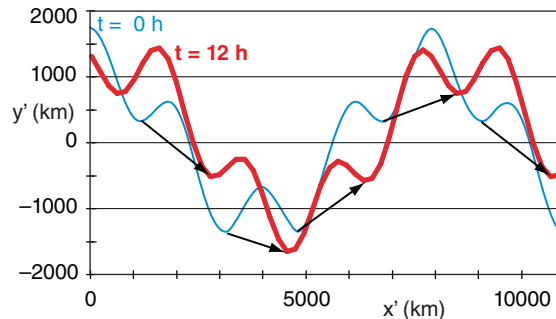
Exposition: Short waves move faster than long ones.

Sample Application (§)

Similar to the previous two Sample Applications, but superimpose the long and short waves.

Find the Answer

The combined long- and short-wave streamline plot:



Check: Physics & units reasonable.

Exposition: The short waves move rapidly along the long-wave streamline similar to trains on a track, except that this long-wave track gradually shifts east.

The short waves travel very fast, so they are in and out of any city very quickly. Thus, they cause rapid changes in the weather. For this reason, weather forecasters pay particular attention to short-wave troughs to avoid surprises. Although short waves are sometimes difficult to spot visually in a plot of geopotential height, you can see them more easily on plots of 50 kPa vorticity. Namely, each short-wave trough has a noticeable positive vorticity that can be highlighted or colored on a forecast map.

11.11.2. Baroclinic Instability

Fig. 11.52 illustrates baroclinic instability using a toy model with thicker atmosphere near the equator and thinner atmosphere near the poles. This mimics the effect of static stability, with cold strongly stable air near the poles that restricts vertical movement of air, vs. warm weakly stable air near the equator that is less limiting in the vertical (see Fig. 5.20 again).

11.11.2.1. Qualitative View

As before, use potential-vorticity conservation:

$$\left[\frac{f_c + (M/R)}{\Delta z} \right]_{initial} = \left[\frac{f_c + (M/R)}{\Delta z} \right]_{later} \quad (11.39)$$

where M is wind speed, the Coriolis parameter is f_c , and the radius of curvature is R . You must include the effective atmospheric thickness Δz because it varies south to north. This captures baroclinic effects that are intentionally neglected for barotropic instability.

For baroclinic waves, follow the jet stream as was done before for barotropic waves, from location **a** to location **d**. All the same processes happen as before, but with an important difference. As the air moves toward location **b**, not only does f_c increase, but Δz decreases. But Δz is in the denominator, hence both f_c and Δz tend to increase the potential vorticity. Thus, the curvature M/R must be even more negative to compensate those combined effect. This means the jet stream turns more sharply.

Similarly, at location **d**, f_c is smaller and Δz in the denominator is larger, both acting to force a sharper cyclonic turn. The net result is that the combined restoring forces are stronger for baroclinic situations, causing tighter turns that create a shorter overall wavelength λ than for barotropic waves.

11.11.2.2. Quantitative View

The resulting north-south displacement y' for the baroclinic wave is:

$$y' \approx A \cdot \cos\left(\pi \cdot \frac{z}{Z_T}\right) \cdot \cos\left[2\pi \cdot \left(\frac{x' - c \cdot t}{\lambda}\right)\right] \quad (11.40)$$

where the tropospheric depth is Z_T (≈ 11 km), the meridional amplitude is A , and where c is phase speed, λ is wavelength, x is distance East, and t is time. Notice that there is an additional cosine factor. This causes the meridional wave amplitude to be zero the middle of the troposphere, and to have opposite signs at the top and bottom.

[ALERT: this is an oversimplification. Waves in the real atmosphere aren't always 180° out of phase between top and bottom of the troposphere. Nonetheless, this simple approach gives some insight into the workings of baroclinic waves.]

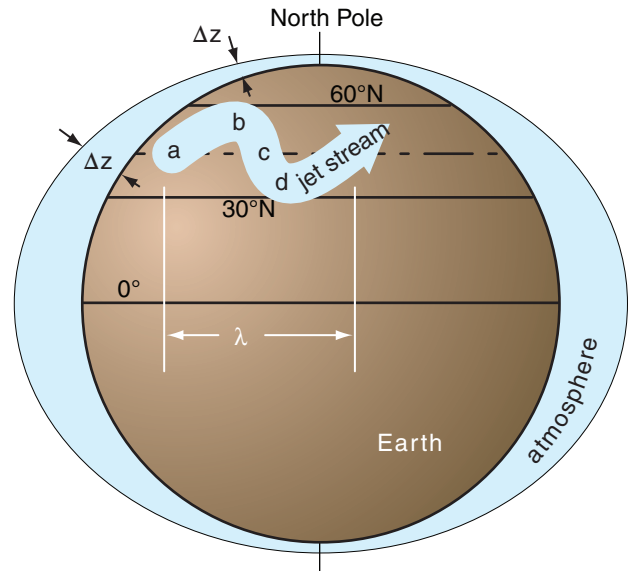


Figure 11.52

Illustration of baroclinic instability, where the effect of static stability is mimicked with an atmosphere that is thicker near the equator and thinner near the poles. The thickness change is exaggerated in this figure.

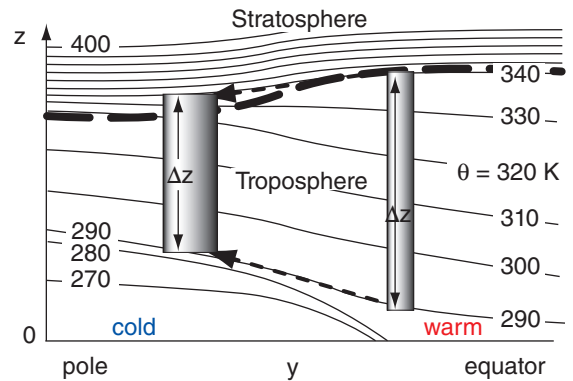


Figure 5.20 (again)

Illustration of how the north-south variation of static stability can be interpreted as a change of effective depth of the atmosphere. Vertical cross section through the atmosphere, showing isentropes (lines of constant potential temperature θ). The depth Δz of column of air on the right will shrink as the column moves poleward, because air tends to follow isentropes during adiabatic processes. Thus, the same $\Delta\theta$ between top and bottom of the air columns spans a shorter vertical distance for the poleward column, meaning that static stability and Brunt-Väisälä frequency are greater there.

Sample Application(s)

The jet stream meanders north and south with amplitude of 900 km relative to reference latitude 50°N. Winds in this jet are 40 m s⁻¹. Temperature decreases 50°C across 12 km thick troposphere, with average temperature -20°C. Calculate the following for a baroclinic wave: Brunt-Väisälä frequency, internal Rossby radius, dominant wavelength, phase speeds, and wave translation distance in 3 h. Also, plot the initial and final wave streamlines y'(x') at both z = 0 and z = 12 km for x' ranging 0 to 5,000 km. β = 1.47x10⁻¹¹ m⁻¹.s⁻¹.

Find the Answer

Given: U_o = 40 m s⁻¹, φ = 50°, A = 900 km, T_{avg} = 253 K, ΔT/Δz = -50K/(12 km), β = 1.47x10⁻¹¹ m⁻¹.s⁻¹, for z=1 & 12 km, t = 0 & 3 h
 Find: N_{BV} = ? s⁻¹, λ_R = ? km, λ = ? km, c_o = ? m s⁻¹, c = ? m s⁻¹, y'(x') = ? km.

Get the N_{BV} eq. from the right column of this page.

$$N_{BV} = \left[\frac{(9.8 \text{ m s}^{-2})}{253 \text{ K}} \left(\frac{-50 \text{ K}}{1.2 \times 10^4 \text{ m}} + 0.0098 \frac{\text{K}}{\text{m}} \right) \right]^{1/2}$$

N_{BV} = **0.0148 s⁻¹**

Apply eq. (10.16):

$$f_c = (1.458 \times 10^{-4} \text{ s}^{-1}) \cdot \sin(50^\circ) = 1.117 \times 10^{-4} \text{ s}^{-1}$$

Apply eq. (11.12):

$$\lambda_R = \frac{(0.0148 \text{ s}^{-1}) \cdot (12 \text{ km})}{1.117 \times 10^{-4} \text{ s}^{-1}} = \mathbf{1590. \text{ km}}$$

Apply eq. (11.43):

$$\lambda = \lambda_d = 2.38 \lambda_R = \mathbf{3784. \text{ km}}$$

Apply eq. (11.41):

$$c_o = \frac{-(1.47 \times 10^{-11} \text{ m}^{-1} \text{ s}^{-1})}{\pi^2 \cdot \left[\frac{4}{(3.784 \times 10^6 \text{ m})^2} + \frac{1}{(1.59 \times 10^6 \text{ m})^2} \right]}$$

$$= \mathbf{-2.21 \text{ m s}^{-1}}$$

Apply eq. (11.42):

$$c = (40 - 2.21) \text{ m s}^{-1} = \mathbf{37.8 \text{ m s}^{-1}}$$

Use eq. (11.40) for z = 0, 12 km, and t = 0, 3 h:

$$y' \approx (900 \text{ km}) \cos\left(\frac{\pi \cdot z}{12 \text{ km}}\right) \cos\left[2\pi\left(\frac{x' - (37.8 \text{ m/s}) \cdot t}{3784 \text{ km}}\right)\right]$$

The results are plotted at right:

Check: Physics & units are reasonable.

Exposition: The Rossby wave at z = 12 km is indeed 180° out of phase from that at the surface. Namely, an upper-level ridge is above a surface trough. In the mid-troposphere (z ≈ 6 km) the baroclinic wave has zero amplitude (not shown). (continues in right column)

The intrinsic phase speed c_o for the baroclinic wave is:

$$c_o = \frac{-\beta}{\pi^2 \cdot \left[\frac{4}{\lambda^2} + \frac{1}{\lambda_R^2} \right]} \quad \bullet(11.41)$$

where eq. (11.35) gives β, wavelength is λ, and eq. (11.12) gives the internal Rossby deformation radius λ_R.

The influence of static stability is accounted for in the **Brunt-Väisälä frequency** N_{BV}, which is a factor in the equation for Rossby deformation radius λ_R (eq. 11.12). Recall from the Atmospheric Stability chapter that N_{BV} = [(|g|/T_v) · (Γ_d + ΔT/Δz)]^{1/2}, where gravitation acceleration is |g| = 9.8 m s⁻², absolute virtual temperature is T_v (where T_v = T for dry air), dry adiabatic lapse rate is Γ_d = 9.8 °C km⁻¹ = 0.0098 K m⁻¹, and ΔT/Δz is the change of air temperature with height.

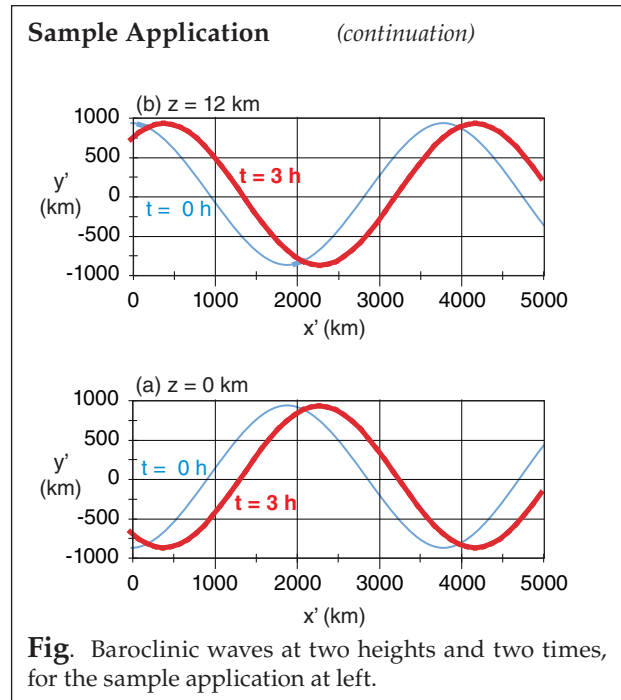
As before, the phase speed relative to the ground is:

$$c = U_o + c_o \quad \bullet(11.42)$$

Although many different wavelengths λ are possible, the dominant wavelength (i.e., the wave for which amplitude grows the fastest) is roughly:

$$\lambda_d \approx 2.38 \cdot \lambda_R \quad (11.43)$$

where λ_R is the internal Rossby radius of deformation (eq. 11.12). Typical values are λ_d ≈ 3 to 4 Mm.



INFO • Baroclinic Wave Characteristics

Baroclinic waves perturb many variables relative to their average background states. Represent the perturbation by $e' = e - e_{background}$ for any variable e . Variables affected include:

- y' = meridional streamline displacement north,
- (u', v', w') = wind components,
- θ' = potential temperature,
- p' = pressure, and
- η' = vertical displacement.

Independent variables are time t and east-west displacement x' relative to some arbitrary location.

Let:
$$a = \pi \cdot z / Z_T \tag{11.44}$$

$$b = 2\pi \cdot (x' - c \cdot t) / \lambda \tag{11.45}$$

Thus:

$$\begin{aligned} y' &= \hat{Y} \cdot \cos(a) \cdot \cos(b) \\ \eta' &= \hat{\eta} \cdot \sin(a) \cdot \cos(b) \\ \theta' &= -\hat{\theta} \cdot \sin(a) \cdot \cos(b) \\ p' &= \hat{P} \cdot \cos(a) \cdot \cos(b) \\ u' &= \hat{U} \cdot \cos(a) \cdot \cos(b) \\ v' &= -\hat{V} \cdot \cos(a) \cdot \sin(b) \\ w' &= -\hat{W} \cdot \sin(a) \cdot \sin(b) \end{aligned} \tag{11.46}$$

Each of the equations above represents a wave, where the wave amplitude is indicated by the factor with the caret (^) over it. These amplitudes are always positive. For Northern Hemispheric baroclinic waves, the amplitudes are:

$$\begin{aligned} \hat{Y} &= A \\ \hat{\eta} &= \frac{A \cdot \pi \cdot f_c \cdot (-c_o)}{Z_T} \cdot \frac{1}{N_{BV}^2} \\ \hat{\theta} &= \frac{A \cdot \pi \cdot f_c \cdot (-c_o)}{Z_T} \cdot \frac{\theta_o}{g} \\ \hat{P} &= A \cdot \rho_o \cdot f_c \cdot (-c_o) \\ \hat{U} &= \left[\frac{A \cdot 2\pi \cdot (-c_o)}{\lambda} \right]^2 \cdot \frac{1}{A \cdot f_c} \\ \hat{V} &= \frac{A \cdot 2\pi \cdot (-c_o)}{\lambda} \\ \hat{W} &= \frac{A \cdot 2\pi \cdot (-c_o)}{\lambda} \cdot \frac{\pi \cdot (-c_o) \cdot f_c}{Z_T \cdot N_{BV}^2} \end{aligned} \tag{11.47}$$

where ρ_o is average density of air at height z , and intrinsic phase speed c_o is a negative number. A (= north-south displacement) depends on the initial disturbance. *(continues in next column)*

INFO • Baroclinic Wave (continuation)

Any atmospheric variable can be reconstructed as the sum of its background and perturbation values; for example: $U = U_{background} + u'$. Background states are defined as follows.

- $U_{background} = U_g$ is the geostrophic (jet-stream) wind.
- $V_{background} = W_{background} = 0$.
- $P_{background}$ decreases with increasing height according to the hydrostatic equation (Chapter 1).
- $\theta_{background}$ increases linearly as altitude increases as was assumed to create a constant value of N_{BV} .
- $Y_{background}$ corresponds to the latitude of zero-perturbation flow, which serves as the reference latitude for calculation of f_c and β .

Background state for η is the altitude z in eq. (11.44).

All variables listed at left interact together to describe the wave. The result is sketched in Fig. 11.53. Although the equations at left look complicated, they are based on a simplified description of the atmosphere. They neglect clouds, turbulence, latent heating, meridional wave propagation, and nonlinear effects. Nonetheless, the insight gained from this simple model helps to explain the behavior of many of the synoptic weather patterns that are covered in the Extratropical Cyclones chapter.

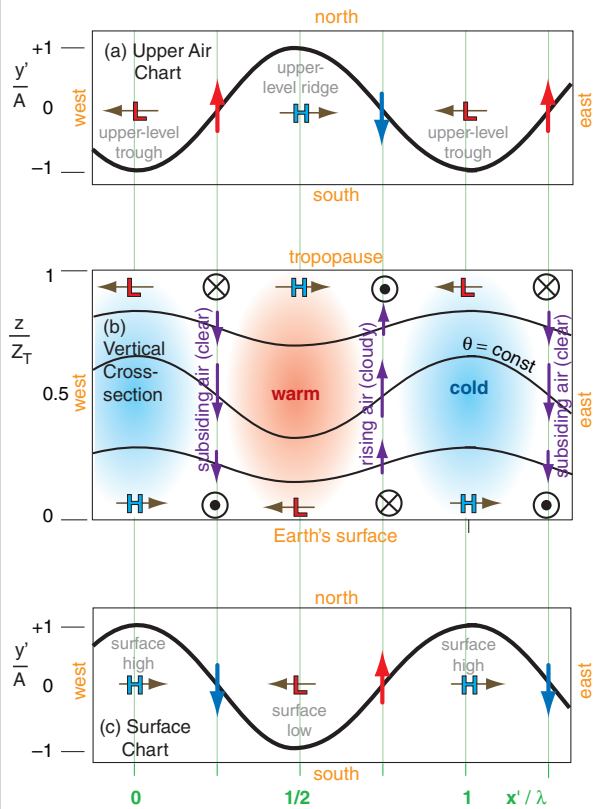


Figure 11.53 Characteristics of a N. Hemisphere baroclinic wave, based on quasi-geostrophic theory. H & L are high and low pressure. Circle-dot and circle-X are flow out-of and into the page, respectively. (after Cushman-Roisin, 1994: "Intro. to Geophysical Fluid Dynamics". Prentice Hall.)

Sample Application

Given $A = 900 \text{ km}$, $\lambda = 3784 \text{ km}$, $c_o = -2.21 \text{ m s}^{-1}$, $Z_T = 12 \text{ km}$, $f_c = 1.117 \times 10^{-4} \text{ s}^{-1}$, $\rho_o = 1 \text{ kg m}^{-3}$, $N_{BV} = 0.0148 \text{ s}^{-1}$, and $|g|/\theta_o = 0.038 \text{ m s}^{-2} \text{ K}^{-1}$. Find the amplitudes for all baroclinic wave variables.

Find the Answer

Given: $A = 900 \text{ km}$, $\lambda = 3784 \text{ km}$, $c_o = -2.21 \text{ m s}^{-1}$, $Z_T = 12 \text{ km}$, $f_c = 1.117 \times 10^{-4} \text{ s}^{-1}$, $\rho_o = 1 \text{ kg m}^{-3}$, $N_{BV} = 0.0148 \text{ s}^{-1}$, and $|g|/\theta_o = 0.038 \text{ m s}^{-2} \text{ K}^{-1}$.

Find: $\hat{Y}, \hat{\eta}, \hat{\theta}, \hat{P}, \hat{U}, \hat{V}, \hat{W}$

Apply eqs. (11.47). $\hat{Y} = A = 900 \text{ km}$.

$$\hat{\eta} = (900 \text{ km}) \cdot \pi \cdot (1.117 \times 10^{-4} \text{ s}^{-1}) \cdot (2.21 \text{ m s}^{-1}) / [(12 \text{ km}) \cdot (0.0148 \text{ s}^{-1})^2] = 265.5 \text{ m}$$

$$\hat{\theta} = 1.53 \text{ K}$$

$$\hat{P} = 0.222 \text{ kPa}$$

$$\hat{U} = 0.109 \text{ m s}^{-1}$$

$$\hat{V} = 3.30 \text{ m s}^{-1}$$

$$\hat{W} = 0.000974 \text{ m s}^{-1} = 3.5 \text{ m h}^{-1}$$

Check: Physics & units are reasonable.

Exposition: Compared to the 40 m s^{-1} jet-stream background winds, the U perturbation is small. In fact, many of these amplitudes are small. They would be larger for larger A and for shorter wavelengths and a shallower troposphere.

11.11.3. Meridional Transport by Rossby Waves

11.11.3.1. Heat Transport Meridionally

As the jet stream meanders north and south while encircling the earth with its west-to-east flow, its temperature changes in response to the regions it flows over (Fig. 11.54). For example, ridges in the planetary wave are where the jet stream is closest to the poles. This air is flowing over colder ground, and is also getting little or no direct solar heating because of the low sun angles (particularly in winter). As a result, the air becomes colder when near the poles than the average jet-stream temperature.

The opposite temperature change occurs in the troughs, where the jet stream is closest to the equator. The air near troughs is flowing over a warmer Earth surface where significant amounts of heat are moved into the jet stream via convective clouds and solar radiation. Define T' as the amount that the temperature deviates from the average value, so that positive T' means warmer (in the troughs), and negative T' means colder (in the ridges) than average.

Define v' as deviation in meridional velocity relative to the mean ($V = 0$). Positive v' occurs where meandering air has a component toward the north, and negative v' means a component toward the south.

Northward movement ($v' = +$) of warm air ($T' = +$) in the N. Hemisphere contributes to a positive (northward) heat flux $v'T'$. This is a kinematic flux, because units are K m/s . Similarly, southward movement ($v' = -$) of cold air ($T' = -$) also contributes to a positive heat flux $v'T'$ (because negative times negative = positive). Adding all the contributions from N different parts of the meandering jet stream gives an equation for the mean meridional heat flux F_y caused by Rossby waves:

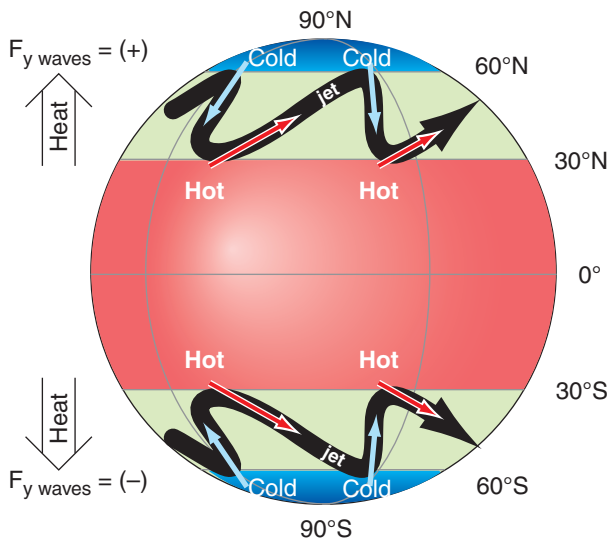


Figure 11.54 Sketch of how Rossby waves (thick black lines) transport heat poleward in midlatitudes. F_y is the meridional heat transport.

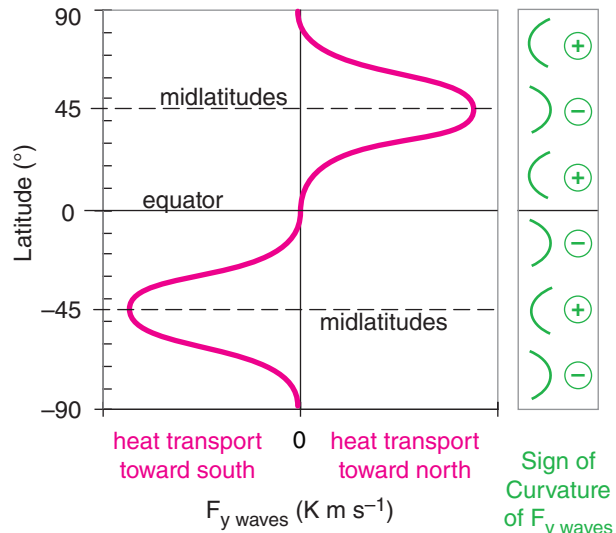


Figure 11.55 Heat flux (magenta line) toward the poles due to Rossby waves. Green icons show whether the curvature of the heat-flux line is positive or negative.

$$F_{y \text{ waves}} = (1/N) \cdot \Sigma(v'T')$$

This flux is positive (negative) in the N. (S.) Hemispheres. Thus, for both hemispheres, Rossby waves move heat from the tropics toward the poles.

The largest magnitudes of v' and T' occur at mid-latitudes, where the jet stream has the largest meridional wind speeds co-located in the region of greatest meridional temperature gradient (Fig. 11.8). Fig. 11.55 shows a sketch of $F_{y \text{ waves}}$ vs. latitude. When this line is concave to the right, it indicates positive curvature (*Curv*). Concave to the left is negative curvature. Curvature of $F_{y \text{ waves}}$ will be used later.

11.11.3.2. Momentum Transport Meridionally

Even if the atmosphere were calm with respect to the Earth's surface, the fact that the Earth is rotating implies that the air is also moving toward the east. Latitude circles near the equator have much larger circumference than near the poles, hence air near the equator must be moving faster toward the east.

As Rossby waves move some of the tropical air poleward (positive v' in N. Hem.; negative v' in S. Hem.), conservation of U angular momentum requires the speed-up (positive U -wind perturbation: u') as the radius from Earth's axis decreases. Similarly, polar air moving equatorward must move slower (negative u' relative to the Earth's surface).

The north-south transport of U momentum is called the average kinematic momentum flux $\overline{u'v'}$:

$$\overline{u'v'} = (1/N) \cdot \Sigma(u'v')$$

For example, consider a N. Hemisphere Rossby-wave. Poleward motion (positive v' ; see brown arrows in Fig. 11.56) transports faster U winds (i.e., positive u'), causing positive $u'v'$. Similarly, equatorward motion (negative v' ; see yellow arrows) transports slower U winds (i.e., negative u'), so again the product is positive $u'v'$. Averaging over all such segments of the jet stream gives positive $\overline{u'v'}$ in the N. Hemisphere, which you can interpret as transport of zonal momentum toward the N. Pole by Rossby waves. In the Southern Hemisphere, $\overline{u'v'}$ is negative, which implies transport of U momentum toward the S. Pole.

To compensate for the larger area of fast U winds (brown in Fig. 11.56) relative to the smaller area of slower U winds (yellow in Fig. 11.56), one can multiply the angular momentum by $a = \cos(\phi_s)/\cos(\phi_d)$:

$$a \cdot u' \approx \Omega \cdot R_{\text{earth}} \cdot \left[\frac{\cos^2 \phi_s}{\cos \phi_d} - \cos \phi_d \right] \cdot \frac{\cos \phi_s}{\cos \phi_d} \quad (11.48)$$

where subscript s represents source location, d is destination, and $\Omega \cdot R_{\text{Earth}} = 463.4 \text{ m s}^{-1}$ as before.

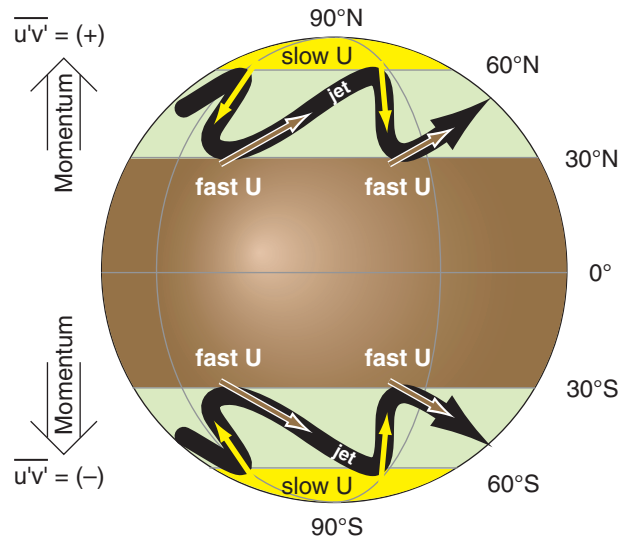


Figure 11.56
Sketch of how Rossby waves (thick black line) transport U momentum toward the poles.

Sample Application

Find the weighted zonal velocity perturbation for air arriving at 50°N from 70°N .

Find the Answer

Given: $\phi_s = 70^\circ\text{N}$, $\phi_d = 50^\circ\text{N}$

Find: $a \cdot u' = ? \text{ m s}^{-1}$

Apply eq. (11.48):

$$a \cdot u' = (463.4 \text{ m/s}) \cdot \left[\frac{\cos^2(70^\circ)}{\cos(50^\circ)} - \cos(50^\circ) \right] \frac{\cos(70^\circ)}{\cos(50^\circ)}$$

$$= -113.6 \text{ m s}^{-1}$$

Check: Physics reasonable, but magnitude too large.

Exposition: The negative sign means air from 70°N is moving slower from the west than any point at 50°N on the Earth's surface is moving. Thus, relative to the Earth, the wind is from the east.

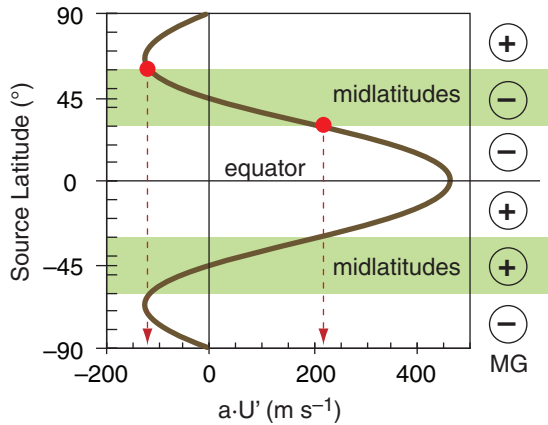


Figure 11.57
Weighted zonal velocity for air that arrives at midlatitude destination 45° from different source latitudes, where the weight is proportional to the amount of air in the source region.

For example, consider the weighted zonal velocity $a \cdot U'$ that reaches destination latitude 45° from other source latitudes, as sketched in Fig. 11.57. Air starting from 30° has much larger magnitude $|a \cdot U'|$ than does air starting from 60°. (*ALERT: Angular-momentum conservation gives unrealistically large velocities, but is qualitatively informative.*)

The change of weighted Rossby-wave momentum flux with latitude is

$$MG = \Delta \overline{u'v'} / \Delta y \quad (11.49)$$

where MG is the north-south gradient of zonal momentum. From Fig. 11.57 we infer that MG is negative (positive) in N. (S.) Hemisphere midlatitudes. This meridional gradient implies that excess zonal momentum from the tropics is being deposited at midlatitudes by the Rossby waves.

Rossby waves that transport U momentum poleward have a recognizable rounded-sawtooth shape, as sketched in Figs. 11.56 & 11.58. Specifically, the equatorward-moving portions of the jet stream are aligned more north-south (i.e., are more meridional), and sometimes even tilt backwards (toward the west as it moves toward the equator). The poleward-moving portions of the jet are more zonal (west to east).

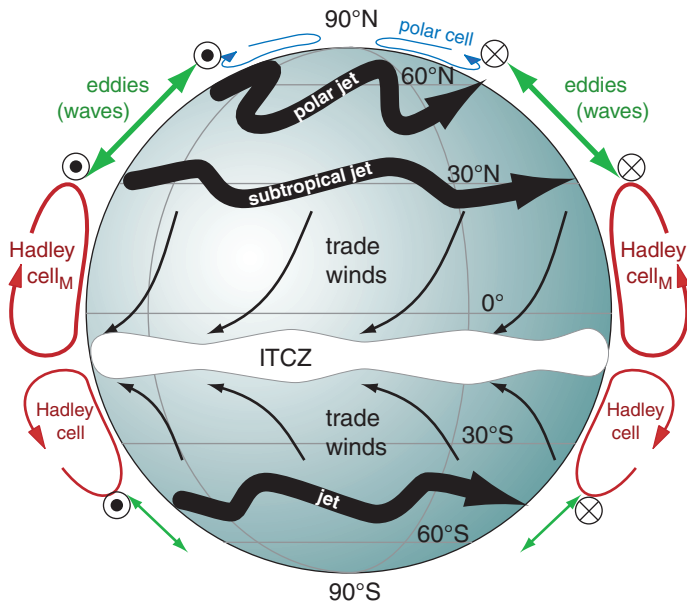


Figure 11.58
Sketch of 3-band global circulation for February (N. Hemisphere winter): 1) a Hadley cell of vertical circulation at low latitudes, 2) Rossby waves with horizontally meandering jet stream at midlatitudes, and 3) a weak polar cell of vertical circulation at high latitudes. For the jet axes, the circle-dot is wind out of the page, and circle-X is wind into the page.

11.12. THREE-BAND GLOBAL CIRCULATION

In the chapter introduction, it was stated that Coriolis force causes the thermally-driven planetary circulation to break down into 3 latitude-bands (Fig. 11.58) in each hemisphere. These bands are: (1) a strong, **direct**, asymmetric, vertical-circulation Hadley cell in low latitudes (0° - 30°); (2) a band of mostly horizontal Rossby waves at mid-latitudes (30° - 60°); and a weak direct vertical circulation cell at high latitudes (60° to 90°). Fig. 11.58 includes more (but not all) of the details and asymmetries explained in this chapter.

The circulation bands work together to globally transport atmospheric heat (Fig. 11.14), helping undo the differential heating that was caused by solar and IR radiation. The Earth-atmosphere-ocean system is in near equilibrium thermally, with only extremely small trends over time related to global warming.

The circulation bands also work together in the meridional transport of zonal momentum. The trade winds, blowing opposite to the Earth's rotation, exert a **torque** (force times radius) that tends to slow the Earth's spin due to frictional drag against the land and ocean surface. However, in mid-latitudes, the westerlies dragging against the Earth's surface and against mountains apply an opposite

INFO • Torques on the Earth

During high-wind episodes in one of the circulation bands, temporary changes in wind-drag torques are large enough to make measurable changes in the Earth's rotation rate — causing the length of a day to increase or decrease 1 - 3 μ s over periods of months. In addition, external influences (lunar and solar tides, solar wind, geomagnetic effects, space dust) cause the Earth to spin ever more slowly, causing the length of a day to increase 1.4 ms/century at present.

torque, tending to accelerate the Earth's spin. On the long term, the opposite torques nearly cancel each other. Thus, the whole Earth-atmosphere-ocean system maintains a near-equilibrium spin rate.

11.12.1. A Metric for Vertical Circulation

Getting back to atmospheric circulations, one can define the strength *CC* of a vertical circulation cell as:

$$CC = \left[\frac{f_c^2}{N_{BV}^2} \frac{\Delta V}{\Delta z} \right] - \frac{\Delta w}{\Delta y} \quad (11.50)$$

Direct circulation cells are ones with a vertical circulation in the direction you would expect if there were no Coriolis force. The units for circulation are s⁻¹.

Using the major Hadley cell as an example of a direct circulation (Fig. 11.59), note that *w* decreases as *y* increases; hence, Δ*w*/Δ*y* is negative. Similarly, Δ*V*/Δ*z* is positive. Thus, eq. (11.50) gives a positive *CC* value for direct circulations, and a negative value for **indirect circulations** (having an opposite rotation direction).

11.12.2. Effective Vertical Circulation

When the forecast equations for momentum and heat are applied to eq. (11.50), the result allows you to anticipate the value of *CC* for a variety of situations— even situations where vertical cells are not dominant:

$$CC \propto - \frac{\Delta E_{net}}{\Delta y} + Curv(F_{y\ wave}) + \frac{\Delta MG}{\Delta z} \quad (11.51)$$

circulation radiation wave-heat wave-momentum

In this equation are factors and terms that were discussed earlier in this chapter. For example, you can use Fig. 11.10 to estimate *E_{net}*, the differential heating due to radiation, and how it varies with *y*. The sign of the curvature (*Curv*) of the Rossby-wave heat flux *F_{y wave}* was shown in Fig. 11.55. If we assume that the meridional gradient of zonal momentum *MG* ≈ 0 near the ground, then Δ*MG*/Δ*z* has the same sign as *MG*, as was sketched in Fig. 11.57.

With this information, you can estimate the sign of *CC* in different latitude bands. Namely, you can anticipate direct and indirect circulations. For the Northern Hemisphere, the results are:

circulation ∝ *radiation* + *wave-heat* + *wave-momentum* = *total*
CC_{polar} ∝ positive + positive + positive = positive
CC_{midlat} ∝ positive + negative + negative = negative
CC_{tropics} ∝ positive + positive + positive = positive

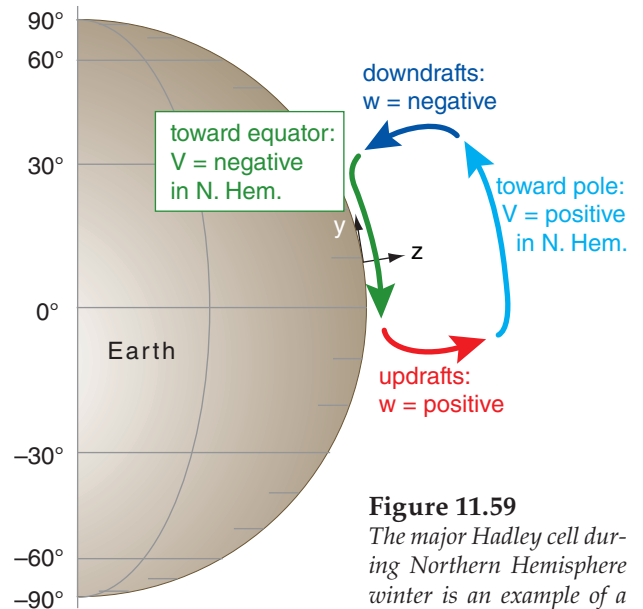


Figure 11.59
 The major Hadley cell during Northern Hemisphere winter is an example of a direct circulation.

Sample Application

Suppose the Hadley cell updraft and downdraft velocities are 6 and -4 mm s⁻¹, respectively, and the meridional wind speeds are 3 m s⁻¹ at the top and bottom of the cell. The major Hadley cell is about 17 km high by 3900 km wide, and is centered at about 10° latitude. Temperature in the tropical atmosphere decreases from about 25°C near the surface to -77°C at 17 km altitude. Find the vertical cell circulation.

Find the Answer

Given: Δ*w* = -10 mm s⁻¹ = -0.01 m s⁻¹, Δ*y* = 3.9 × 10³ km
 Δ*V* = 6 m s⁻¹, Δ*z* = 17 km, φ = 10°, Δ*T* = -102°C.
 Find: *CC* = ? s⁻¹.

First, use eq. (10.16):

$$f_c = (1.458 \times 10^{-4} \text{ s}^{-1}) \cdot \sin(10^\circ) = 2.53 \times 10^{-5} \text{ s}^{-1}$$

Next, for the Brunt-Väisälä frequency, we first need:

$$T_{avg} = 0.5 \cdot (25 - 77)^\circ\text{C} = -26^\circ\text{C} = 247 \text{ K}$$

$$\text{In the tropics } \Delta T / \Delta z = -6^\circ\text{C km}^{-1} = -0.006 \text{ K m}^{-1}$$

Then use eq. (5.4), and assume *T_v* = *T*:

$$N_{BV} = \sqrt{\frac{9.8 \text{ m/s}^2}{247 \text{ K}} (-0.006 + 0.0098)} \frac{\text{K}}{\text{m}} = 0.0123 \text{ s}^{-1}$$

Finally, use eq. (11.50):

$$CC = \left[\left(\frac{2.53 \times 10^{-5} \text{ s}^{-1}}{0.0123 \text{ s}^{-1}} \right)^2 \cdot \frac{6 \text{ m/s}}{17000 \text{ m}} \right] - \frac{-0.01 \text{ m/s}}{3.9 \times 10^6 \text{ m}}$$

$$CC = 1.493 \times 10^{-9} + 2.564 \times 10^{-9} \text{ s}^{-1} = \mathbf{4.06 \times 10^{-9} \text{ s}^{-1}}$$

Check: Physics & units are reasonable.

Exposition: Both terms contribute positively to the circulation of the major Hadley cell during Northern Hemisphere winter.

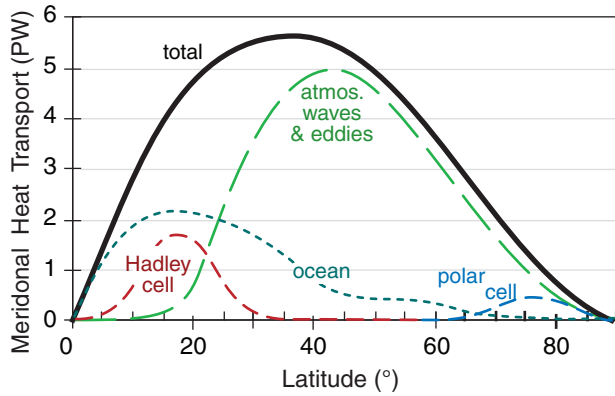


Figure 11.60
Contributions of direct circulations (medium dashed line, for Hadley cell and polar cell) and indirect circulations (long dashed line, for Rossby waves and eddies) to total meridional heat transport T_r in the N. Hemisphere

Rossby waves so efficiently transport heat and momentum at midlatitudes that the effective vertical circulation is negative. This indirect circulation is called the **Ferrel cell**.

Fig. 11.60 redraws the N. Hemisphere portion of Fig. 11.14, qualitatively highlighting the relative contributions of the direct (Hadley and polar cells) and indirect (Ferrel cell/Rossby waves) atmospheric circulations to the total meridional heat transport. At mid-latitudes, the main circulation feature is the Rossby-wave meanders of the jet stream near the tropopause, and the associated low- and high-pressure centers near the surface. High- and low-latitudes are dominated by direct vertical circulations.

Ocean currents also contribute to global heat redistribution. Although ocean-circulation details are not within the scope of this book, we will introduce one ocean topic here — the Ekman spiral. This describes how wind drag can drive some ocean currents, including hurricane storm surges.

11.13. EKMAN SPIRAL OF OCEAN CURRENTS

Frictional drag between the atmosphere and ocean enables winds to drive ocean-surface currents. Coriolis force causes the surface current to be 45° to the right of the wind direction in the Northern Hemisphere. Drag between that surface-current and deeper water drives deeper currents that are slower, and which also are to the right of the current above. The result is an array of ocean-current vectors that trace a spiral (Fig. 11.61) called the **Ekman spiral**.

The equilibrium horizontal ocean-current components (U , V , for a rotated coordinate system having U aligned with the wind direction) as a function of depth (z) are:

$$U = \left[\frac{u_{*water}^2}{(K \cdot f_c)^{1/2}} \right] \cdot \left[e^{z/D} \cdot \cos\left(\frac{z}{D} - \frac{\pi}{4}\right) \right] \quad (11.52a)$$

$$V = \left[\frac{u_{*water}^2}{(K \cdot f_c)^{1/2}} \right] \cdot \left[e^{z/D} \cdot \sin\left(\frac{z}{D} - \frac{\pi}{4}\right) \right] \quad (11.52b)$$

where z is negative below the ocean surface, f_c = Coriolis parameter, and u_{*water} is a **friction velocity** ($m\ s^{-1}$) for water. It can be found from

$$u_{*water}^2 = \frac{\rho_{air}}{\rho_{water}} \cdot u_{*air}^2 \quad (11.53)$$

where the density ratio $\rho_{air}/\rho_{water} \approx 0.001195$ for sea water. The friction velocity ($m\ s^{-1}$) for air can be approximated using **Charnock's relationship**:

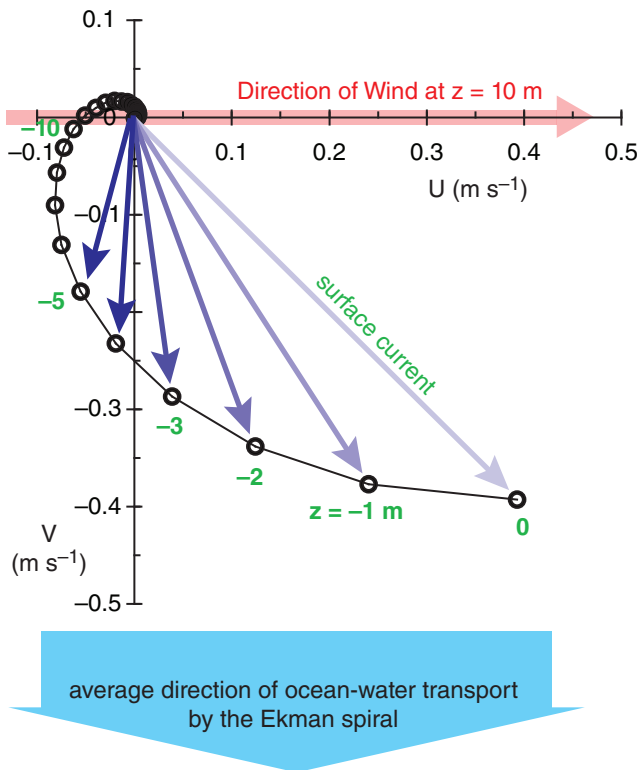


Figure 11.61
Example of an Ekman spiral in the ocean. Blue arrows show ocean currents at different depths (numbers in green). U current direction is aligned with the near-surface wind direction. Red arrow shows the wind direction, but speed is much greater. This example is based on a $10\ m\ s^{-1}$ wind at 45° latitude.

$$u_{air}^2 \approx 0.00044 \cdot M^{2.55} \tag{11.54}$$

where M is near-surface wind speed (at $z = 10$ m) in units of $m\ s^{-1}$.

The Ekman-layer depth scale is

$$D = \sqrt{\frac{2 \cdot K}{f_c}} \tag{11.55}$$

where K is the ocean eddy viscosity (a measure of ability of ocean turbulence to mix momentum). One approximation is $K \approx 0.4 |z| u_{water}$. Although K varies with depth, for simplicity in this illustration I used constant K corresponding to its value at $z = -0.2$ m, which gave $K \approx 0.001\ m^2\ s^{-1}$.

The average water-mass transport by Ekman ocean processes is 90° to the right (left) of the near-surface wind in the N. (S.) Hemisphere (Fig. 11.61). This movement of water affects sea-level under hurricanes (see the Tropical Cyclone chapter).

11.14. REVIEW

The combination of solar radiation input and IR output from Earth causes polar cooling and tropical heating. In response, a global circulation develops due to buoyancy, pressure, and geostrophic effects, which transports heat from the tropics toward the polar regions, and which counteracts the radiative differential heating.

Near the equator, warm air rises and creates a band of thunderstorms at the ITCZ. The updrafts are a part of the Hadley-cell direct vertical circulation, which moves heat away from the equator. This cell cannot extend beyond about 30° to 35° latitude because Coriolis force turns the upper-troposphere winds toward the east, creating a subtropical jet near 30° latitude at the tropopause. Near the surface are the trade-wind return flows from the east.

A strong meridional temperature gradient remains at mid-latitudes, which drives westerly winds via the thermal-wind effect, and creates a polar jet at the tropopause. But instabilities of the jet stream cause meridional meanders called Rossby waves.

These waves are very effective at moving heat poleward, leaving only a very weak indirect-circulating Ferrel cell in midlatitudes. Near the poles is a weak direct-circulation cell. Ocean currents can be driven by the overlying winds in the atmosphere. All these ceaseless global circulations in both the atmosphere and the ocean can move enough momentum and heat to keep our planet in near equilibrium.

Sample Application

For an east wind of $14\ m/s$ at $30^\circ N$, graph the Ekman spiral.

Find the Answer

Given: $M = 14\ m \cdot s^{-1}$, $\phi = 30^\circ N$

Find: $[U, V]$ ($m\ s^{-1}$) vs. depth z (m)

Using a relationship from the Forces and Winds chapter, find the Coriolis parameter: $f_c = 7.29 \times 10^{-5}\ s^{-1}$.

Next, use Charnock's relationship. eq. (11.54):

$$u_{air}^2 = 0.00044 (14^{2.55}) = 0.368\ m^2\ s^{-2}$$

Then use eq. (11.53):

$$u_{water}^2 = 0.001195 \cdot (0.368\ m^2\ s^{-2}) = 0.00044\ m^2\ s^{-2}$$

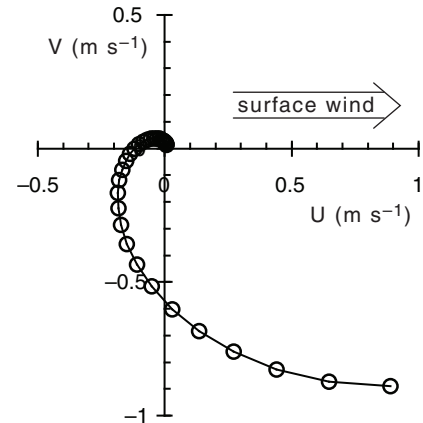
Estimate K at depth 0.2 m in the ocean from

$$K \approx 0.4 \cdot (0.2\ m) \cdot [0.00044\ m^2\ s^{-2}]^{1/2} = 0.00168\ m^2\ s^{-1}$$

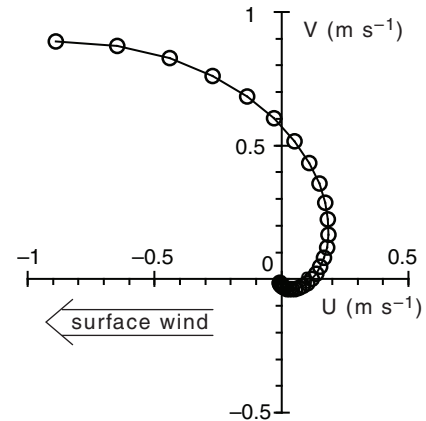
Use eq. (11.55):

$$D = [2 \cdot (0.00168\ m^2\ s^{-1}) / (7.29 \times 10^{-5}\ s^{-1})]^{1/2} = 6.785\ m$$

Use a spreadsheet to solve for (U, V) for a range of z , using eqs. (11.52). I used $z = 0, -1, -2, -3$ m etc.



Finally, rotate the graph 180° because the wind is from the East.



Check: Physics & units are reasonable.

Exposition: Net transport of ocean water is toward the north for this East wind case.

11.15. HOMEWORK EXERCISES

11.15.1. Broaden Knowledge & Comprehension

B1. From hemispheric weather maps of winds near the tropopause (which you can access via the internet), identify locations of major global-circulation features including the jet stream, monsoon circulations, tropical cyclones and the ITCZ.

B2. Same as the previous exercise, except using water-vapor or infrared image loops from geostationary satellites to locate the features.

B3. From the web, find a rawinsonde sounding at a location in the trade-wind region, and confirm the wind reversal between low and high altitudes.

B4. Use a visible, whole-disk image from a geostationary satellite to view and quantify the cloud-cover fraction as a function of latitude. Speculate on how insolation at the Earth's surface is affected.

B5. Download a series of rawinsonde soundings for different latitudes between the equator and a pole. Find the tropopause from each sounding, and then plot the variation of tropopause height vs. latitude.

B6. Download a map of sea-surface temperature (SST), and discuss how SST varies with latitude.

B7. Most satellite images in the infrared show greys or colors that are related to brightness temperature (see the legend in whole-disk IR images that you acquired from the internet). Use these temperatures as a function of latitude to estimate the corresponding meridional variation of IR-radiation out. Hint, consider the Stefan-Boltzmann law.

B8. Download satellite-derived images that show the climatological average incoming and outgoing radiation at the top of the atmosphere. How does it relate to the idealized descriptions in this chapter?

B9. Download satellite-derived or buoy & ship-derived ocean currents for the global oceans, and discuss how they transport heat meridionally, and why the oceanic transport of heat is relatively small at mid to high latitudes in the N. Hemisphere.

B10. Use a satellite image to locate a strong portion of the ITCZ over a rawinsonde site, and then download the rawinsonde data. Plot (compute if needed) the variation of pressure with altitude, and discuss how it does or doesn't deviate from hydrostatic.

B11. Search the web for sites where you can plot "re-analysis data", such as the NCEP/NCAR reanalysis or any of the ECMWF reanalyses. Pick a month during late summer from some past year in this database, and plot the surface pressure map. Explain how this "real" result relates to a combination of the "idealized" planetary and monsoonal circulations.

B12. Same as B11, but for monthly average vertical cross sections that can be looped as movies. Display fields such as zonal wind, meridional wind, and vertical velocity, and see how they vary over a year.

B13. Capture a current map showing 85 kPa temperatures, and assume that those temperatures are surrogates for the actual average virtual temperature between 100 and 70 kPa. Compute the thermal wind magnitude and direction for a location assigned by your teacher, and see if this theoretical relationship successfully explains the wind shear between 100 and 70 kPa. Justify your reasoning.

B14. Capture a current map showing the thickness between 100 and 50 kPa, and estimate the thermal wind direction and magnitude across that layer.

B15. Use rawinsonde soundings from stations that cross the jet stream. Create your own contour plots of the jet-stream cross section for (a) heights of key isobaric surfaces; (b) potential temperature; and (c) wind magnitude. Compare your plots with idealized sketches presented in this chapter.

B16. What are the vertical and horizontal dimensions of the jet stream, based on weather maps you acquire from the internet.

B17. Acquire a 50 kPa vorticity chart, and determine if the plotted vorticity is isentropic, absolute, relative, or potential. Where are positive-vorticity maxima relative to fronts and foul weather?

B18. Calculate the values for the four types of vorticity at a location identified by your instructor, based on data for winds and temperatures. Namely, acquire the raw data used for vorticity calculations; do not use vorticity maps captured from the web.

B19. For the 20 kPa geopotential heights, use the wavy pattern of height contours and their relative packing to identify ridges and troughs in the jet stream. Between two troughs, or between two ridges, estimate the wavelength of the Rossby wave. Use that measured length as if it were the dominant wavelength to estimate the phase speed for baroclinic and barotropic waves.

B20. Confirm that the theoretical relationship between horizontal winds, temperatures, vertical velocities, and heights for baroclinic waves is consistent with the corresponding weather maps you acquire from the internet. Explain any discrepancies.

B21. Confirm the three-band nature of the global circulation using IR satellite image movie loops. In the tropics, compare the motion of low (warm) and high (cold) clouds, and relate this motion to the trade winds and Hadley circulation. In mid-latitudes, find the regions of meandering jet stream with its corresponding high and low-pressure centers. In polar regions, relate cloud motions to the polar cell.

B22. Are the ocean-surface current directions consistent with near-surface wind directions as observed in maps or animations acquired from the internet, given the dynamics describe for the Ekman spiral?

11.15.2. Apply

A1(S). For the “toy” model, make a graph of zonally-averaged temperature (°C) vs. latitude for the altitude (km) above ground level (AGL) given here:

- a. 0.5 b. 1 c. 1.5 d. 2 e. 2.5 f. 3 g. 3.5
- h. 4 i. 4.5 j. 5 k. 5.5 l. 6 m. 6.6 n. 7
- o. 8 p. 9 q. 10 r. 11 s. 12 t. 13 u. 14

A2(S). For the “toy” model, make a graph of zonally-averaged $\Delta T/\Delta y$ (°C km⁻¹) vs. latitude for the altitude (km AGL) given here:

- a. 0.5 b. 1 c. 1.5 d. 2 e. 2.5 f. 3 g. 3.5
- h. 4 i. 4.5 j. 5 k. 5.5 l. 6 m. 6.6 n. 7
- o. 8 p. 9 q. 10 r. 11 s. 12 t. 13 u. 14

A3. Estimate the annual average insolation (W m⁻²) at the following latitude:

- a. 90° b. 85° c. 80° d. 75° e. 70° f. 65° g. 60°
- h. 55° i. 50° j. 45° k. 40° l. 35° m. 30° n. 25°
- o. 20° p. 15° q. 10° r. 5° s. equator

A4. Estimate the annual average amount of incoming solar radiation (W m⁻²) that is absorbed in the Earth-ocean-atmosphere system at latitude:

- a. 90° b. 85° c. 80° d. 75° e. 70° f. 65° g. 60°
- h. 55° i. 50° j. 45° k. 40° l. 35° m. 30° n. 25°
- o. 20° p. 15° q. 10° r. 5° s. equator

A5. Using the idealized temperature near the middle of the troposphere (at $z = 5.5$ km), estimate the outgoing infrared radiation (W m⁻²) from the atmosphere at the following latitude:

- a. 90° b. 85° c. 80° d. 75° e. 70° f. 65° g. 60°
- h. 55° i. 50° j. 45° k. 40° l. 35° m. 30° n. 25°
- o. 20° p. 15° q. 10° r. 5° s. equator

A6. Using the results from the previous two exercises, find the net radiation magnitude (W m⁻²) that is input to the atmosphere at latitude:

- a. 90° b. 85° c. 80° d. 75° e. 70° f. 65° g. 60°
- h. 55° i. 50° j. 45° k. 40° l. 35° m. 30° n. 25°
- o. 20° p. 15° q. 10° r. 5° s. equator

A7. Using the results from the previous exercise, find the latitude-compensated net radiation magnitude (W m⁻²; i.e., the differential heating) at latitude:

- a. 90° b. 85° c. 80° d. 75° e. 70° f. 65° g. 60°
- h. 55° i. 50° j. 45° k. 40° l. 35° m. 30° n. 25°
- o. 20° p. 15° q. 10° r. 5° s. equator

A8. Assuming a standard atmosphere, find the internal Rossby deformation radius (km) at latitude:

- a. 90° b. 85° c. 80° d. 75° e. 70° f. 65° g. 60°
- h. 55° i. 50° j. 45° k. 40° l. 35° m. 30° n. 25°
- o. 20° p. 15° q. 10° r. 5° s. equator

A9. Given the following virtual temperatures at your location (20°C) and at another location, find the change of geostrophic wind with height [(m s⁻¹)/km]. Relative to your location, the other locations are:

$\Delta x(\text{km})$	$\Delta y(\text{km})$	$T_v(^\circ\text{C})$	$\Delta x(\text{km})$	$\Delta y(\text{km})$	$T_v(^\circ\text{C})$
a. 0	100	15	k. 100	0	15
b. 0	100	16	l. 100	0	16
c. 0	100	17	m. 100	0	17
d. 0	100	18	n. 100	0	18
e. 0	100	19	o. 100	0	19
f. 0	100	21	p. 100	0	21
g. 0	100	22	q. 100	0	22
h. 0	100	23	r. 100	0	23
i. 0	100	24	s. 100	0	24
j. 0	100	25	t. 100	0	25

A10. Find the thermal wind (m s⁻¹) components, given a 100 to 50 kPa thickness change of 0.1 km across the following distances:

- $\Delta x(\text{km}) =$ a. 200 b. 250 c. 300 d. 350
- e. 400 f. 450 g. 550 h. 600 i. 650
- $\Delta y(\text{km}) =$ j. 200 k. 250 l. 300 m. 350
- n. 400 o. 450 p. 550 q. 600 r. 650

A11. Find the magnitude of the thermal wind (m s⁻¹) for the following thickness gradients:

- $\frac{\Delta TH(\text{km})}{\Delta x(\text{km})}$ & $\frac{\Delta TH(\text{km})}{\Delta y(\text{km})}$
- a. -0.2 / 600 and -0.1 / 400
- b. -0.2 / 400 and -0.1 / 400
- c. -0.2 / 600 and +0.1 / 400
- d. -0.2 / 400 and +0.1 / 400
- e. -0.2 / 600 and -0.1 / 400
- f. -0.2 / 400 and -0.1 / 400
- g. -0.2 / 600 and +0.1 / 400
- h. -0.2 / 400 and +0.1 / 400

A12. For the toy model temperature distribution, find the wind speed (m s^{-1}) of the jet stream at the following heights (km) for latitude 30° :

- a. 0.5 b. 1 c. 1.5 d. 2 e. 2.5 f. 3 g. 3.5
h. 4 i. 4.5 j. 5 k. 5.5 l. 6 m. 6.6 n. 7
o. 8 p. 9 q. 10 r. 11 s. 12 t. 13 u. 14

A13. If an air parcel from the starting latitude 5° has zero initial velocity relative to the Earth, then find its U component of velocity (m s^{-1}) relative to the Earth when it reaches the following latitude, assuming conservation of angular momentum.

- a. 0° b. 2° c. 4° d. 6° e. 8° f. 10° g. 12°
h. 14° i. 16° j. 18° k. 20° l. 22° m. 24° n. 26°

A14. Find the relative vorticity (s^{-1}) for the change of (U , V) wind speed (m s^{-1}), across distances of $\Delta x = 300$ km and $\Delta y = 600$ km respectively given below.

- a. 50, 50 b. 50, 20 c. 50, 0 d. 50, -20 e. 50, -50
f. 20, 50 g. 20, 20 h. 20, 0 i. 20, -20 j. 20, -50
k. 0, 50 l. 0, 20 m. 0, 0 n. 0, -20 o. 0, -50
p. -20, 50 q. -20, 20 r. -20, 0 s. -20, -20 t. -20, -50
u. -50, 50 v. -50, 20 x. -50, 0 y. -50, -20 z. -50, -50

A15. Given below a radial shear ($\Delta M/\Delta R$) in [$\text{m s}^{-1}/\text{km}$] and tangential wind speed M (m s^{-1}) around radius R (km), find relative vorticity (s^{-1}):

- a. 0.1, 30, 300 b. 0.1, 20, 300 c. 0.1, 10, 300
d. 0.1, 0, 300 e. 0, 30, 300 f. 0, 20, 300
g. 0, 10, 300 h. -0.1, 30, 300 i. -0.1, 20, 300
j. -0.1, 10, 300 k. -0.1, 0, 300

A16. If the air rotates as a solid body of radius 500 km, find the relative vorticity (s^{-1}) for tangential speeds (m s^{-1}) of:

- a. 10 b. 20 c. 30 d. 40 e. 50 f. 60 g. 70
h. 80 i. 90 j. 100 k. 120 l. 140 m. 150

A17. If the relative vorticity is $5 \times 10^{-5} \text{ s}^{-1}$, find the absolute vorticity at the following latitude:

- a. 90° b. 85° c. 80° d. 75° e. 70° f. 65° g. 60°
h. 55° i. 50° j. 45° k. 40° l. 35° m. 30° n. 25°
o. 20° p. 15° q. 10° r. 5° s. equator

A18. If absolute vorticity is $5 \times 10^{-5} \text{ s}^{-1}$, find the potential vorticity ($\text{m}^{-1} \cdot \text{s}^{-1}$) for a layer of thickness (km) of:

- a. 0.5 b. 1 c. 1.5 d. 2 e. 2.5 f. 3 g. 3.5
h. 4 i. 4.5 j. 5 k. 5.5 l. 6 m. 6.6 n. 7
o. 8 p. 9 q. 10 r. 11 s. 12 t. 13 u. 14

A19. The potential vorticity is $1 \times 10^{-8} \text{ m}^{-1} \cdot \text{s}^{-1}$ for a 10 km thick layer of air at latitude 48°N . What is the change of relative vorticity (s^{-1}) if the thickness (km) of the rotating air changes to:

- a. 9.5 b. 9 c. 8.5 d. 8 e. 7.5 f. 7 g. 6.5
h. 10.5 j. 11 k. 11.5 l. 12 m. 12.5 n. 13

A20. If the absolute vorticity is $3 \times 10^{-5} \text{ s}^{-1}$ at 12 km altitude, find the isentropic potential vorticity (PVU) for a potential temperature change of ___ $^\circ \text{C}$ across a height increase of 1 km.

- a. 1 b. 2 c. 3 d. 4 e. 5 f. 6 g. 6.5
h. 7 i. 8 j. 9 k. 10 l. 11 m. 12 n. 13

A21. Find the horizontal circulation associated with average relative vorticity $5 \times 10^{-5} \text{ s}^{-1}$ over area (km^2):

- a. 500 b. 1000 c. 2000 d. 5000 e. 10,000
f. 20,000 g. 50,000 h. 100,000 i. 200,000

A22. For the latitude given below, what is the value of the beta parameter ($\text{m}^{-1} \text{ s}^{-1}$):

- a. 90° b. 85° c. 80° d. 75° e. 70° f. 65° g. 60°
h. 55° i. 50° j. 45° k. 40° l. 35° m. 30° n. 25°
o. 20° p. 15° q. 10° r. 5° s. equator

A23. Suppose the average wind speed is 60 m s^{-1} from the west at the tropopause. For a barotropic Rossby wave at 50° latitude, find both the intrinsic phase speed (m s^{-1}) and the phase speed (m s^{-1}) relative to the ground for wavelength (km) of:

- a. 1000 b. 1500 c. 2000 d. 2500 e. 3000
f. 3500 g. 4000 h. 4500 i. 5000 j. 5500
k. 6000 l. 6500 m. 7000 n. 7500 o. 8000

A24. Plot the barotropic wave (y' vs x') from the previous exercise, assuming amplitude 2000 km.

A25. Same as exercise A23, but for a baroclinic Rossby wave in an atmosphere where air temperature decreases with height at 4°C km^{-1} .

A26(§). Plot the baroclinic wave (y' vs x') from the previous exercise, assuming amplitude 2000 km and a height (km):

- (i) 2 (ii) 4 (iii) 6 (iv) 8 (v) 10

A27. What is the fastest growing wavelength (km) for a baroclinic wave in a standard atmosphere at latitude:

- a. 90° b. 85° c. 80° d. 75° e. 70° f. 65° g. 60°
h. 55° i. 50° j. 45° k. 40° l. 35° m. 30° n. 25°
o. 20° p. 15° q. 10° r. 5° s. equator

A28. For the baroclinic Rossby wave of exercise A25 with amplitude 2000 km, find the wave amplitudes of the:

- (i). vertical-displacement perturbation
(ii). potential-temperature perturbation
(iii). pressure perturbation
(iv). U-wind perturbation
(v). V-wind perturbation
(vi). W-wind perturbation

A29(S). For a vertical slice through the atmosphere, plot baroclinic Rossby-wave perturbation amount for conditions assigned in exercise A28.

A30. Find the latitude-weighted $a-u'$ momentum value (m s^{-1}) for air that reaches destination latitude 50° from source latitude: a. 80° b. 75° c. 70° d. 65° e. 60° f. 55° g. 45° h. 40° i. 35°

A31. Suppose the ____ cell upward and downward speeds are ____ and ____ mm s^{-1} , respectively, and the north-south wind speeds are 3 m s^{-1} at the top and bottom of the cell. The cell is about ____ km high by ____ km wide, and is centered at about ____ latitude. Temperature in the atmosphere decreases from about 15°C near the surface to -57°C at 11 km altitude. Find the vertical circulation.

cell	W_{up} (mm s^{-1})	W_{down} (mm s^{-1})	Δz (km)	Δy (km)	ϕ ($^\circ$)
a. Hadley	6	-4	17	3900	10
b. Hadley	4	-4	15	3500	10
c. Hadley	3	-3	15	3500	5
d. Ferrel	3	-3	12	3000	45
e. Ferrel	2	-2	11	3000	45
f. Ferrel	2	-2	10	3000	50
g. polar	1	-1	9	2500	75
h. polar	1	-1	8	2500	75
i. polar	0.5	-0.5	7	2500	80

A32. Find the friction velocity at the water surface if the friction velocity (m s^{-1}) in the air (at sea level for a standard atmosphere) is:

- a. 0.05 b. 0.1 c. 0.15 d. 0.2 e. 0.25
 f. 0.3 g. 0.35 h. 0.4 i. 0.45 j. 0.5
 k. 0.55 l. 0.6 m. 0.65 n. 0.7 o. 0.75

A33. Find the Ekman-spiral depth scale at latitude 50°N for eddy viscosity ($\text{m}^2 \text{ s}^{-1}$) of:

- a. 0.0002 b. 0.0004 c. 0.0006 d. 0.0008 e. 0.001
 f. 0.0012 g. 0.0014 h. 0.0016 i. 0.0018 j. 0.002
 k. 0.0025 l. 0.003 m. 0.0035 n. 0.004 o. 0.005

A34(S). Create a graph of Ekman-spiral wind components (U, V) components for depths from the surface down to where the velocities are near zero, for near-surface wind speed of 8 m s^{-1} at 40°N latitude.

11.15.3. Evaluate & Analyze

E1. During months when the major Hadley cell exists, trade winds cross the equator. If there are no forces at the equator, explain why this is possible.

E2. In regions of surface high pressure, descending air in the troposphere is associated with dry (non-rainy) weather. These high-pressure belts are where

deserts form. In addition to the belts at $\pm 30^\circ$ latitude, semi-permanent surface highs also exist at the poles. Are polar regions deserts? Explain.

E3. The subtropical jet stream for Earth is located at about 30° latitude. Due to Coriolis force, this is the poleward limit of outflow air from the top of the ITCZ. If the Earth were to spin faster, numerical experiments suggest that the poleward limit (and thus the jet location) would be closer to the equator. Based on the spins of the other planets (get this info from the web or a textbook) compared to Earth, at what latitudes would you expect the subtropical jets to be on Jupiter? Do your predictions agree with photos of Jupiter?

E4. Horizontal divergence of air near the surface tends to reduce or eliminate horizontal temperature gradients. Horizontal convergence does the opposite. Fronts (as you will learn in the next chapter) are regions of strong local temperature gradients. Based on the general circulation of Earth, at what latitudes would you expect fronts to frequently exist, and at what other latitudes would you expect them to rarely exist? Explain.

E5. In the global circulation, what main features can cause mixing of air between the Northern and Southern Hemispheres? Based on typical velocities and cross sectional areas of these flows, over what length of time would be needed for the portion 1/e of all the air in the N. Hemisphere to be replaced by air that arrived from the S. Hemisphere?

E6. In Fig. 11.4, the average declination of the sun was listed as 14.9° to 15° for the 4-month periods listed in those figures. Confirm that those are the correct averages, based on the equations from the Solar & Infrared Radiation chapter for solar declination angle vs. day of the year.

E7. Thunderstorms are small-diameter (15 km) columns of cloudy air from near the ground to the tropopause. They are steered by the environmental winds at an altitude of roughly 1/4 to 1/3 the troposphere depth. With that information, in what direction would you expect thunderstorms to move as a function of latitude (do this for every 10° latitude)?

E8. The average meridional wind at each pole is zero. Why? Also, does your answer apply to instantaneous winds such as on a weather map? Why?

E9. Can you detect monsoonal (monthly or seasonal average) pressure centers on a normal (instantaneous) weather map analysis or forecast? Explain.

E10. Figs. 11.3a & 11.5a showed idealized surface wind & pressure patterns. Combine these and draw a sketch of the resulting idealized global circulation including both planetary and monsoon effects.

E11. Eqs. (11.1-11.3) represent an idealized (“toy model”) meridional variation of zonally averaged temperature. Critically analyze this model and discuss. Is it reasonable at the ends (boundaries) of the curve; are the units correct; is it physically justifiable; does it satisfy any budget constraints (e.g., conservation of heat, if appropriate), etc. What aspects of it are too simplified, and what aspects are OK?

E12. (a) Eq. (11.4) has the 3rd power of the sine times the 2nd power of the cosine. If you could arbitrarily change these powers, what values would lead to reasonable temperature gradients ($\Delta T/\Delta y$) at the surface and which would not (Hint: use a spreadsheet and experiment with different powers)?

(b) Of the various powers that could be reasonable, which powers would you recommend as fitting the available data the best? (Hint: consider not only the temperature gradient, but the associated meridional temperature profile and the associated jet stream.) Also, speculate on why I chose the powers that I did for this toy model.

E13. Concerning differential heating, Fig. 11.9 shows the annual average insolation vs. latitude. Instead, compute the average insolation over the two-month period of June and July, and plot vs. latitude. Use the resulting graph to explain why the jet stream and weather patterns are very weak in the summer hemisphere, and strong in the winter hemisphere.

E14. At mid- and high-latitudes, Fig. 11.9 shows that each hemisphere has one full cycle of insolation annually (i.e., there is one maximum and one minimum each year).

But look at Fig. 11.9 near the equator.

a. Based on the data in this graph (or even better, based on the eqs. from the Solar & Infrared Radiation chapter), plot insolation vs. relative Julian day for the equator.

b. How many insolation cycles are there each year at the equator?

c. At the equator, speculate on when would be the hottest and coldest “seasons”.

d. Within what range of latitudes near the equator is this behavior observed?

E15. Just before idealized eq. (11.6), I mentioned my surprise that E_2 was approximately constant with latitude. I had estimated E_2 by subtracting my toy-

model values for E_{insol} from the actual observed values of E_{in} . Speculate about what physical processes could cause E_2 to be constant with latitude all the way from the equator to the poles.

E16. How sensitive is the toy model for E_{out} (i.e., eq. 11.7) to the choice of average emission altitude z_m ? Recall that z_m , when used as the altitude z in eqs. (11.1-11.3), affects T_m . Hint: for your sensitivity analysis, use a spreadsheet to experiment with different z_m and see how the resulting plots of E_{out} vs. latitude change. (See the “A SCIENTIFIC PERSPECTIVE” box about model sensitivity.)

E17(S). Solve the equations to reproduce the curves in figure: a. 11.10 b. 11.11 c. 11.12 d. 11.13

E18. We recognize the global circulation as a response of the atmosphere to the instability caused by differential heating, as suggested by **LeChatelier’s Principle**. But the circulation does not totally undo the instability; namely, the tropics remain slightly warmer than the poles. Comment on why this remaining, unremoved instability is required to exist, for the global circulation to work.

E19. In Fig. 11.12, what would happen if the surplus area exceeded the deficit area? How would the global circulation change, and what would be the end result for Fig. 11.12?

E20. Check to see if the data in Fig. 11.12 does give zero net radiation when averaged from pole to pole.

E21. The observation data that was used in Fig. 11.14 was based on satellite-measured radiation and differential heating to get the total needed heat transport, and on estimates of heat transport by the oceans. The published “observations” for net atmospheric heat transport were, in fact, estimated as the difference (i.e., residual) between the total and the ocean curves. What could be some errors in this atmosphere curve? (Hint: see the A SCIENTIFIC PERSPECTIVE box about Residuals.)

E22. Use the total heat-transport curve from Fig. 11.60. At what latitude is the max transport? For that latitude, convert the total meridional heat-flux value to horsepower.

E23. For Fig. 11.15, explain why it is p' vs. z that drive vertical winds, and not P_{column} vs. z .

E24. a. Redraw Figs. 11.16 for downdraft situations.

b. Figs. 11.16 both show updraft situations, but they have opposite pressure couplets. As you al-

ready found from part (a) both pressure couplets can be associated with downdrafts. What external information (in addition to the pressure-couplet sign) do you always need to decide whether a pressure couplet causes an updraft or a downdraft? Why?

E25. a. For the thermal circulation of Fig. 11.17(iv), what needs to happen for this circulation to be maintained? Namely, what prevents it from dying out?

b. For what real-atmosphere situations can thermal circulations be maintained for several days?

E26. a. Study Fig. 11.18 closely, and explain why the wind vectors to/from the low- and high-pressure centers at the equator differ from the winds near pressure centers at mid-latitudes.

b. Redraw Fig. 11.5a, but with continents and oceans at the equator. Discuss what monsoonal pressures and winds might occur during winter and summer, and why.

E27. a. Redraw Fig. 11.19, but for the case of geostrophic wind decreasing from its initial equilibrium value. Discuss the resulting evolution of wind and pressure fields during this geostrophic adjustment.

b. Redraw Fig. 11.19, but for flow around a low-pressure center (i.e., look at gradient winds instead of geostrophic winds). Discuss how the wind and pressure fields adjust when the geostrophic wind is increased above its initial equilibrium value.

E28. How would the vertical potential temperature gradient need to vary with latitude for the “internal Rossby radius of deformation” to be invariant? Assume constant troposphere depth.

E29. In the Regional Winds chapter, gap winds and coastally-trapped jets are explained. Discuss how these flows relate to geostrophic adjustment.

E30. At the top of **hurricanes** (see the Tropical Cyclones chapter), so much air is being continuously pumped to the top of the troposphere that a high-pressure center is formed over the hurricane core there. This high is so intense and localized that it violates the conditions for gradient winds; namely, the pressure gradient around this high is too steep (see the Forces & Winds chapter).

Discuss the winds and pressure at the top of a hurricane, using what you know about geostrophic adjustment. Namely, what happens to the winds and air mass if the wind field is not in geostrophic or gradient balance with the pressure field?

E31. In the thermal-wind relationship (eqs. 11.13), which factors on the right side are constant or vary

by only a small amount compared to their magnitude, and which factors vary more (and are thus more important in the equations)?

E32. In Fig. 11.20, how would it change if the bottom isobaric surface were tilted; namely, if there were already a horizontal pressure gradient at the bottom?

E33. Draw a sketch similar to Fig. 11.20 for the thermal-wind relationship for the Southern Hemisphere.

E34. In maps such as Fig. 11.21, explain why thickness is related to average temperature.

E35. Redraw Fig. 11.22 for the case cold air in the west and warm air in the east. Assume no change to the bottom isobaric surface.

E36. Copy Fig. 11.24. a. On your copy, draw the G_1 and G_2 vectors, and the M_{TH} vector at point B. Confirm that the thermal wind relationship is qualitatively satisfied via vector addition. Discuss why point B is an example of veering or backing.

b. Same as (a) but calculate the actual magnitude of each vector at point B based on the spacing between isobars, thickness contours, or height contours. Again, confirm that the thermal wind relationship is satisfied. (1° latitude = 111 km)

E37. Using a spreadsheet, start with an air parcel at rest at the tropopause over the equator. Assume a realistic pressure gradient between the equator and 30° latitude. Use dynamics to solve for acceleration of the parcel over a short time step, and then iterate over many time steps to find parcel speed and position. How does the path of this parcel compare to the idealized paths drawn in Fig. 11.26d? Discuss.

E38. In the thunderstorms at the ITCZ, copious amounts of water vapor condense and release latent heat. Discuss how this condensation affects the average lapse rate in the tropics, the distribution of heat, and the strength of the equatorial high-pressure belt at the tropopause.

E39. Summarize in a list or an outline all the general-circulation factors that make the mid-latitude weather different from tropical weather.

E40. Explain the surface pressure patterns in Figs. 11.31 in terms of a combination of idealized monsoon and planetary circulations.

E41. Figs. 11.31 show mid-summer and mid-winter conditions in each hemisphere. Speculate on what the circulation would look like in April or October.

E42. Compare Figs. 11.32 with the idealized planetary and monsoon circulations, and discuss similarities and differences.

E43. Based on Figs. 11.32, which hemisphere would you expect to have strong subtropical jets in both summer and winter, and which would not. What factors might be responsible for this difference?

E44. For the Indian monsoon sketched in Fig. 11.33, where are the updraft and downdraft portions of the major Hadley cell for that month? Also, what is the relationship between the trade winds at that time, and the Indian monsoon winds?

E45. What are the dominant characteristics you see in Fig. 11.34, regarding jet streams in the Earth's atmosphere? Where don't jet streams go?

E46. In Figs. 11.35, indicate if the jet-stream winds would be coming out of the page or into the page, for the: a) N. Hemisphere, (b) S. Hemisphere.

E47. Although Figs. 11.36 are for different months than Figs. 11.32, they are close enough in months to still both describe summer and winter flows.

a. Do the near-tropopause winds in Figs. 11.36 agree with the pressure gradients (or height gradients) in Figs. 11.32?

b. Why are there easterly winds at the tropopause over/near the equator, even though there is negligible pressure gradient there?

E48. Describe the mechanism that drives the polar jet, and explain how it differs from the mechanism that drives the subtropical jet.

E49. In Fig. 11.37b, we see a very strong pressure gradient in the vertical (indicated by the different isobars), but only small pressure gradients in the horizontal (indicated by the slope of any one isobar). Yet the strongest average winds are horizontal, not vertical. Why?

E50. Why does the jet stream wind speed decrease with increasing height above the tropopause?

E51. a. Knowing the temperature field given by the toy model earlier in this chapter, show the steps needed to create eq. (11.17) by utilizing eqs. (11.2, 11.4 and 11.13). b. For what situations might this jet-wind-speed equation not be valid? c. Explain what each term in eq. (11.17) represents physically.

E52. Why does an air parcel at rest (i.e., calm winds) near the equator possess large angular momentum?

What about for air parcels that move from the east at typical trade wind speeds?

E53. At the equator, air at the bottom of the troposphere has a smaller radius of curvature about the Earth's axis than at the top of the troposphere. How significant is this difference? Can we neglect it?

E54. Suppose that air at 30° latitude has no east-west velocity relative to the Earth's surface. If that air moves equatorward while preserving its angular momentum, which direction would it move relative to the Earth's surface? Why? Does it agree with real winds in the general circulation? Elaborate.

E55. Picture a circular hot tub of 2 m diameter with a drain in the middle. Water is initially 1.2 m deep, and you made rotate one revolution each 10 s. Next, you pull the plug, allowing the water depth to stretch to 2.4 m as it flows down the drain. Calculate the new angular velocity of the water, neglecting frictional drag. Show your steps.

E56. In eq. (11.20), why is there a negative sign on the last term? Hint: How does the rotation direction implied by the last term without a negative sign compare to the rotation direction of the first term?

E57. In the Thunderstorm chapters, you will learn that the winds in a portion of the tornado can be irrotational. This is surprising, because the winds are traveling so quickly around a very tight vortex. Explain what wind field is needed to give **irrotational winds** (i.e., no relative vorticity) in air that is rotating around the tornado. Hint: Into the wall of a tornado, imagine dropping a neutrally-buoyant small paddle wheel the size of a flower. As this flower is translated around the perimeter of the tornado funnel, what must the local wind shear be at the flower to cause it to not spin relative to the ground? Redraw Fig. 11.43 to show what you propose.

E58. Eq. (11.25) gives names for the different terms that can contribute toward vorticity. For simplicity, assume Δz is constant (i.e., assume no stretching). On a copy of Fig. 11.44, write these names at appropriate locations to identify the dominant factors affecting the vorticity max and min centers.

E59. If you were standing at the equator, you would be rotating with the Earth about its axis. However, you would have zero vorticity about your vertical axis. Explain how that is possible.

E60. Eq. (11.26) looks like it has the absolute vorticity in the numerator, yet that is an equation for a form of

potential vorticity. What other aspects of that equation make it like a potential vorticity?

E61. Compare the expression of horizontal circulation C with that for vertical circulation CC .

E62. Relate Kelvin's circulation theorem to the conservation of potential vorticity. Hint: Consider a constant Volume = $A \cdot \Delta z$.

E63. The jet stream sketched in Fig. 11.49 separates cold polar air near the pole from warmer air near the equator. What prevents the cold air from extending further away from the poles toward the equator?

E64. If the Coriolis force didn't vary with latitude, could there be Rossby waves? Discuss.

E65. Are baroclinic or barotropic Rossby waves faster relative to Earth's surface at midlatitudes? Why?

E66. Compare how many Rossby waves would exist around the Earth under barotropic vs. baroclinic conditions. Assume an isothermal troposphere at 50°N.

E67. Once a Rossby wave is triggered, what mechanisms do you think could cause it to diminish (i.e., to reduce the waviness, and leave straight zonal flow).

E68. In Fig. 11.50 at point (4) in the jet stream, why doesn't the air just continue turning clockwise around toward points (2) and (3), instead of starting to turn the other way?

E69. Pretend you are a newspaper reporter writing for a general audience. Write a short article describing how baroclinic Rossby waves work, and why they differ from barotropic waves.

E70. What conditions are needed so that Rossby waves have zero phase speed relative to the ground? Can such conditions occur in the real atmosphere?

E71. Will Rossby waves move faster or slower with respect to the Earth's surface if the tropospheric static stability increases? Why?

E72. For a baroclinic wave that is meandering north and south, consider the northern-most point as the wave crest. Plot the variation of this crest longitude vs. altitude (i.e., x vs. z). Hint: consider eq. (11.40).

E73. Use tropopause-level Rossby-wave trough-axes and ridge-axes as landmarks. Relative to those landmarks, where east or west is: (a) vertical velocity

the greatest; (b) potential-temperature deviation the greatest; and (c) vertical displacement the greatest?

E74. In Figs. 11.51 and 11.53 in the jet stream, there is just as much air going northward as there is air going southward across any latitude line, as required by mass conservation. If there is no net mass transport, how can there be heat or momentum transport?

E75. For the Southern Hemisphere: (a) would a direct circulation cell have positive or negative CC ? (b) for each term of eq. (11.51), what are their signs?

E76. Compare definitions of circulation from this chapter with the previous chapter, and speculate on the relevance of the static stability and Earth's rotation in one or both of those definitions.

E77. Consider a cyclonic air circulation over an ocean in your hemisphere. Knowing the relationship between ocean currents and surface winds, would you anticipate that the near-surface wind-driven ocean currents are diverging away from the center of the cyclone, or converging toward the center? Explain, and use drawings. Note: Due to mass conservations, horizontally diverging ocean surface waters cause upwelling of nutrient-rich water toward the surface, which can support ocean plants and animals, while downwelling does the opposite.

11.15.4. Synthesize

S1. Describe the equilibrium general circulation for a non-rotating Earth.

S2. Circulations are said to **spin-down** as they lose energy. Describe general-circulation spin-down if Earth suddenly stopped spinning on its axis.

S3. Describe the equilibrium general circulation for an Earth that spins three times faster than now.

S4. Describe the **spin-up** (increasing energy) as the general circulation evolves on an initially non-rotating Earth that suddenly started spinning.

S5. Describe the equilibrium general circulation on an Earth with no differential radiative heating.

S6. Describe the equilibrium general circulation on an Earth with cold equator and hot poles.

S7. Suppose that the sun caused radiative cooling of Earth, while IR radiation from space caused warming of Earth. How would the weather and climate be different, if at all?

- S8. Describe the equilibrium general circulation for an Earth with polar ice caps that extend to 30° latitude.
- S9. About 250 million years ago, all of the continents had moved together to become one big continent called **Pangaea**, before further plate tectonic movement caused the continents to drift apart. Pangaea spanned roughly 120° of longitude ($1/3$ of Earth's circumference) and extended roughly from pole to pole. Also, at that time, the Earth was spinning faster, with the solar day being only about 23 of our present-day hours long. Assuming no other changes to insolation, etc, how would the global circulation have differed compared to the current circulation?
- S10. If the Earth was dry and no clouds could form, how would the global circulation differ, if at all? Would the tropopause height be different? Why?
- S11. Describe the equilibrium general circulation for an Earth with tropopause that is 5 km high.
- S12. Describe the equilibrium general circulation for an Earth where potential vorticity isn't conserved.
- S13. Describe the equilibrium general circulation for an Earth having a zonal wind speed halfway between the phase speeds of short and long barotropic Rossby waves.
- S14. Describe the equilibrium general circulation for an Earth having long barotropic Rossby waves that had slower intrinsic phase speed than short waves.
- S15. Describe the nature of baroclinic Rossby waves for an Earth with statically unstable troposphere.
- S16. Describe the equilibrium general circulation for an Earth where Rossby waves had no north-south net transport of heat, momentum, or moisture.
- S17. Describe the equilibrium general circulation for an Earth where no heat was transported meridionally by ocean currents.
- S18. Describe the equilibrium ocean currents for an Earth with no drag between atmosphere and ocean.
- S19. Suppose there was an isolated small continent that was hot relative to the surrounding cooler ocean. Sketch a vertical cross section in the atmosphere across that continent, and use thickness concepts to draw the isobaric surfaces. Next, draw a plan-view map of heights of one of the mid-troposphere isobaric surfaces, and use thermal-wind effects to sketch wind vectors on this same map. Discuss how this approach does or doesn't explain some aspects of monsoon circulations.
- S20. If the Rossby wave of Fig. 11.50 was displaced so that it is centered on the equator (i.e., point (1) starts at the equator), would it still oscillate as shown in that figure, or would the trough of the wave (which is now in the S. Hem.) behave differently? Discuss.
- S21. If the Earth were shaped like a cylinder with its axis of rotation aligned with the axis of the real Earth, could Rossby waves exist? How would the global circulation be different, if at all?
- S22. In the subtropics, low altitude winds are from the east, but high altitude winds are from the west. In mid-latitudes, winds at all altitudes are from the west. Why are the winds in these latitude bands different?
- S23. What if the Earth did not rotate? How would the Ekman spiral in the ocean be different, if at all?